Location of Refueling Stations for Alternative Fuel Vehicles Considering Driver Deviation Behavior and Uneven Consumer Demand: Model, Heuristics, and GIS

by

Jong-Geun Kim

A Dissertation Presented in Partial Fulfillment
of the Requirements for the Degree
Doctor of Philosophy

Approved in November 2010 by the
Graduate Supervisory Committee:

Michael J. Kuby, Chair
Elizabeth A. Wentz
Alan T. Murray

ARIZONA STATE UNIVERSITY

December 2010

ABSTRACT

Concerns about Peak Oil, political instability in the Middle East, health hazards, and greenhouse gas emissions of fossil fuels have stimulated interests in alternative fuels such as biofuels, natural gas, electricity, and hydrogen. Alternative fuels are expected to play an important role in a transition to a sustainable transportation system. One of the major barriers to the success of alternative-fuel vehicles (AFV) is the lack of infrastructure for producing, distributing, and delivering alternative fuels. Efficient methods that locate alternative-fuel refueling stations are essential in accelerating the advent of a new energy economy.

The objectives of this research are to develop a location model and a Spatial Decision Support System (SDSS) that aims to support the decision of developing initial alternative-fuel stations. The main focus of this research is the development of a location model for siting alt-fuel refueling stations considering not only the limited driving range of AFVs but also the necessary deviations that drivers are likely to make from their shortest paths in order to refuel their AFVs when the refueling station network is sparse. To add reality and applicability of the model, the research is extended to include the development of efficient heuristic algorithms, the development of a method to incorporate AFV demand estimates into OD flow volumes, and the development of a prototype SDSS. The model and methods are tested on real-world road network data from state of Florida.

The Deviation-Flow Refueling Location Model (DFRLM) locates facilities to maximize the total flows refueled on deviation paths. The flow volume is assumed to be decreasing as the deviation increases. Test results indicate that the specification of the maximum allowable deviation and specific deviation penalty functional form do have a measurable effect on the optimal locations of facilities and objective function values as well. The heuristics (greedy-adding and greedy-adding with substitution) developed here have been identified efficient in solving the DFRLM while AFV demand has a minor effect on the optimal facility locations. The prototype SDSS identifies strategic station locations by providing flexibility in combining various AFV demand scenarios.

This research contributes to the literature by enhancing flow-based location models for locating alternative-fuel stations in four dimensions: (1) drivers' deviations from their shortest paths, (2) efficient solution approaches for the deviation problem, (3) incorporation of geographically uneven alt-fuel vehicle demand estimates into path-based origin-destination flow data, and (4) integration into an SDSS to help decision makers by providing solutions and insights into developing alt-fuel stations.

ACKNOWLEDGMENTS

I was fortunate to have a graduate committee that has been extremely supportive and allowed me to explore my research interests. First, I would like to thank my mentor, Dr. Michael Kuby, for his guidance, encouragement, and expertise during the course of my study. His complete confidence in me has enabled me to overcome the many obstacles I encountered. Dr. Elizabeth Wentz provided me heart-warming support and perspectives every time I met her. I am very grateful to Dr. Alan Murray for his invaluable insight and enlightening advice.

I want to gratefully acknowledge the continued support I received from Jana Hutchins, Shea Lemar, and Ayan Mitra from Institute for Social Science Research. I would also like to thank Dr. Seow Lim for his exceptional work, Dr. Lee Lines from Rollins College, Dr. Ronald Schultz and Dr. Zhixiao Xie from Florida Atlantic University who worked together on the Florida Hydrogen Initiative project.

I cannot thank enough to my friends BK, YB, Won, Min, and Hang-A for their support. I appreciate the sustained interest of my colleagues Drs. Lee, Shin, Hong, Park, Kim, and Chun. I would like to thank my parents, my brother and sister for their constant love and support over the length of my study. At last, my deepest thanks belong to my wife Nayoung for her love, support, and patience.

TABLE OF CONTENTS

CHAPTER Page

CHAPTER Page

CHAPTER Page

LIST OF TABLES

Table Page

LIST OF FIGURES

Figure Page

Figure Page

LIST OF ALGORITHMS

1 INTRODUCTION AND PURPOSE

1.1 Alternative Fuel Needs and Barriers

Petroleum-based automobiles are the dominant mode of modern transportation systems. Concerns about Peak Oil, political instability in the Middle East, health hazards, and greenhouse gas (GHG) emissions of fossil fuels have challenged humankind to make a transition to a more sustainable transportation system. Greater sustainability may be accomplished by improving vehicles' fuel economy (Greene 2004) or by designing an efficient traffic control system (McQueen and McQueen 1999). In addition, planning measures such as "smart growth" (Duany, Plater-Zyberk, and Speck 2000) and telecommuting may also contribute to reducing transportation demand. However, the efficiency gained could be offset by the induced demand generated through increased system capacity, or the projected increase in population and economic wealth (EIA 2009) may generate much more demand. For instance, the percentage of light truck sales increased from about 30% of new personal sales in 1990 to about 50% in 2005 (BTS 2008). Considering the above limits, policy makers, automobile manufacturers, and fuel providers have become increasingly interested in alternative fuels such as biofuels, natural gas, electricity, and hydrogen and they will play an important role in a transition to a sustainable transportation system.

One of the major barriers to the success of alternative-fuel vehicles (AFVs) is the lack of infrastructure for producing, distributing, and delivering alternative fuels (Greene 1996; Ogden 1999a; Melendez 2006; NAS 2004). It is clear that availability of alt-fuel stations will accelerate the market acceptance of AFVs. Based on a survey of the literature and of experts involved in alternative fuel deployment, Melendez (2006) identified the following as four major barriers of infrastructure development: lack of availability of alt-fuel stations; the high construction costs of alt-fuel stations; the high costs of AFVs; and the relatively short range of AFVs between refueling. The short range of AFVs is especially relevant given the current technological state of battery electric vehicle and hydrogen fuel cell vehicles. The high construction costs of alt-fuel stations imply that drivers need to deviate to refuel their AFVs. The high costs of AFVs result in the uneven demand where everyone is not equally likely to purchase an AFV.

1.2 Location Models for Refueling Stations and Consideration of Deviations

Efficient methods that locate alternative-fuel refueling stations are essential in accelerating the advent of a new energy economy. Such methods should suggest strategic station locations such that even a limited number of stations can achieve a satisfactory level of coverage. In addition, such methods need to be based on realistic assumptions about the characteristics of consumer demand for AFVs and drivers' refueling behavior when the stations are scarce. Kuby and Lim (2005) developed the Flow Refueling Location Model (FRLM), which determines the location and combination of refueling stations to be built in order to maximize the flows covered by a given number of facilities. The model takes into account the paths of drivers from their origins to destinations, the amount of flows on the paths, and the driving range of vehicles. In the initial stages of the transition to alternative fuels, the lack of stations will require drivers to deviate from their regular or pre-planned routes. Berman, Bertsimas, and Larson (1995) relaxed the assumption of basic flow-intercepting models that all flows follow the shortest paths between pairs of nodes, but no one has looked at deviations for flow refueling.

1.3 Enhanced Representation of Alternative Fuel Demand

Realistic representation of demand is critical for facility location models. Given the costs of purchasing and maintaining AFVs initially will be more expensive than conventional vehicles, the consumers' likelihood to purchase AFVs will be geographically uneven. Melendez and Milbrandt (2006) of the National Renewable Energy Laboratory used a Geographic Information System (GIS) to model the potential hydrogen demand using demographic characteristics and policy variables by census boundary. This approach has not been widely used in estimating the flow volumes of AFVs for recommending optimal refueling station sites.

1.4 Managing Uncertainty in Site Selection through SDSS

Facility location models are often deterministic. However, data used as inputs for such models have errors in representing real entities as digital objects. In addition, specification of the objective function and constraints in a location model is also an abstraction process. A spatial decision support system (SDSS) is "a framework that integrates key computer-based components to support spatial decision making" (Densham 1991). A facility location model's inherent uncertainties can be alleviated by utilizing an SDSS with efficient solution algorithms, exploratory tools, and various outputs. Users can conduct experiments on the location model with varying parameters and dynamically visualize results in a series of maps representing criteria outcomes and decision options. By comparing many alternatives, users can obtain insight into the nature of the spatial decision problem and eventually reach a better decision.

1.5 General Objectives

The general objectives of this research are to develop a location model and a spatial decision support system (SDSS) that aims to support the decision of building initial alternative-fuel stations. The focus of this research is on the incorporation of drivers' deviations and uneven distribution of alt-fuel vehicle demand into the model and the SDSS as well. The research formulates a location model that extends a flow-based location model, the FRLM, develops heuristic algorithms to solve the problem, and integrates them within a GIS environment by building a SDSS. In addition, this research proposes and compares methods that integrate the AFV demand and trip volumes and explore results of different scenarios. The model and methods are applied to real-world road network data from the state of Florida.

The developed location model for planning alt-fuel refueling station network considers not only vehicles' range but also the deviations that drivers are likely to make from their shortest paths in order to refuel their AFVs. The model is formulated as a mixed-integer linear programming and global optimal solutions for problem instances are obtained.

The flow-refueling model is considerably more complex than the flow-intercepting model because longer paths can only be covered by combinations of facilities. In fact, the number of possible combinations on long paths can be so large that it is not even practical to generate the linear program for the FRLM for a realistic network, let alone solve it (Lim and Kuby 2010). Therefore, this research also develops a heuristic solution method to solve the flow-refueling model with deviation paths on a network of a realistic size.

For the developed location model to provide a more realistic solution in planning a network of alt-fuel refueling facilities, the geographical variation of AFV demand needs to be incorporated into the model. Given that the matrix of trip volumes between origins and destinations is required for the FRLM, traffic data need to be weighted by alternative-fuel purchasing likelihood for the model. This is an enhanced representation of demand in the early stages of the transition to alternative-fuel vehicles.

This dissertation develops a prototype SDSS designed to support a roll-out plan for siting alt-fuel refueling facilities. The SDSS integrates into a GIS (ESRI ArcGIS) the developed location model, heuristic algorithms, and AFV demand estimation method. The SDSS enables the user to generate a variety of scenarios and to explore alternatives that will be important to the planners in mitigating the effect of the uncertainty in the data or the model.

1.6 Significance

This research has theoretical and societal significance. On the theoretical side, it expands the location modeling literature by providing more realistic representation of demands. Many theories and models of facility location have been developed to serve point-based demand. In addition, demand is usually assumed to be served by one facility. Recently, there is growing research interest in developing models for flow-based demands (Hodgson 1990; Mirchandani, Rebello, and Agnetis 1995; Kuby and Lim 2005; Zeng, Castillo, and Hodgson 2010a) or the need of multiple facilities for a full coverage of one unit of demand (Kuby and Lim 2005; Murray, Tong, and Kim 2010). However, the provision of partial coverage of flow-based demand by a group of facilities has not been studied. To put this in an application level, understanding of the effects of deviating flows on facility location is lacking. There are no station location models in the literature that account for deviations and vehicles' range at the same time not to mention the absence of the approaches that add reality and applicability to the model: development of efficient heuristics; incorporation of AFV demand estimates into flow-based demand; development of a framework to explore different AFV demand scenarios to reduce uncertainty.

On a broad societal level, this work contributes to mitigating the impact of transportation energy on the environment, as discussed above. The lack of models for understanding and locating the refueling stations for deviation flows and AFV flows has important implications for private sector's efforts to commercialize AFVs and the government's need to plan required subsidies. Until the AFV market becomes mature, alt-fuel stations will need to be located strategically. Convenient and more accessible location of alt-fuel stations will make full advantage of the necessary public-private partnerships. It will minimize the government subsidies required by fuel providers to make the final costs of alternative fuels competitive with gasoline by maximizing the utilization of alt-fuel stations constructed.

1.7 Organization of the Dissertation

Chapter 1 has introduced the backgrounds of this research and articulated the objectives. Chapter 2 reviews related literature in the fields of location modeling, refueling infrastructure analysis and modeling, and spatial decision support systems. Chapter 3 provides a detailed research statement. Chapter 4 presents the concept, formulation, and solution procedure of deviation-flow location model. It also includes discussion of experimental results. Chapter 5 explains the heuristic algorithms to solve the deviation-flow refueling location (DFRLM) problems when its size becomes large. Detail of the algorithm steps and implementation considerations are presented with numerical experiments on test networks. Chapter 6 suggests a method to integrate demand for alternative-fuel vehicles and traffic flow volume. It includes a sub-model that estimates alt-fuel vehicle demand. The chapter then explores the sensitivity of AFV demand estimate to its model parameters and its subsequent effects on the results of a flow-based location model. Chapter 7 describes the developed GIS-based spatial decision support system for refueling service infrastructure planning. This chapter explains functional components of the SDSS. Chapter 8 provides conclusions and suggests future research topics.

2 LITERATURE REVIEW

This research has intellectual roots in the interdisciplinary literatures on optimal facility location modeling (Section 2.1), analysis and modeling of alternative fuels and alt-fuel vehicles (Section 2.2), and spatial decision support systems and GIS (Section 2.3). The overlapping areas of study are subsequently presented. Section 2.4 reviews optimization models for locating alt-fuel refueling stations whereas Section 2.5 discusses GIS-based approaches for estimating alt-fuel demand. Section 2.6 provides a review of the research on the SDSSs specifically for optimal facility location models.

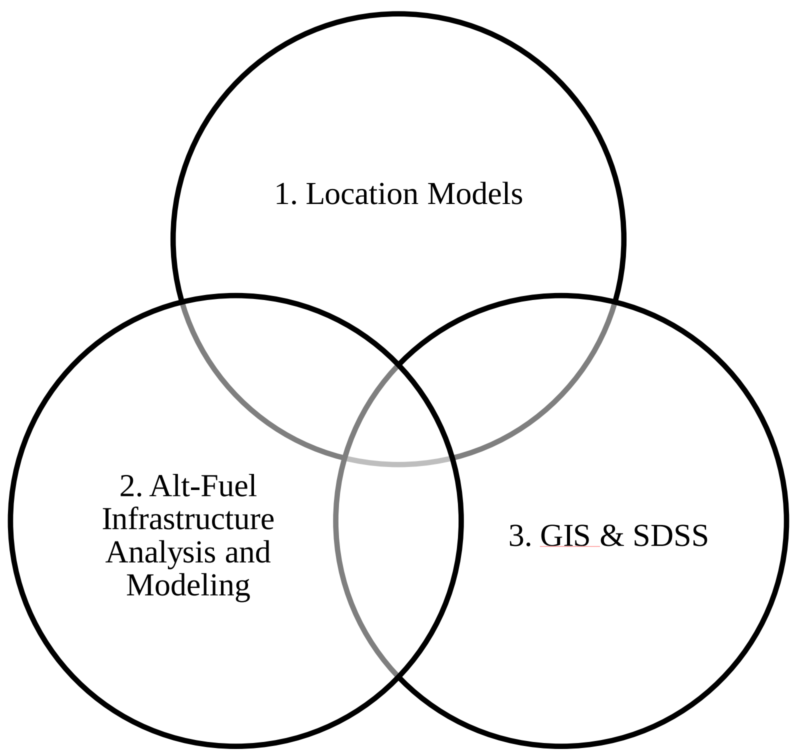

Figure 2.1 Classification of Reviewed Literature.

2.1 Classical and Flow-based Location Models

2.1.1 *Classical Location Models*

Facility location models attempt to find optimal or near-optimal locations for activities such as retail stores, public-sector facilities, and emergency facilities. Many facility location models have been developed with different objectives and constraints and thus, there is no universally accepted taxonomy. For instance, Daskin (2008) classified location models into three broad areas: covering-based models, median-based models, and other models. On the other hand, Ghosh, McLafferty, and Craig (1995) categorized retail location models into 5 groups: p-median, covering, p-choice, consumer preference, and franchise models. The models differ in their assumptions about consumer's spatial behavior, the environment in which the facilities operate, and many other aspects. The following is to provide a broad and coarse overview of location models that are referred to in later sections. Refer to other literature (Drezner and Hamacher 2002; Drezner 1995) for a more complete review. Church and Murray (2009) provide a concise and practical overview on location models with a focus on GIS.

Covering models assume that there is a critical coverage distance or time within which demands need to be served if they are to be counted as "covered" or "served adequately." Such models are typically used in designing emergency services but increasingly, they are also being used in the private sectors. Within the class of covering models, three prototypical models are the location set-covering model (LSCP), the maximal covering model, and the *p*-center model.

The objective of the location set-covering model is to minimize the number of sites needed to cover all demands (Toregas et al. 1971), whereas the max covering model (Church and ReVelle 1974) takes the number of facilities as given and solves for the locations of *p* facilities to maximize the covered demand.

The *p*-center model (Hakimi 1965) minimizes the coverage distance that is needed to cover all demands with a given number of facilities. This is sometimes referred to as the "minimax" facility location problem. On a network the absolute *p*-center model allows facilities to be located on the nodes and the links, while the vertex *p*-center model restricts sites to the nodes. (In other taxonomies, the *p*-center problem can be viewed as more closely related to the *p*-median problem, in the sense that it minimizes the maximum rather than the average distance.)

Median-based models minimize the demand-weighted average distance between a demand node and the facility to which it is assigned. Such models are typically used in public-sector non-emergency contexts or distribution planning contexts in which minimizing the total outbound or inbound transport cost is essential. The *p*-median model minimizes the population-weighted average distance of all nodes to the nearest facility, given a fixed number, *p*, of facilities (ReVelle and Swain 1970; Hakimi 1964). This very basic model can be used to locate private facilities such as retail centers, or public facilities such as libraries. An important difference between median models and covering and center models is that some demand nodes can be quite far away from their closest facility if that allows the average demand node to be as close as possible.

The fixed-charge model minimizes total location-sensitive costs, which includes the cost of building facilities and the cost of transportation between facilities and demand nodes (Balinski 1965). This model attempts to optimize the trade-off between transportation and investment costs, as the more facilities are built, the less transportation costs will be, and vice versa. It is the basis for many private-sector models, and can be extended to optimize supply chain infrastructure problems, such as where to locate factories, warehouses, and distribution centers.

The allocation-to-the-nearest-center hypothesis used in most classic location models lacks empirical support. Huff (1964) proposed a stochastic model of choice based on spatial interaction. It incorporates attractiveness of a store as well as distance for a consumer to visit the store. Attractiveness represents store characteristics such as service level, size, and charging price. There exist many different model specifications depending on how to formulate the probabilistic choice rules. In the retail location literature, multiplicative competitive interaction (Nakanishi and Cooper 1974) and multinomial logit models (McFadden 1974; Williams 1977) are commonly used for that purpose.

There are models that do not fall into either of these categories such as the *p*-dispersion model (Kuby 1987) and anti-cover problem. The *p*-dispersion model maximizes the minimum distance between any pair of facilities. This model is useful in locating franchise outlets, where minimizing the cannibalization of one outlet's market by another franchisee is desirable. The model can also be used in locating weapon supplies (e.g., nuclear weapons) where minimizing the likelihood that the destruction of any one would impact other supplies is desirable. The anti-cover problem locates the maximum number of facilities with the restriction that no two are closer than a specified distance from each other (Erkut and Neuman 1989).

2.1.2 *Location Models for Flow-based Demand*

Most of above location models involve providing service to point-based demands. Recently there has been increasing research interest in flow-based demand that is expressed by flows travelling on paths between origin-destination (O–D) pairs in a traffic network. The flow-intercepting location model (FILM) sites facilities within a transportation network and explicitly considers the flow over the network arcs. Refueling stations (Kuby and Lim 2005), convenience stores, and automated teller machines, vehicle inspection stations (Hodgson, Rosing, and Zhang 1996), and billboards (Hodgson and Berman 1997) are examples of flow-dependent facilities. Boccia, Sforza, and Sterle (2009) add three more application categories such as location of traffic counting sensors for O-D matrix estimation problems, location of inspection stations for the hazardous material transportation or for control problems, and location of variable message signs for route guidance.

Hodgson (1990) and later (independently) Berman, Larson, and Fouska (1992) designed the Flow Capturing (Intercepting) Location Model (FCLM, FILM) to locate these kinds of flow-dependent facilities. The objective of this model is to locate the facilities so as to maximize the total flow of customers that are "intercepted" during their travel. Hodgson (1990) pointed out using link traffic counts in an evaluation of retail facilities does not deal with the *cannibalization* problem, which is an self-competition problem that is caused by counting flows multiple times along nodes.

In the FCLM, an O-D pair (q) is the basic unit of demand and it exerts a demand equal to its flow. The formulation of the problem is structurally identical to the maximum-covering location problem (MCLP). In the FCLM, $\boldsymbol{N_q}$ is the set of nodes capable of capturing flow q and the flow is captured when there is at least one open facility along the path q.

Formulation of the FCLM

$$\text{Maximize } Z = \sum_{q \in Q} f_q Y_{q}, \tag{1}$$

subject to

$$\sum_{k \in N_q} X_k \geq Y_{q}, \quad \forall q \in Q, \tag{2}$$

$$\sum_{k \in K_q} X_k = p \tag{3}$$

$$X_k, Y_q \in \{0,1\} \quad \forall k, q \tag{4}$$

where:

q = a particular O-D pair (implicitly, the shortest path for each pair)
Q = set of all O-D pairs
f_q = flow volume between O-D pair q
Y_q = 1 if f_q is captured, 0 otherwise.
k = index of a potential facility location
K = set of all potential facility locations
X_k = 1 if there is a facility at location k, 0 otherwise.
N_q = set of nodes capable of capturing f_q (that is, the set of nodes on the path q)
p = the number of facilities to be located

The objective function (1) denotes the objective of the model, which is to maximize the flow volume captured. Constraint (2) denotes that a flow is captured only if at least one potential facility capable of capturing the flow (i.e., on the shortest path) is opened. Constraint (3) limits the number of facilities located to a fixed number. Constraint (4) is the binary constraint.

Wang and Lin (2009) developed a flow-based set covering model using an O-D distance matrix as the required data. Because their model is structurally similar to the set covering location model (Toregas et al. 1971), all the flow-based demand has to be covered and thus consideration on the number of flow is not required. Therefore, the model's focus was on determining a set of stations in order to capture every path in the inter-city road network.

The pick-up problem (Zeng, Hodgson, and Castillo 2009) is another extension to the FCLM so that allocation of demand is tracked and thus the model maximizes the total benefit of capturing flows in the network by considering the relative location on the path where the flow is captured. For instance, in the problem of locating pizza shops, it is beneficial for the customers to pick up the pizza as close as possible to their destinations, whereas in the problem of locating coffee shops, customers may want to pick up their coffee as close as possible to their origination of the trip so that they can enjoy it while driving.

In a review of models for flow-based demand, Berman, Hodgson, and Krass (1995) discussed the basic model and its variant extensions including most of above models, the maximal market size problem with congestion, and probabilistic flow-interception models.

The FCLM itself does not consider the allocation of demand to the open facility (Zeng, Castillo, and Hodgson In Press). They proposed a generalized flow-interception location-allocation model (GFIM) into which most current deterministic flow-interception models can be transformed. They provide a good overview on the FCLM and its variant extensions from the framework of GFIM.

2.1.3 *Extensions of the FCLM considering Deviations*

Berman, Larson, and Fouska (1995) presented several generalizations of the basic FCLM by relaxing a key assumption required by the basic FCLM: customers can make no deviation, no matter how small, from their pre-planned paths to visit the facilities. Thus locations somewhat close to pre-planned paths may be also candidates for locating the facilities. They discussed three extensions of the basic problem considering deviations from pre-planned tours: the delta coverage problem, the maximal market size problem, and the problem of minimizing expected inconvenience (Hodgson 1981).

Assume a network *G= (N, A)* where *N* is the set of nodes with cardinality *n* and *A* is the set of arcs. As a special case of the basic problem, the Delta Coverage Problem is identical to the basic FCLM except for the binary variable y'_q, which replaces y_q. They defined y'_q to be equal to 1 if there exists a node *j* on path *q* whose shortest distance to the closest facility in *K* is less than or equal to deviation Δ as in equation (5).

$$y'_q = \begin{cases} 1 \text{ if there exists } j \in q \mid d(j,k) \leq \Delta \\ 0 \text{ otherwise} \end{cases} \qquad (5)$$

where

$$d(j,k) \leq \Delta = \min_{k \in K}\{d(j,k)\}$$

Berman, Hodgson, and Krass (1995) defined the set N'_q to include the set of nodes in N_q, and all points along the arc *G* that are exactly Δ units of distance away from a node. The problem can be formulated identically to the basic problem, with the minor modification that x_k is now defined as a binary variable for any $k \in N'_q$ (instead of $k \in N_q$).

In extending the FCLM, the deviation distance was defined as the additional distance incurred when a customer deviates from the pre-planned trip. For any path *q*, they let node 1 designate the origin and node l designate the destination. They distinguished between two main cases: (1) the case in which all travel occurs on shortest paths; (2) another case in which travel in the network may visit nodes off the shortest path *q* but all nodes on *q* must be visited in the original sequence. The deviation distance $D(q,K)$ for the first and second cases is given by equations (6) – (7):

$$D(q,K) = \min_{k \in K} D(q,k) \equiv \min_{k \in K}\{d(1,k) + d(k,l) - d(1,l)\} \tag{6}$$

$$D(q,K) = \min_{j \in q, j \neq l}\{\min_{k \in K}\{d(j,k) + d(k, j+1) - l(j, j+1)\}\} \tag{7}$$

where

$l(j, j+1)$ is the length of link (*j*, *j*+1)

Based on the above definition of deviation distance, the Maximal Market Size Problem assumes that as the deviation distance gets larger, fewer customers will visit their closest facility. The function $g(D(q,k))$ represents the fraction of customers traveling on path *q* who deviate to the closest facility in *K*. The problem is formulated in equation (8):

$$\underset{k \in G}{Max} \sum_{q \in Q} f_q g(D(q,k)) \tag{8}$$

To apply this criterion, it is required to have on hand, in addition to all the distances (deviation or shortest), information on the relationship between users' demand and distances—which may not be easy to determine. It is proved in Berman, Bertsimas and Larson (1995) that when *g(*)* is a convex decreasing function, an optimal set of locations for maximal market size problem exists in *N* and thus *N* can replace *G* in equation (8).

The assumption of the Problem of Minimizing Expected Inconvenience (Hodgson 1981) is that all customers will travel from their pre-planned trips to a service facility that is closest in terms of the deviation distance. The problem is to minimize the total deviation distance traveled per unit of time as shown in equation (9):

$$\underset{k \in G}{Min} \sum_{q \in Q} f_q D(q,k) \tag{9}$$

Overall, the introduction of function $g(D(q,k))$, which denotes fractional demand at *q* to use the facility at *k,* enables users to model how demand is allocated to facilities. In other words, it opens the possibility to account for the effects of a facility at a node to flow-based demand and full coverage of demand by a facility is relaxed.

Berman and Krass (1998) and similarly Wu and Lin (2003) extended the FCLM so that competition among facilities are incorporated by merging Huff's gravity model (1964) into the FCLM. In this model, customer's utility increases with the attractiveness of the facility and decreases with the deviation distance. By modeling a "dummy" path from demand node to itself, the model accounts for both flow-based demand and point-based demand. However, these "spatial interaction" type models are typically used to analyze the competitive situation at the proposed location site, and require significantly more data and resources to apply than covering-type models. In contrast, covering-type models ignore the competitive aspect of the location decision, instead maximizing the total demand covered by all the facilities—which, incidentally, is always assumed to be 100% in the spatial interaction models.

2.2 Alternative Fuel Refueling Infrastructure Analysis and Modeling

A great deal of research and analysis has focused on infrastructure development for the transition to a new transportation system. Consideration of all related fuels and AFV technologies is beyond the scope of this research. This section focuses more on hydrogen from among the different types of alternative fuels. For an overview of general aspects of the hydrogen economy, including various possible scenarios to develop the hydrogen economy, "well-to-wheel" analysis, supply models, and lessons learned from other alternative fuels, we refer the reader to other literature (Ogden 1999b; DOE 2002; NAS 2004; Sperling and Cannon 2004; DOE 2008). The focus of this section is on the literature that estimates hydrogen demand and models hydrogen refueling infrastructure. Even though some papers and reports reviewed here do not involve optimal infrastructure modeling, investigation of the models that estimate demand should provide insights into a better understanding of spatial demand patterns, which is important in facility location modeling.

2.2.1 *Hydrogen Demand Estimation*

Hydrogen demand models in the literature incorporate a variety of assumptions and rules. For the purpose of discussing their application to hydrogen infrastructure planning they can be grouped into five categories according to modeling method employed: logistic choice models, supply chain models, system dynamics simulation models, GIS approaches, and operation research (OR) facility location models. This review focuses on the way in which each approach estimates demand.

In the lifecycle of an automobile, there are two interrelated cycles: the fuel cycle and the vehicle cycle (Tester 2005). To investigate the relationship between availability of alt-fuel stations and alt-fuel price, a nested multinomial logit analysis on a survey of stated preferences was used in a vehicle choice and fuel choice analysis (Greene 1996). This relationship was incorporated into a market transition model (HyTrans) that simulates the use and cost of alternative fuels and AFVs (Greene 2001; Greene and Bowman 2007). In the transition model, endogenous elements include fuel price, vehicle prices, and vehicle choices; however the vehicle sales target is exogenously given. Scale economy, learning by doing, and availability of fuels are the factors that generate dynamics in the model. The transition model had not accounted for spatial arrangement of alt-fuel stations until it was integrated with the work of Melendez and Milbrandt (2006) and later that of Welch (2006). The results of the integrated models were reported in Greene et al. (2008), which put more emphasis on the phased rollout of refueling stations in regions of high potential demand. A similar model and projection was suggested in Germany (Keles et al. 2008). With regard to ways of estimating demand, all variants of the model estimate hydrogen demand from the given number of AFVs by multiplying it with a constant[1], average hydrogen consumption per vehicle, which was derived from the Hydrogen Analysis Project (H2A) (Ogden 2004).

In examining the hydrogen supply chain from production center to refueling stations, Ogden (2004) built a database on the costs of delivery system components, proposed a set of base cases that depict market types and demand penetration levels, and estimated delivery costs for these base cases. The database and base cases were tested on an idealized city model (ICM) with regularly sited stations of the same size. The ICM assumes a circular shape of cities and a homogenous distribution of population and road networks. Trucks travel from the city gate to each station individually while pipelines connect each station to another. Demand is assumed to be a linear function of the number of hydrogen vehicles. Yang and Ogden (2007) revised the ICM and applied it to US cities to model the lowest-cost hydrogen delivery option from a large central production plant to vehicles. The ICM provides information on pipeline length and truck

[1] Hydrogen consumption for a vehicle: 0.72 kg/day (mature market), 0.96 kg/day (early fleet market). (Ogden 2004, 3)

travel distance for connecting a network of fuelling stations. Similar to Ogden (2004), demand is a linear function of population.

Welch (2006, 2007a; 2007b) analyzed consumer sensitivity to alt-fuel station coverage using a discrete choice model. The choice model was implemented in a system dynamics simulation model (HyDIVE) to estimate required vehicle price, vehicle makes, and fuel cost to meet DOE's (Greene et al. 2008) AFV market sales target. In the model, demand is proportional to population and a log-normal driver trip frequency distribution is assumed. In the sensitivity analysis of the choice model, station convenience attributes are measured in terms of possibility of mid- or long-distance trips (20-150, +150 mile from home) rather than percentage of existing stations. However, in implementing trip distribution, the model does not seem to consider either the limits of spatial extent constrained by the physical configuration of road network or dominant directional flow patterns that would emerge as a result of distributed urban functions. Therefore, the model's driving pattern is still similar to population distribution, which may not reflect the actual spatial pattern of trips.

2.3 Spatial Decision Support Systems

This section provides a brief review on the research trends in SDSS development with the examples of location model-based SDSSs.

A spatial decision support system (SDSS) is "a framework that integrates key computer-based components to support spatial decision making" (Densham 1991). Pivotal components in identifying an SDSS are spatial database management tools, spatial modeling tools, spatial analysis tools, visualization tools and a user interface (Densham 1994; Nyerges et al. 1997). Since a GIS is an information system capable of storing, ana1yzing, manipulating, displaying, and representing complex spatial data (Burrough 1992), it provides core functionalities for an SDSS. GIS becomes a more powerful SDSS when integrated with other domain-specific models devised for solving spatial problems. For example, facility location problems have been efficiently solved by integrating GIS and optimization-based models (Church 2002; Church and Murray 2009; Murray 2010). Moreover, a modern GIS is equipped with an array of powerful spatial analytic capabilities and this enables its contribution to go beyond an input generator or an output visualization tool (Murray 2010), including its potential to represent facilities and demands in various geometric objects (Miller 1996). However, GIS can serve as an SDSS without the addition of any domain-specific models, as illustrated by a GIS for suitability analysis (McHarg 1969), which identifies feasible potential facility locations, can be easily performed utilizing map algebra (Tomlin 1990) in GIS.

2.3.1 *Research Trends in SDSS Development*

Many prototype SDSS are introduced in the literature and each of them is designed to solve domain-specific problems. Here, research trends are classified according to the main component that the research aims to develop or contribute rather than by application domains.

2.3.1.1 Interoperability

Developing SDSS by definition involves integration of multiple information systems or models. Since the adoption of GIS as a platform for SDSS, because of its lack of analytic and modeling capabilities in GIS, integration of separate systems by means of data exchange has been a main research agenda in the GIS community (Goodchild 1991; Fedra 1994; Abel, Kilby, and Davis 1994; Steyaert and Goodchild 1994; Jankowski 1995; Goodchild 1987, 1990; Goodchild et al. 1992; Anselin and Getis 1992; Anselin, Dobson, and Hudak 1993; Anselin and Bao 1997; Church, Loban, and Lombard 1992; Fotheringham and Rogerson 1994; Openshaw 1992; Batty and Xie 1994a, 1994b; Densham and Rushton 1991; Ralston, Tharakan, and Liu 1994; Longley and Batty 1996).

The levels of integration between GIS and analytical models can take a loose coupling strategy where GIS and models are linked using a disconnected file exchange mechanism, a tight coupling that provides a common user interface with shared files being seamlessly exchanged under the scene, and a full integration into GIS with shared memory and a common file structure (Fedra 1993). GIS The full integration of location model and GIS is rare because the application domains for GIS are broad (Church and Murray 2009) but there are some commercial software where widely-used heuristic algorithms (Teitz and Bart 1968; Densham and Rushton 1992) are included in a basic analytic tool. However, in most cases one encounters and deals with interoperability of different systems in developing a SDSS for location problem solving.

Interoperability is a broader term that refers to integrating independent and heterogeneous systems. It spans the data modeling levels from semantics to data structures as well as encompasses hardware, software, and network protocol compatibility. Research on GIS interoperability tends to focus on the highest levels: data model and application semantic interoperability (Bishr 1998). Data model interoperability ensures that users have access to a virtual global data model that abstracts all specific data models in underlying remote (spatial database) systems. Application semantic interoperability allows seamless integration among systems without requiring prior knowledge of the data assumptions and semantics.

Recent advancements in information technology (e.g. component based software, visual object-oriented programming language and analysis, and open source libraries) enable system integration between desktop platforms much easier, and thus this problem is becoming less significant (O'Sullivan and Unwin 2003; Argent 2004; Miller and Shaw 2001). However, in an internet-based environment, interoperability is again an important research theme (Rinner 2003).

2.3.1.2 Geographic Visualization

SDSS require interactive/dynamic data manipulation and visual displays of different what-if scenarios. Geographic visualization (GV) techniques encompass a wide range of uses, including exploration, analysis, synthesis and presentation of geographic data (MacEachren 1994). Visualization of uncertainty is considered to be helpful to enable SDSS users to cope with uncertain information (MacEachren et al. 2005). Even though empirical results provide mixed results in relation to the role of visualization, more efforts to achieve agreed strategies for effectively visualizing uncertainty are required. This should be accompanied by further understanding on human cognition and perception on spatial phenomena.

Integration of SDSS with advanced geographical visualization tools provides more insights into the problems and alternatives. More specifically, GV techniques can be used in *before-run exploration* stage (Fotheringham 1998) to gain insights on the problem and *after-run exploration* stage to evaluate conflicting decision alternatives. The need for such tools becomes more critical in a collaborative decision making environment (Armstrong and Densham 2008).

2.3.1.3 Collaborative SDSS

Spatial decisions are often made by groups of people, involving them in collaborative efforts. Collaborative SDSS (CSDSS) should include consensus-building component that typically requires technology for interactive geographic visualization, information sharing, electronic voting, data transmission, and computer conferencing (Ahearn and Osleeb 1993; Nyerges et al. 1997; MacEachren 2001; MacEachren et al. 2005). CSDSS is often developed in a web-based environment, since public access to SDSS is one of the main motivations for developing a web-based SDSS (Rinner 2003). Such technologies and new collaborative environment could not be fully utilized until solutions or alternatives are promptly provided. Thus, even though CSDSS may use a robust heuristic solution approach to find solutions efficiently, more powerful computing resource would be often required to solve large problems.

2.3.1.4 Geocomputation and Heuristics

Geocomputation refers to methods that heavily rely on the existence of computer power for the analysis of geographic information (O'Sullivan and Unwin 2003). Many geocomputation methods are inspired by and derived from artificial intelligence techniques. They include expert systems, artificial neural networks, and genetic algorithms. These techniques are used in SDSS to mimic human decision processes and provide decision rules and criteria weighting scheme.

Given that SDSS should deal with large problems in a reasonable time, the heuristics that are developed for relatively small location problems in a lab environment may not perform as well as preferred. Thus, testing of heuristics on real-world data is essential. These needs become clearer when considering the requirement of fast solution provision for CSDSS. Parallel super computer, a geocomputation approach, exists at one “extreme” in solving such problems (Clarke 2003). However, it seems that the research trend is development and testing of heuristics for the size of problems that SDSS and CSDSS will encounter. Development of heuristic solution approach for such large problems using genetic algorithms is one of the areas that research interest converges (Lim 2007; Xiao 2008; Zeng and Church 2009).

2.3.1.5 Uncertainty

SDSS utilizes spatial data extensively, which naturally bear uncertainty. Geographers have identified sources of spatial data error (Goodchild and Gopal 1989; Burrough and McDonnell 1998; Unwin 1995) and propagation of error (Heuvelink 1999). If the input data have uncertainty, reliability of the results needs to be tested. The normal approach is through repeated numerical simulation (Monte Carlo simulation), by which random numbers and probability are used to iteratively solve the problems. In this way, deterministic models effectively turn into stochastic models. Another element that is subject to uncertainty is the parameters in the model. Model users need to conduct some form of sensitivity analysis, examining each parameter in turn to see how much influence it has on the results (Longley et al. 2005).

Visualization of uncertainty may be helpful in decision-making. One way of visualizing the uncertainty in a location model is to show buffers around model-selected sites indicating the uncertainty of site locations. In an attempt to measure the effect of inexact siting prescription, Murray (2003) perturbed the identified sites within a given buffer radius and compared the objective values with optimal ones. Analytic efforts to address uncertainty in location modeling is reviewed in Murray (2003).

Instead of reporting or visualizing uncertainty, SDSS can utilize such models that domain-specific scientists have developed to deal explicitly with inherent uncertainty in the models. For example, in the literature of facility location, dynamic models and stochastic models are an attempt to locate facilities over a specified time horizon and to take into account the stochastic nature of real-world data (Owen and Daskin 1998; Snyder 2006). Dynamic models are concerned with uncertainty related to planning for future conditions, while stochastic models are for uncertainty due to limited knowledge of model input parameters. Research on stochastic location problems can be broken down into two primary approaches. In a probabilistic approach, probability distributions of random variables are explicitly considered, while in a scenario planning approach, a generated set of possible future variable values are considered. An example of robust optimization is illustrated in Church and Murray (2009). It is a reformulation of one classic location model, the *p*-median problem, in such a way that multiple demand scenarios are weighted, and then the model finds the best one from the different scenarios.

As a response to the uncertainty, in the decision science literature there is a growing interest in shifting the focus from a predictive (consolidative) approach to an anticipatory (exploratory) approach for long-term policy analysis (Bankes 1993; Lempert, Popper, and Bankes 2003). The new approach changes the question from "What will the long-term future bring?" to "How can we choose actions today that will be consistent with our long-term interest?" Lempert, Popper, and Bankes (2003) proposed four key elements in a successful long-term (35 to 200 years to the future) policy analysis: a broad range (hundreds to millions) of scenarios, robust (not necessarily optimal) strategies to deal with the plausible futures, robustness achievement while evolving over time in response to new information, and interactive exploration of the wide range of plausible futures.

2.4 Optimization Models for Locating Refueling Stations

Many approaches for modeling and analyzing alternative fuel refueling infrastructure reviewed in the previous section (See section 2.2) deal with diverse modeling aspects in alt-fuel station development. However, they do not provide a solution that satisfies a given set of conditions by examining all possible combinations of locations. This section reviews optimization models for locating refueling stations. It corresponds to the overlap of the sets in Figure 2.1 representing the literature on location science (Section 2.1) and the literature on alternative-fuel infrastructure (Section 2.2). Within the intersection of those two sets of literature are the optimal facility location models specifically for alt-fuel stations. These are divided here into two groups depending on the geometric representation of demand: models for point-based and flow-based demands.

2.4.1 *Models for Point-based Demand*

Bapna, Thakur, and Nair (2002) used a multi-objective model to locate unleaded gasoline stations in India. One objective minimizes the sum of travelers' costs and station investment costs, while the second maximizes the population on enabled links. These objectives are optimized subject to a constraint that requires the resultant sub-graph to be able to span the network connecting all nodes given the driving range of vehicles, that is, a minimum spanning tree constraint.

Bersani et al. (2009) took into account competition by incorporating the Huff model in a multi-objective model. The highly non-linear model minimizes a petrol (gasoline and unleaded petrol) station company's conversion (fixed and storage) cost to additionally provide hydrogen while maximizing the demand in a competitive environment. Demand for the new fuel, hydrogen, is assumed to be geographically even and proportional to gasoline sales. Whereas they assumed that competitors' sales data were available, without detailed information about the competing company's plan for hydrogen distribution network, the competitors' station that is the closest to each selected station was assumed to be converted to provide hydrogen and "the optimal set of chosen stations has no ability to attract those new customers who are usually served by competing companies." (Bersani et al. 2009, 58)

Many median-based models have been used for siting refueling stations. Goodchild and Noronha (1987) developed a model to decide which gasoline stations of a firm to keep open or close to maximize the market. They recognized that refueling trips are composed of a mix of traffic-originated demand and population-originated demand. With the limited information, consumer's spatial behavior with respect to actual or hypothetical distribution of facilities was assumed to be linear to distance. As a result, their model became a *p*-median problem that minimizes the two different distributions of demand.

Other researchers have continued to use the *p*-median model. Chan, Padmanabhan, and Seetharaman (2007) reported on government use of the *p*-median model to locate gasoline stations in Singapore. Lin et al.(2008) proposed the fuel-travel-back model, which uses link traffic as the weight and locates stations to minimize the sum of average weighted distance. The model is structurally identical to *p*-median model with link traffic as the weight at each road intersection.

Analysis by Nicholas, Handy, and Sperling (2004) using a *p*-median approach determined the number of stations by the average driving time per refueling trip. Their model was similar to the *p*-median model except that the model added two stations at a time until it reached the number of stations with which the station network can provide given accessibility to the customers which were measured by average driving time to the nearest station. In this way, the *p*-median approach could provide station locations and numbers to build. They suggested that 10% of stations in Sacramento County would be within 3 minute driving distance from home.

It is important to note that *p*-median based models tend to locate stations closer to population centers or link traffic centers. In addition, if population is used as a weight, the implicit assumption is that drivers would make special trips for refueling. On the other hand, if link traffic is used as the weight, the model partially accounts for drivers' behavior to refuel when needed while driving. However, the link traffic might be doubly counted by more than one station along the path, as pointed out by Hodgson (1990), which could lead to duplicative siting and cannibalization of a station's demand by other stations. In addition, given the limited range of AFVs, p-median based models may not site stations to enable a long inter-regional (e.g. LA to San Francisco) trip. This is exactly why location models for flow-based demand is needed for locating stations of range-limited alternative-fuel vehicles, which is discussed in the next section.

2.4.2 *Models for Flow-based Demand*

Wang and Lin (2009) developed a flow-based set-covering location model using an O-D distance matrix as the required data. Because their model is structurally similar to the location set covering model, all the flow-based demand has to be covered and thus consideration on the amount of flow is not required.

Kuby and Lim (2005) extended the FCLM to locate a given number of facilities to maximize the number of flows they can refuel. The two models are similar in that both avoid multi-counting of flows along the nodes that paths of the flows pass through. The major difference between the two is the need for multiple stops. The FCLM counts a flow as captured if a facility is located anywhere along the path of the flow because one stop will satisfy consumers' need, whereas the FRLM regards a flow as refueled only when a satisfactory number of facilities (stations) are spaced properly along the path because consumers on the path need multiple stops. The development intent of the FRLM was to deal with location of refueling stations for range-limited vehicles such as alt-fuel vehicles. In the FRLM, therefore, vehicle range is the key element. A limited driving range means that one facility anywhere on the path cannot necessarily succeed in refueling a trip on a given shortest path—a combination of facilities may be needed. The subscript *h* is introduced to represent a combination of facilities *k* that is able to refuel path *q*. With the combination *h*, variable v_h is also introduced which equals 1 if all the facilities in combination *h* are open, and 0 otherwise:

Formulation of the FRLM

$$\text{Maximize } Z = \sum_{q \in Q} f_q y_{q,} \tag{10}$$

subject to

$$\sum_{h \in H} b_{qh} v_h \geq y_q \quad \forall q \in Q \tag{11}$$

$$a_{hk} x_k \geq v_h \qquad \forall h \in H; k \mid a_{hk} = 1 \tag{12}$$

$$\sum_{k \in K} x_k = p \tag{13}$$

$$x_k, v_h, y_q \in \{0,1\} \quad \forall k, h, q \tag{14}$$

where:

q a particular OD pair (implicitly the shortest paths for each pair)

Q set of all OD pairs

f_q flow between OD pair q

y_q = 1 if f_q is captured, 0 otherwise.

k a potential facility location

K set of all potential facility locations

x_k = 1 if there is a facility at location k , 0 otherwise

p the number of facilities to be located

h index of combinations of facilities

H set of all potential facility combinations

a_{hk} = 1 if facility k is in combination h, 0 otherwise

b_{qh} = 1 if facility combination h can refuel OD pair q, 0 otherwise

v_h = 1 if all facilities in combination h are open, 0 otherwise

The objective function (10) locates p facilities to maximize the total flow that can be refueled. Constraints (11) ensure that for an O-D pair q to be open, at least one combination of facilities h has to be open. Determination of the eligible combination is exogenous in that it is generated outside the model and depends on the network structure and the given vehicle range. An algorithm to generate the combination h for each path q and other considerations such as obtaining a tighter set H by removing supersets are discussed in Kuby and Lim (2005). Constraints (12) bind v_h to one only after all the facilities in combination h are open. Constraint (13) requires exactly p facilities to be open. Constraints (14) are integrality constraints. The facility location variables x_k are defined as binary variables in (14). Kuby and Lim (2005) discussed how the other two variables (v_h and y_q,) can be relaxed so that they become continuous variables with an upper bound of 1, which will result in great reduction in the number of binary variables, and yet the model still yields an all-integer solution.

The elegantly simple formulation of the FRLM may not reveal the computational effort of obtaining the set *H* of all feasible combinations of facilities but it could be substantial especially when considering the possible valid combinations for the paths with many nodes. The algorithm developed by Kuby and Lim (2005) generates the valid facility combinations of refueling stations that enable drivers to complete their round trips between an O-D pair without running out of fuel given the vehicles' range. From the list of all possible combinations of stations on a path, they provide the following principles for generating the valid combinations to include in the model: a valid combination of stations should enable round trips; each trip starts with a half tank full unless there is a station at the origin because if one can reach the next refueling station without a problem with half tank from origin, he/she, on the way back, should be able to travel from the station and origin; only one direction of a round trip needs to be evaluated for refueling validity because of the above two conditions; and supersets of other valid combinations should be removed to reduce the number of valid combinations. The algorithm first generates shortest paths for all O-D pairs and for each pair it obtains the node sequence along the path. It then generates a list of all possible combinations of the nodes on the path, and thus the size of this list is $\sum_{k=1}^{n} C_{k}^{n}$, where $n\ (>1)$ is the number of nodes on the path. The algorithm determines whether each combination can refuel the given path and removes one from the list unless it can refuel a vehicle with the given range. The remaining range in a vehicle is set at half the vehicle range unless there is a station at the starting node. It moves to the next node in the sequence while subtracting the link distance traveled from the vehicle's remaining range. The remaining range becomes full when the visiting node already has a facility. If the round-trip taking the shortest path of the O-D pair successfully ends without running out of fuel, the path is considered feasible with the station combination. After all combinations are evaluated for the path, the algorithm removes combinations that are supersets of other valid combinations. The algorithm runs for all the paths and outputs a list of path q and its corresponding set of facility combination h that can refuel the path q. Note that there is a many-to-many relationship between the set Q and set H. The innovative component of the FRLM is the use of facility combinations to refuel network paths. This element is devised because the FRLM is considering range-limited vehicles, which hold true for AFVs such as hydrogen fuel cell and battery electricity vehicles.

Kuby and Lim (2007) proposed methods to add candidate locations along arcs to improve the FRLM's solution. As a covering based model, the FRLM incorporates limits in the extent of a facility's coverage. Nodal candidate locations, therefore, may not constitute a finite dominating set from which optimal solutions are guaranteed to be obtained (Hooker, Garfinkel, and Chen 1991). For the max cover model, Church and Meadows (1979) suggested nodes be augmented with network intersection points, which were the cover distance away from demand nodes. Even though the number of candidate sites required to ensure optimal solutions is much larger than the number of demand nodes, the problem is still much reduced one for not having to evaluate an infinite number of possible sites anywhere on the network. For the FCLM, nodal locations constitute a finite dominating set, because a flow that is captured by a mid-link location can also be captured by a facility by a node on the flow path (Hodgson 1990; Berman, Larson, and Fouska 1992). However, this does not apply to the FRLM, where some flows can only be refueled by mid-link locations because of the model's consideration on vehicle's range and combination of facilities. In other words, nodes do not form a finite dominating set in the FRLM. To deal with this, Kuby and Lim (2007) proposed three methods to add candidate locations along arcs. The first method was to add mid-path segments. The other two methods (Kuby, Lim, and Upchurch 2005) employed *p*-dispersion (Kuby 1987) approaches to disperse added nodes along arcs of a network. Added nodes split an arc into sub-arcs. One approach used a minimax method, while the other used a maximin. With the minimax approach, nodes were added so that they minimized the maximum sub-arc length in the network, whereas the maximin approach ensured that added nodes maximized the minimum sub-arc length.

Upchurch, Kuby, and Lim (2009) extended the FRLM to consider capacity of facilities. Several assumptions in FRLM are relaxed. For example, the location variable x_k represents a standard refueling module that a station can install and replace, and thus it becomes an integer variable rather than binary to account for possibility of adding multiple modules in a location. To account for the possibility that a combination of facilities h not providing enough fuel for customers because of the capacity constraint, multiple h may be required for a flow and the fraction of the flow refueled by each combination also need to be tracked. For this, a continuous variable, y_{qh}, is used to represent the flow allocation to combinations of facilities.

To solve the FRLM optimally, the set of all combinations *H* has to be identified for each O-D pair *q*, if a combination *h* can refuel the path *q*, and then it is tested whether a combination *h* has any tighter subset that can also refuel the same path. This process is computationally very complex, let alone the complexity of finding optimal solution for mixed integer formulation by using branch and bound algorithm. In an experiment with a subset of real-world road network, Lim and Kuby (2010) found that generation of all combinations for just 39 O-D paths took 13 hours[2]. Therefore, Lim (2007) developed three heuristic algorithms (greedy, greedy with substitution, and genetic) for an integration of the FRLM and GIS. These heuristics were used to propose strategic locations of hydrogen refueling stations in the state of Florida (Kuby et al. 2009) with real-world data.

Capar, Kuby, and Rao (2010) provided a new MILP formulation for the FRLM that exploits the logics of Kuby and Lim (2005)'s algorithm that generates the feasible combinations for a path. They added new variables to indicate two conditions at the same time: whether there is an open station at a node on a specific path, and whether a vehicle that was refueled at the node can reach next

[2] In addition to it they mentioned "*Of these 39 paths, the one with the most arcs has 23 arcs. However, even in this medium-sized network, there are 900 paths that have at least 23 arcs, with a maximum of 59 arcs*." (Lim and Kuby 2010, 57)

open station along the path. In addition, newly added constraints ensure that the sub-path from origin to the node in evaluation can be traversed without running out of fuel considering the relative location of the node (origin, in the middle, or near at the destination of a path) and existence of station at the node. They also provided a strategy to improve the solution time by adding low-bounds and by prioritizing the nodes that were included in the previous solutions. Their new MILP formulation resulted in remarkably fast solution time yet with a substantially increased number of constraints.

2.5 GIS-based Approaches for Hydrogen Demand Estimation

This section of the literature review corresponds loosely to the intersection of the sets in Figure 2.1 representing the literature on alternative-fuel infrastructure (Section 2.2) and the literature on SDSSs (Section 2.3). The term "loosely" is used because it includes GIS-based approaches that may not quite rise to the formal definition of SDSS, and it focuses mainly on hydrogen demand estimation. GIS-based approaches for estimating hydrogen demands generally used two types of data: existing gasoline stations and demographics.

2.5.1 *Use of Gasoline Station Data*

Based on the data of existing conventional stations, a series of studies have focused on various aspects of size and number of refueling stations needed. The approaches employed for this kind of analysis are not only unique but diverse and exploratory, and the proposed results may be valuable for refueling network planners.

Melaina (2003) proposed three approaches to estimate alt-fuel station numbers. The first approach is based on the percentage of existing stations. It was assumed that 5% of high-volume stations will initiate the transition and 15% of all census stations for the next stage. In earlier work, Kitamura and Sperling (1987) provided a survey result that a 10% share of existing gasoline stations would make fuel availability a minor issue when customers are choosing AFVs. Melaina's second approach is based on the ratio of total stations' land area to the total of major metropolitan land area. Since each station was assigned the same land area, the difference between the two is attributed to the number of stations. The third approach is spacing stations on the road network at regular intervals. It was suggested that for rural areas the interval for development phases 1 and 2 should be 50 miles and 20 miles, whereas for urban areas they were 20 miles and 10 miles, respectively. Based on these approaches, it was estimated that 4,500 ~ 17,700 stations would be needed to initiate the transition. The methods only deal with number of stations and do not identify where those stations should go, nor do they estimate demand.

Based on existing network gasoline stations, Melaina and Bremsona (2008) suggested a method to determine a sufficient number of stations for urban areas. It is a function of population density, with higher density cities having a denser network of stations. A power function was specified from observing high correlation between station density and population density. Assuming a low-density station network should provide sufficient coverage, a curve that fits those cities with relatively low-density station networks was derived. They estimated that some 51,000 urban stations would be required to provide this sufficient level of coverage to all major urban areas and this number was 33 percent less than their estimate of total urban stations.

Showing that gasoline station size has regularities in US urban areas, Melaina (2005) proposed an simple point aggregation method for designing an ideal refueling network. The method used GIS to ensure a given “dispersion” distance between aggregated points that represent stations. Melaina and Bremson (2006) argue that idealized station network rollout scenario would favor refueling availability over competitive advantages of stations. In other word, each station’s competitive advantage might be compromised to achieve or provide a satisfactory level of coverage to customers. Thus, they designed an idealized refueling network using a modified Melaina (2005)’s algorithm, from which they estimated the cost to provide adequate refueling availability. Even though regularities in rank-size distribution are commonly observed in many empirical distributions, using it for planning purpose is innovative especially when such a scheme is incorporated with dispersion, an important design principle.

2.5.2 *Use of Demographic Data*

Ni et al. (2005) used GIS to determine hydrogen center demands given a certain penetration rate in the vehicle stock in a region. Instead of using city boundaries, demand centers are identified on the basis of population density, car ownership, market penetration rate, and fuel use. Certain areas whose demand density is higher than a given threshold are selected and clustered using a buffer. After aggregating hydrogen demand within a cluster, only a subset of clusters whose demand is higher than a threshold for maintaining a station remains. Because all the metrics used in estimating hydrogen demand are constant except for population density, this method essentially identifies population centers. This clustering may also overestimate regional demand by aggregating all hydrogen demand of the areas that fall within a buffer.

One of the most important pieces of research underlying this dissertation is by Melendez and Milbrandt (2005), who developed a plan for a national hydrogen network to make interstate trips possible by regularly placing stations along highways in areas of high potential hydrogen demand. In as series of analyses, Melendez and Milbrandt (2006) identified the areas of highest FCV demand, and then assessed how many stations would be needed to fuel these vehicles and where they might realistically be located. As a first step, a literature search and interviews with vehicle technology experts were conducted to identify key demographic attributes affecting hydrogen vehicle adoption in consumer markets. Each attribute was standardized by assigning a classification rank value, and then weights were assigned to each attribute to calculate a total rank score. The rank score is expected to represent the relative likelihood of a consumer's purchasing a hydrogen vehicle.

It is worth noting that their method is essentially a suitability analysis (McHarg 1969) using map algebra (Tomlin 1990), which have now become standard practices in GIS. Suitability analysis is mainly used for a raster data format, where continuous space is represented in discrete forms of regularly spaced points or polygons (Burrough and McDonnell 1998). In fact they converted nationwide census tracts into a raster format by applying a 20 by 20 mile grid, which arguably implies that the household is evenly distributed within each grid.

From this analysis, they identified 20 urban areas with the highest potential hydrogen vehicle demand. It is important to this research because it seems to be the only analysis that took into account geographically uneven hydrogen vehicle demand, and because it was later employed in other research. Greene et al. (2008) located hydrogen stations in the identified 20 areas, and Kuby et al. (2009) adapted their weighting method for use in analyzing initial hydrogen stations for Florida.

One of the analytic issues in estimating consumer demand is the possibility of errors introduced by integrating data that are based on different zoning systems such as census tracts, traffic analysis zones, and regularly spaced polygons. The fundamental reason for this problem is the fact that continuous space is usually represented in discrete forms, which results in loss of geographic details (Goodchild 1979; Murray 2003). Given that any zoning system cannot contain all the details, a method that reduces or eliminates errors in integrating attributes from different zoning systems is required. Goodchild and Lam (1980) referred to this as the areal interpolation problem and suggested a straightforward method. Furthermore, Goodchild, Anselin, and Deichmann (1993) discussed and suggested a framework that utilizes complementary information to derive control zones where a uniform distribution of source zone attributes is assumed. Gan (1994) proposed that network density can be used as the complementary data.

2.6 Integration of SDSS and Optimal Facility Location Models

This section reviews literature in Figure 2.1 representing the intersections of the literatures on optimal facility location models (Section 2.1) and SDSSs (Section 2.3). In location modeling and analysis, SDSSs have been successfully developed for solving complex facility location problems including area and corridor location problems and location-routing problems. The role of GIS in SDSSs ranges from an input generator or important component to the sole platform to solve the problem by itself.

2.6.1 *Coupling-based Integration*

Church, Loban, and Lombard (1992) employed suitability analysis to represent the impact of an area being included in a corridor. The suitability scores were provided as an input in solving the corridor location problem formulated as a multi-objective optimization problem. The interface designed in a GIS environment showed both decision space and objective space to allow exploratory analysis of the solutions.

Yeh and Chow (1996) applied a *p*-median heuristic solution approach (Cooper 1963, 1967) in planning open space in Hong Kong. In their system, spatial data were exported to an external custom program that runs the heuristic.

Camm et al. (1997) integrated MapInfo and LINDO using a loose coupling strategy. They divided their problem into two components: distribution center location and product sourcing problems. The former was formulated as an uncapacitated fixed charge location problem and the latter as a transportation problem.

Johnson (2001) developed a SDSS for housing mobility program planning that was based on ESRI MapObjects and ILOG-CPLEX. The problem was modeled as a multi-objective problem, with a “center” (minimax) equity objective and a median objective that minimizes the weighted sum of total economic impacts of the housing mobility to certain groups. The two output types (objective values and decision variables) were displayed at the same time. The objective values were displayed as either a value path (Revelle 1987) or a tradeoff surface to enable the decision makers to explore the conflicting objectives.

Ribeiro and Antunes (2002) developed an application based on ESRI MapObjects that internally used Xpress-MP to solve uncapacitated fixed charge, capacitated fixed charge, and p-median problems. The application was intended to support decisions for planning public facilities such as hospitals and schools.

Bender et al. (2002) developed an open source library of location algorithms (LoLA), some of which can be loosely integrated with ArcView GIS through a menu developed with Avenue script. The link between LoLA and ArcView allows the user to solve *p*-median, *p*-center, and uncapacitated fixed charge location problems using exact and heuristic solution algorithms. Standalone LoLA provides more models and algorithms for planar and network problems. The library is extensible in that the source code is open to public who may add location models and algorithms to it.

Liu, Huang, and Chandramouli (2006) integrated an ant colony heuristic algorithm with ArcGIS to suggest locations for fire stations. They formulated the problem as a multi-objective optimization problem that reduces the response time, ensures suitable distance among fire stations, and maximizes the coverage by the station. For simplicity of computation, they converted vector data into a raster format.

Snediker, Murray, and Matisziw (2008) developed a decision support system for supporting network infrastructure protection planning. The system was composed of ESRI MapObjects, ILOG CPLEX, and a charting library (GigaSoft ProEssentials). With the system, network planners can generate interdiction scenarios, assess the impacts of the interdiction by using indices or visually exploring the impacts, and derive protection strategies. The system has the feature to generate all possible interdiction scenarios, and the network elements related to the user-selected scenarios can be interactively visualized. The effect of reinforcing a network element can also be visualized while a table reports the reinforcement effect in terms of impact difference.

Murawski and Church (2009) formulated the maximal covering network improvement model (MC-NIP) to improve the accessibility to rural health services and took a loose coupling strategy in solving the problems. ArcGIS was used to export data into a spreadsheet file and then it was converted to CPLEX model to solve optimally. The results were imported back to GIS to visualize as a map.

2.6.2 *Advanced Use of GIS for Location Modeling*

Modern GIS provides not only input data but valuable information to location analysis and modeling (Church 2002; Murray 2005; Church and Murray 2009; Murray 2010). This section provides recent research trend where GIS is used as a spatial analytic tool in efficiently identifying and providing valuable spatial information required for solving complex location problems. Refer to Murray (2010) for a more complete review.

Gerrard et al. (1997) used GIS to modify spatial data in selecting reserve sites. They modified their reserve site selection model into a special form of MCLP (Church and ReVelle 1974) and pre-processed the publicly available data into a format that would work with ArcInfo's internal location analysis tool.

Basic GIS functions such as buffer generation and Voronoi diagram generation have been extensively used to provide enhanced input for solving problems for continuous space. Suzuki and Okabe (1995) provided a heuristic to solve a continuous space p-center problem by iteratively generating Voronoi diagrams. Murray and Kim (2008) developed a GIS-based approach to identify enough cliques required for efficiently solving an anti-covering location problem.

Spaulding and Cromley (2007) used GIS operations (service area and buffer) to generate inputs for solving the maximal capture location problem (ReVelle 1986). They represented the demand as areas delineated by a given network distance rather than nodes and investigated the spatial property of the problem. They formulated the problem and exploited the output data that were generated from iterative runs of GIS operations. In addition, they utilized auxiliary data in mitigating aggregation errors while estimating demands for newly generated zones.

Zeng, Castillo, and Hodgson (2010b) suggested a framework to aggregate O-D flow data for use in the FCLM. They integrated ArcGIS, CPLEX, and heuristics in aggregating flow data. Their iterative procedure systematically removes O-D pairs with lower flow volumes; removes nodes with low passing flows; identifies nodes with higher probability of being included in the optimal solution; and then finally solves the problem to optimality when the size is small enough. They exploited the property of FCLM where high-flow nodes are good candidates for optimal solution.

Classical covering location models: LSCP, MCLP, and the Backup Covering Location Problem (BCLP) were reformulated by Murray (2005), Tong and Murray (2008), and Kim and Murray (2008) respectively with the help of analytic capabilities of GIS. Each developed a new location model that is less sensitive to scale and unit definition variation, which is collectively referred to as the modifiable areal unit problem (Openshaw and Taylor 1981).

3 STATEMENT OF RESEARCH

3.1 Research Needs

This dissertation research is rooted in the three literatures reviewed in Chapter 2: optimal facility location models, alternative-fuel infrastructure and demand analysis, and spatial decision support systems. In particular, this research takes place in the area of overlap of all three literatures (Figure 3.1). The literature review shows that flow-based location models for locating alternative-fuel stations need enhancements in four dimensions: (1a) drivers' deviations from their shortest paths, (1b) efficient solution approaches for the deviation problem, (2) incorporation of geographically uneven alt-fuel vehicle demand estimates into path flows, and (3) integration into an SDSS to help decision makers by providing solutions and insights into developing alt-fuel stations.

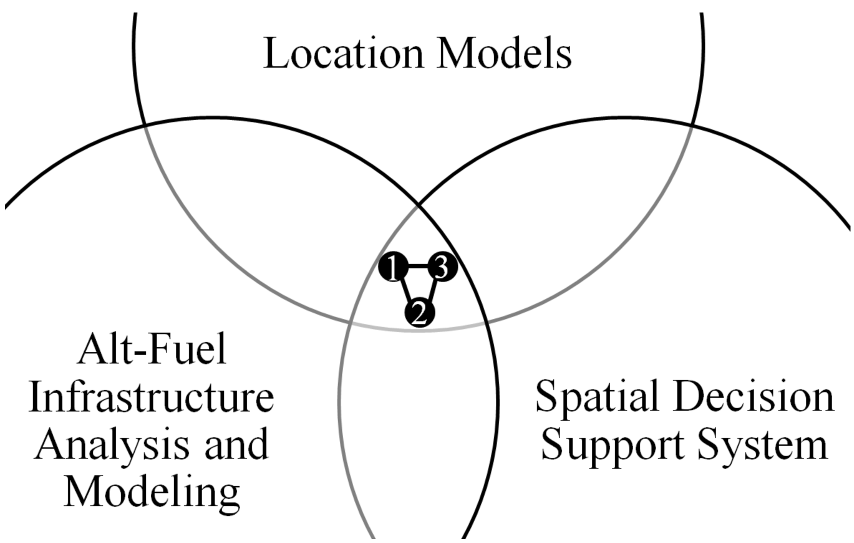

Figure 3.1 Contributions of the dissertation.[a]

[a] (1) represents the flow refueling location model (1a) and heuristic solution method (1b); (2) represents the uneven demand model for path flows; and (3) represents the SDSS for the entire model including (1) and (2).

The first major gap is that, despite the FRLM's ability to model driver behavior more realistically by basing it on drivers stopping along their way rather than making trips from home to station and back, there is still room to make the driver behavior in the model even more realistic. Most prominently, the FRLM does not account for the necessary deviations that many early AFV adopters will need to take when the network of station is sparse. Therefore, an extension of the FRLM that considers deviation is necessary. An important input for the new model is to potentially include *all* deviation paths between O-D pairs. Given that the problem of finding all possible paths between an O-D pair in a real world network is hard to solve, the generation of feasible deviation paths requires additional constraints that reflect more realistic assumptions on drivers' refueling behavior in a sparse refueling network. In addition, without available empirical data as to how many AFV drivers will deviate from their pre-determined paths and how far they would do so for refueling purposes, an explorative model taking into account this uncertainty is required. With such a model integrated into an SDSS, planners could perform experiments with different upper bounds of deviation distance or apply different functional forms to fit the decreasing willingness of drivers to deviate from their paths as deviations get larger. Both of the above inputs need to consider vehicle range at the same time. With these requirements satisfied, flow-based models will become even more realistic and more widely applicable. It is expected that allowing drivers to deviate from their shortest paths will increase each station's utilization level, and in turn it will result in less investment costs and a more successful transition to a new transportation system.

Another gap in the literature is an absence of efficient heuristic solution algorithms for the suggested flow refueling location model that allows for drivers to make *any possible deviation* from their shortest path that is within some maximum user-specified deviation. While a mixed-integer programming formulation of the problem can lead to optimal solutions, the required computation time can be prohibitively long, and thus application of the approach to a real world network will be limited when its size is large. Heuristic algorithms provide sub-optimal solutions within a reasonable time. Lim (2007) proposed heuristic approaches for the FRLM. A heuristic for the FCLM with deviation cases was suggested in Berman (1995). The heuristic in Boccia, Sforza, and Sterle (2009) was developed for the FCLM with inspection case. However, given that no one has published a model for the FRLM with deviations, it is not surprising that there is also no reported heuristic method for the FRLM with deviation cases. A heuristic for the FRLM with deviation can be directly used to solve problem instances of original FCLM (Hodgson 1990; Berman, Larson, and Fouska 1992), FCLM with deviation (Berman, Bertsimas, and Larson 1995), and the original FRLM (Kuby and Lim 2005). In addition, given that there is an absence of a generic heuristic to solve any flow-based demand location models, the new heuristic might be modified to solve flow-based models generally, if not for all.

The third gap is the absence of a method to incorporate NREL's raster-based demand estimation model using map algebra into the path-based FRLM.

Even though NREL's approach is valuable in that it explicitly considers the spatial variation of AFV demands, the conversion of census tracts into a raster format introduces representation errors. One straightforward solution may be to use the smallest unit consistently, but it may not be always feasible. Therefore, an areal interpolation method needs to be employed. On the other hand, from the perspective of input requirements for the FRLM, the area-based demand estimates need to be converted to a "proportion estimate" so that original flow volume is weighted by it. Essentially the product of the two values represents the AFV flows traveling between an OD pair. Even though it may not the best approach, this simple method accounts for the obvious uneven demand in the early stages of the transition to alternative-fuel vehicles. Complementarily, by varying the scenarios of estimating AFV demands and exploring its effects on the optimal station locations, the planners may obtain valuable insight in making a decision.

The fourth gap is related to uncertainty management through the use of an SDSS that integrates the proposed spatial optimization model and GIS. Previous research has also considered to some degree uncertainties in planning alt-fuel stations or modeling demand for alternative fuels and alt-fuel vehicles. One such approach was utilizing sensitivity analyses. However, not only is the future AFV demand unknown but their demand is geographically uneven. These uncertain and spatial factors have not been accounted for in the optimization based alt-fuel infrastructure planning models. Exploring the sensitivity of estimated AFV demand to its model parameters and its subsequent effects on the results of flow-based models can improve the reliability of the result. Moreover, an SDSS can provide a framework to explore design alternatives. Especially when the design is related to the unknown phenomenon such as the deviation of AFV drivers and unequal likelihood of AFV adoption rate, the capabilities of an SDSS to generate multiple scenarios and to compare those alternatives are important. If a site is repeatedly selected as optimal with given range of acceptable input parameters, it is highly likely that locating facility at the site will constitute a more robust solution. Therefore, given the absence of an SDSS designed to support a planning decision of a refueling facility network that considers drivers' deviation and AFV demands, development of such a flexible SDSS is necessary.

3.2 Research Questions

This research addresses the gaps identified above by developing a flow-based location model and a Spatial Decision Support System (SDSS) that incorporates heuristic algorithms for the purpose of deploying initial networks of alternative-fuel stations. The focus of this research is on the incorporation of drivers' required deviation from their pre-planned routes and uneven distribution of alt-fuel vehicle demand. These deviation behaviors and spatial variations in demands are incorporated into not only the FRLM but also an SDSS that enables the user to deal with the inherent uncertainties in predicting or estimating them. In addition, this research proposes and compares methods that integrate the AFV demand and trip volumes and explores results of different scenarios. The models and methods are applied to a real-world road network data from state of Florida. To achieve the research goals mentioned above, specific research questions can be enumerated as follows:

- What are the important characteristics of drivers' deviations from their shortest paths to formulate in mathematical terms, and in what ways does the structure of the new model need to differ from previous models?
- What are the critical aspects in the design of a heuristic algorithm that can solve general flow-capturing and flow-refueling models with deviations, and what are the important considerations when implementing the suggested heuristic algorithm in an SDSS environment?
- What are the possible ways of integrating estimates of categorically measured potential alt-fuel vehicle demand with origin-destination path-based trip data using a GIS? How do the results from these methods differ from each other with regard to facility locations?
- What are the important aspects that need to be considered in integrating the location model and a GIS so the resulting SDSS manages the uncertainty in the model or data in designing an alternative-fuel refueling network?

These four research questions correspond to the four chapters that follow, but are represented in Figure 3.1 as a triangle in the area of intersection of the three literatures. The corners of this triangle are positioned in "literature space" to represent in a conceptual sense where these new contributions to these literatures can be placed. The literature gaps and research contributions relating to the deviation flow-refueling problem are combined into a single point of the triangle in Figure 3.1, although they are presented in two separate chapters (Chapter 4 on the deviation location model and Chapter 5 on the heuristic solution methods). The research question on demand modeling is shown in Figure 3.1 as a second component of this research, and is presented in Chapter 6. Finally, the SDSS is presented in Chapter 7 and is shown as a third point of the triangle in Figure 3.1.

4 DEVIATION-FLOW REFUELING LOCATION MODEL

The key aspect of this research is to extend the FRLM to consider the ability of drivers to deviate from their shortest paths for the purpose of stopping at a refueling station that is not on their shortest path. By considering deviations, we relax the assumption of the flow-refueling location model that customers do not deviate from their preplanned trips to refuel their vehicles. Thus locations *somewhat close* to pre-planned paths may be also candidates for locating the facilities. This is believed to better reflect drivers' behavior when the refueling network is sparse and the required deviation to the facility is acceptable. We assume that the number of customers who need to travel to a facility at such a less convenient location decreases as a function of required deviation distance. The objective of the new model, which is called the Deviation-Flow Refueling Location Model (DFRLM), is to locate p facilities to maximize the expected number of potential customers who refuel their range-limited vehicles at the facilities.

An important input for the new model is *all* deviation paths between O-D pairs. Given that the problem of finding all possible paths between an O-D pair in a real world network is hard to solve, the generation of feasible deviation paths requires additional constraints that reflect more realistic assumptions on drivers' refueling behavior in a sparse refueling network. In addition, without available empirical data as to how many AFV drivers would deviate from their pre-determined paths and how far they would do so for refueling purposes, an explorative model is required. With the model, planners can perform experiments with different upper bounds of deviation distance or apply different forms of functions to fit anticipated drivers' decreasing willingness to deviate. Both of the above inputs need to consider vehicle range at the same time. With these requirements satisfied, flow-based models will expand their applicability.

This chapter first illustrates the logic of deviation-flow refueling using an example network. Because we can model deviations in various ways, assumptions of this research are explained in Section 4.2. Section 4.3 presents a mixed-integer programming model for the DFRLM and it is followed by an explanation of the algorithms and applications that are developed for generating deviation paths and for modeling distance decay of flows in Section 4.4 Section 4.5 explains solution procedure. Section 4.6 presents preliminary results on a 25-node network. Section 4.7 offers conclusions and future research.

4.1 An Example Network

The simple network in Figure 4.1 with 6 nodes and 3 paths illustrates the difference among the FCLM with deviation, the FRLM, and the suggested DFRLM model. For simplicity, all path flow will be assumed to be 1 as in Table 4.1. Suppose that the driving range of an AFV is 70 and one station (p = 1) is to be built at one of the nodes to maximize the flows that can be served by it. If the FCLM with deviation is applied in this situation, and the maximum deviation is considered to be large, then stations can be located at any node in the network. However, when the basic FRLM (with no deviations allowed) is used to solve the problem, only node C can provide service to the customers on path 2 and path 3.

Path 1 cannot be served by node C, because C is not on path 1. Any of other nodes (O, A, B, D, and E) alone cannot refuel round-trip flows because of the vehicle's range limit (See section 2.3 for more discussion on generating the combinations of facilities that can refuel a path).

When deviation from the shortest path is allowed, either B or C can be chosen for siting the station. Node B can refuel path 1 with deviation distance 5 ($\overline{OABD} - \overline{OAD}$), path 2 with deviation distance of 10 ($\overline{OABCE} - \overline{OCE}$). The customer flows refueled by node B, however, should be less than the sum of each flow because the number of visiting customers should decrease as deviation distance increases. The station at node C can refuel path 1 with deviation distance of 15 ($\overline{OCD} - \overline{OAD}$) while serving paths 2 and 3 without any deviations. When evaluating B and C, locating the station at C is likely to be superior to locating at B because of its higher objective value (this of course depends on the deviation penalty function). It is worth noting, however, that even though the optimal location(s) from the two models (FRLM and DFRLM) may be the same (node C), the objective value of the DFRLM will be greater than that of the FRLM because the former accounts for the additional customer flows that deviated from their shortest paths. This example shows that allowing deviations in modeling flow-refueling will increase the utility of stations by serving more customers.

Table 4.1   O-D Flow Paths

Origin-Destination Pair q	Flow	Shortest path by nodes	Shortest path distance (time)
1 (O-D)	1	O A D	45
2 (O-E)	1	O C E	40
3 (D-E)	1	D C E	40

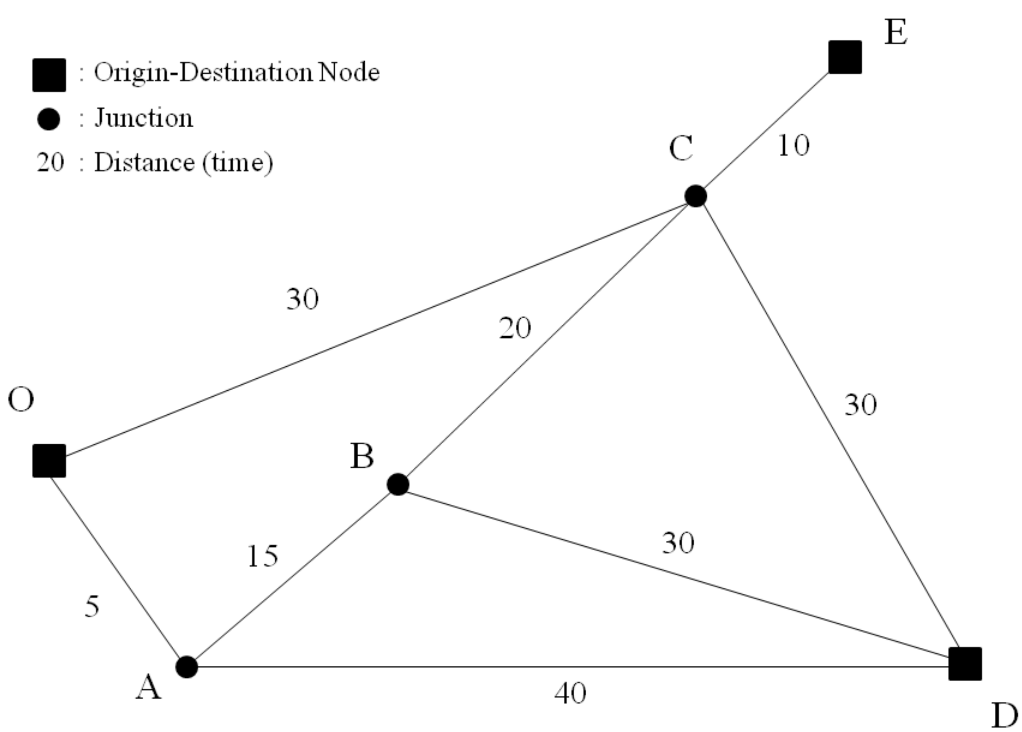

Figure 4.1   A 6-Node Network.

4.2 Assumptions

4.2.1 *Shortest Deviation Path*

An assumption related to the deviation distance[3] calculation is that drivers take the shortest or least cost deviation path to their required refueling stations and then to their final destination. That is, we assume they have perfect information and choose the best way to deviate from their shortest path to the off-path station(s) and then to their final destination. Such behavior is expected to be more common in the future due to the increasing availability of onboard vehicle navigation systems. In sum, we assume that drivers who need to take a deviation path for refueling may have to visit multiple stations and the sequence of them has to be optimized so that the total deviation path distance is minimized.

4.2.2 *Flow Volume Decay with the Increase of Deviation*

Another assumption relates to modeling of penalties on deviations. This has been handled in a few different ways in FCLM-deviation models. One possible assumption is that a given Δ unit of distance away from a node in the pre-planned trip path is regarded not affecting the flow volumes. If the driver then returns to their shortest path, this assumption implies that all customers are willing to take up to 2Δ unit deviation from their original paths. Alternatively one may choose not to impose an upper limit on deviation distance no matter how long it may be, as in Hodgson (1981). Another possible assumption is that the

[3] Deviation distance was defined as the additional distance incurred when a customer deviates from the pre-planned (shortest) trip. For discussion on other types of deviation distance, see section 2.3.1.

fraction of customers deviating to a facility can be specified as a decreasing function. Here we assume the latter, namely that capturing of flows by stations off the shortest path declines from 100% to 0% according to some exogenously given deviation penalty function.

This research does not assume a specific curve shape of the decreasing function to describe the fraction of flows on deviation paths, but loosely defines it as a decreasing function of deviation distance.[4] The reliability of a penalty function is highly dependent on the specific situations to which the model will be applied. Previous research employed exponential decay (Berman, Bertsimas, and Larson 1995; Zeng, Hodgson, and Castillo 2009). In the transportation literature, inverse distance functions have been widely accepted. The exact shape and steepness may need to be calibrated to empirical survey data, which is beyond the scope of this dissertation. Given that this research focuses on unknown demand, exploration with various types of distance decay functions and parameters is more appropriate. Note that depending on the specification, the extent to which customers show indifference to the required deviation could also be modeled.

In addition, we assume that there is an upper limit of deviation distance that drivers can tolerate. In other words, drivers would not take the deviation path whose total distance is longer than a certain distance, even though the path might be refuelable. It may be a psychological limit that is dependent on consumers' perception on deviation.

[4] Deviation distance is directly calculated by subtracting shortest path distance from deviation path distance.

Both distance decay function and upper limit of deviation distance can be specified in relative or absolute terms. In the case of a penalty function, the spatial extent of distance decay is referred to here as bandwidth. Large bandwidth implies more gradual distance decay, where a small bandwidth results in a rapid decrease. The bandwidth can be a fixed distance or can be relatively derived from each reference path distance (i.e. some percentage of the shortest path distance). Likewise, the upper limit of deviation distance can be a fixed value or it can be specified as percentage of shortest path distance.

One of the tasks carried out for this research is a development of a program that allows users to specify parameters for 5 different types of distance decay functions: no distance decay, linear, exponential, sigmoid, and inverse distance. Design and implementation details are described in section 4.4.3.

4.2.3 *Common Assumptions of Flow-Refueling Location Model*

DFRLM is an extension of the FRLM, and therefore it follows assumptions of its precedent model, which are presented in Kuby and Lim (2005). The following is a summary of them.

- Flow-refueling location models are formulated to locate facilities that make round-trips feasible.
- The starting level of a vehicle's fuel is half the fuel tank, which ensures that the round trip will be feasible.
- Fuel consumption is strictly a function of distance.

- Facility location is limited to network nodes. It will be, however, possible to extend DFRLM to add candidate locations at anywhere along the links as the extensions of FRLM do.

4.3 Formulation of the Deviation-Flow Refueling Location Model

This section presents a mixed integer programming formulation of the deviation-flow refueling location model (DFRLM). The model relaxes the FRLM (Kuby and Lim 2005) such that it allows driver's deviations to the facilities that are near customers' preplanned shortest paths as considered in Berman, Bertsimas, and Larson (1995). A new subscript *r* is introduced to represent deviations.

Formulation of the DFRLM

$$\text{Maximize } \sum_q \sum_r f_q g_{qr} y_{qr} \qquad (14)$$

Subject to

$$\sum_{r \in R_q} y_{qr} \le 1 \qquad \forall q \in Q \qquad (15)$$

$$\sum_{h \in H_{qr}} v_h \ge y_{qr} \qquad \forall r \in R_q, q \in Q \qquad (16)$$

$$x_k \ge v_h \qquad \forall h \in H, k \in K_h \qquad (17)$$

$$\sum_{k \in K} x_k = p \qquad (18)$$

$$x_k, v_h, y_{qr} \in \{0,1\} \quad \forall k \in K, h \in H, q \in Q, r \in R_q \qquad (19)$$

where:

q = a particular O-D pair (the shortest path for each pair)

Q = set of all O-D pairs

f_q = flow between O-D pair q

r = index of deviation paths

R = set of all deviations

R_q = set of deviation paths r for O-D pair q

g_{qr} = fraction of normal path q customers who would be willing to take deviation path r (that is, the penalty function value for deviation r)

y_{qr} = 1 if path r is the highest-volume path for O-D pair q that can be refueled, 0 otherwise

k = a potential facility location

K = set of all potential facility locations

K_h = set of facilities k that are in combination h

x_k = 1 if there is a facility at location k, 0 if not

h = index of combinations of facilities

H = set of all potential facility combinations

H_{qr} = set of facility combinations h that can refuel deviation path r that is originated from O-D pair q

v_h = 1 if all facilities in combination h are open, 0 otherwise

p = the number of facilities to be located

The objective function (14) maximizes the total flow that can be refueled. Constraints (15) limit the contribution to the objective function to at most one deviation path *r*. The set of paths *r* for OD pair *q* includes *q* itself, as *q* is the shortest path from OD pair *q* with deviation distance = 0. The number of possible

r is very large, and thus without this constraints, double counting of flows on deviation paths might also be possible. Constraints (16) are similar to constraints (6) in the FRLM, except instead of requiring at least one eligible combination of facilities h to be open for path q if q is to be refueled, they require at least one valid combination h to be open for any deviation path r. Constraints (17) ensure all the facilities in combination h are open before $v_{\underline{h}}$ becomes one. Constraints (18) specify the number of facilities to open, and (19) are the integrality constraints for the variables.

4.4 Algorithms to Generate Input Data for DFRLM

Three algorithms were implemented to prepare input data for the MILP formulation of DFRLM (Figure 4.2). One algorithm generates deviation paths for each OD pair given the upper limit of deviation distance. Another algorithm computes the fraction of flows on deviation paths. This algorithm reads in the user's input parameters to formulate a distance decay function. This research develops these two algorithms. The last algorithm determines whether a particular combination of facilities can refuel a deviation path. This algorithm is the one from Kuby and Lim (2005) except that it runs on all deviation paths rather than on shortest paths. The three algorithms are implemented in an application using the C# programming language.

4.4.1 *Generating Deviation Paths: Modified k-Shortest Path Algorithm*

This algorithm generates the set of deviation paths R and R_q. It first reads in an upper limit of deviation distance, which could be in relative term or absolute term. The next step is to run Hoffman and Pavely's (1959) k-shortest paths (KSP) algorithm with $k = 1$, and then the algorithm evaluates if its deviation distance is shorter than the upper limit. If so, the algorithm increases k by 1 and keeps generating alternative paths by running the KSP algorithm until the deviation distance reaches the upper limit. Note, however, that if the upper limit equals 0, no deviation is allowed, and the KSP generates only shortest paths, which in effect converts the DFRLM into the FRLM. It is, however, possible that the KSP may generate multiple paths with the same distance, in which case, one may consist of more edges with shorter distances while others are made up of fewer edges with longer distances. Even in such cases, only one deviation path contributes to objective value because constraints (15) in the MILP of the DFRLM ensure the inclusion of one deviation path per an OD pair. The algorithm stops when all OD pairs are evaluated.

One modeling issue is whether or not deviation paths should contain loops. In many implementations of KSP algorithms, loops are not allowed; the paths are simple. Yen (1971), Dreyfus (1969), Shier (1979), and Eppstein (1994) provide more complete reviews on KSP algorithms. If we consider the refueling behavior when stations are scarce, however, drivers may have to take a short deviation that has a loop to fill up enough fuel to reach the next stations or destination. For example, if there is a station at node *A* close to origin *O*, drivers may take a path *O*-*A*-*O*-*B*-*D* to reach the destination *D*. With the inclusion of loops or cycles in computing KSPs, the sequence of nodes in the path may not best reflect typical drivers' behavior. For example, paths *O*-*A*-*O*-*B*-*D* and *O*-*A*-*O*-*A*-*O*-*B*-*D* are recognized as different deviation paths. But in fact, because the set of facilities that can refuel the former is also able to refuel the latter path, and only the shorter deviation path will contribute to objective, the MILP model works with deviation paths with loops (See section 4.4.3 for discussion on refueling feasibility). Given that typical drivers would take only one necessary loop to refuel, removing multiple loops in KSP algorithm will be more preferable to reduce the size of problem. This research does not implement such an advance KSP algorithm but just allows loops to take into account drivers' necessary cyclic refueling trips. . Even with this relaxation, there may be some deviation paths that the KSP algorithm implemented here cannot generate.

Another modeling issue is related to the FRLM's round trip assumption. A KSP algorithm generates routes from an origin to a destination, but it usually does not find a round trip path from origin to a destination and back. Note that a driver's ingress path might be different from egress path. For example, an ingress path q_{in} is O-A-R_1-D if a driver refuels at R_1 that is off of his/her preplanned path. But the egress path q_{out} could be D-R_2-A-O, where R_1 is not the same as R_2 and R_2 is closer to destination node but farther to A than R_1. In this case, q_{in} is feasible but visiting the nodes of q_{in} in the reverse order may not be feasible. Similarly q_{out} might be feasible only for the returning trip. From a different perspective, one might think such a round trip path can be generated from algorithms for traveling salesman problem (TSP). But a deviation refueling path is different from traveling salesman path in that visiting nodes are not pre-determined as in TSP; we need multiple deviation round trip paths; and that TSP by nature does not allow a cycle in the tour. Along with the need for considering possible cycles, the construction of round trip paths complicates the generation of deviation paths for refueling.

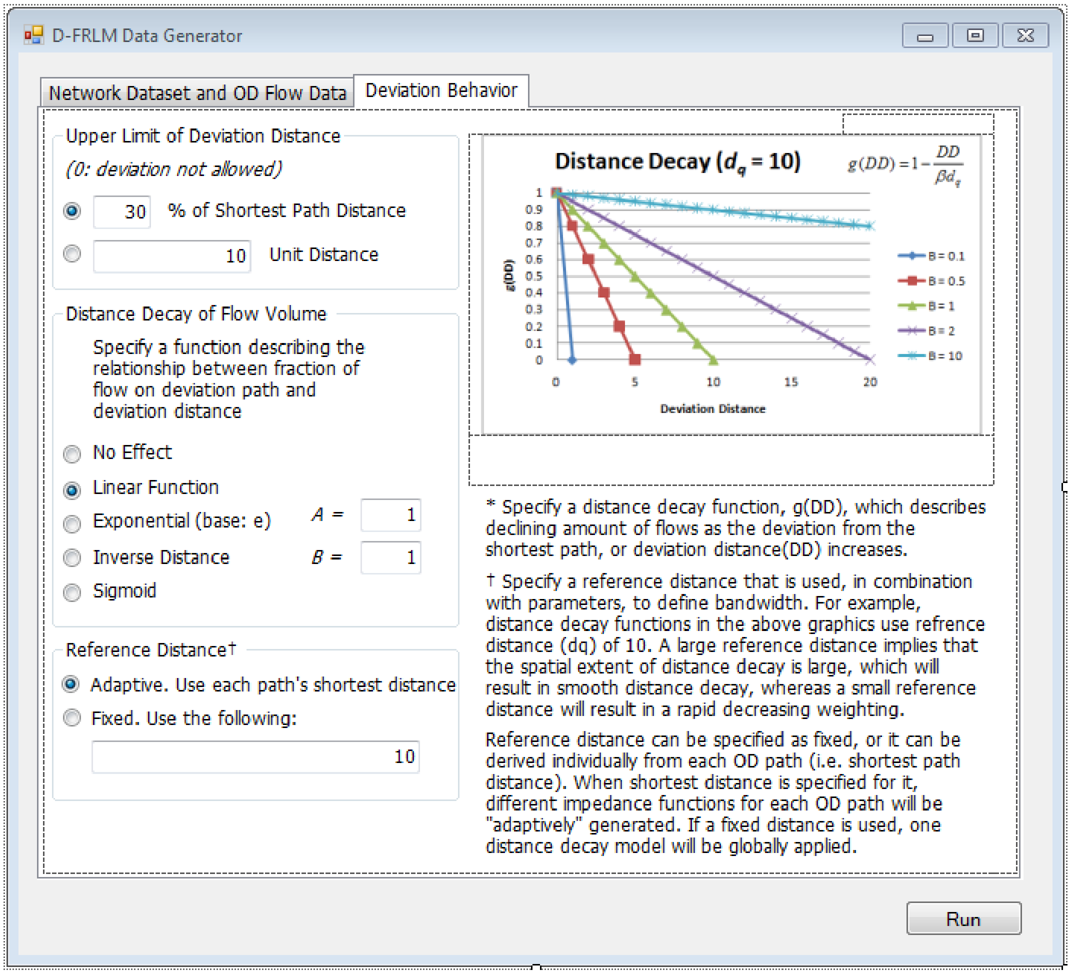

Figure 4.2 Input Data Generation for DFRLM.

4.4.2 *Computing the Fraction of Flow Volume on Deviation Paths*

This algorithm computes the fraction of path *q* customers who take deviation path *r*, which is denoted as g_{qr} in the MILP formulation of the DFRLM (Section 4.3). Let *DD* , d_q, and *g(DD)* be the deviation distance, reference distance, and the fraction of flows specified by function *g* and input *DD*. Users can choose a distance decay function type from 5 available types: no decay, linear, exponential, inverse distance, and sigmoid. Each function can be expressed as below:

$$g(DD)_{\text{No Decay}} = 1 \tag{20}$$

$$g(DD)_{\text{linear}} = 1 - \frac{DD}{\beta d_q} \tag{21}$$

$$g(DD)_{\text{exponential}} = 1 - (\alpha e^{\beta(DD - d_q)}) \tag{22}$$

$$g(DD)_{\text{inverse distance}} = (\alpha e^{-\beta \bullet DD}) \tag{23}$$

$$g(DD)_{\text{sigmoid}} = \frac{1}{1 + \alpha e^{(\beta \bullet DD) - d_q}} \tag{24}$$

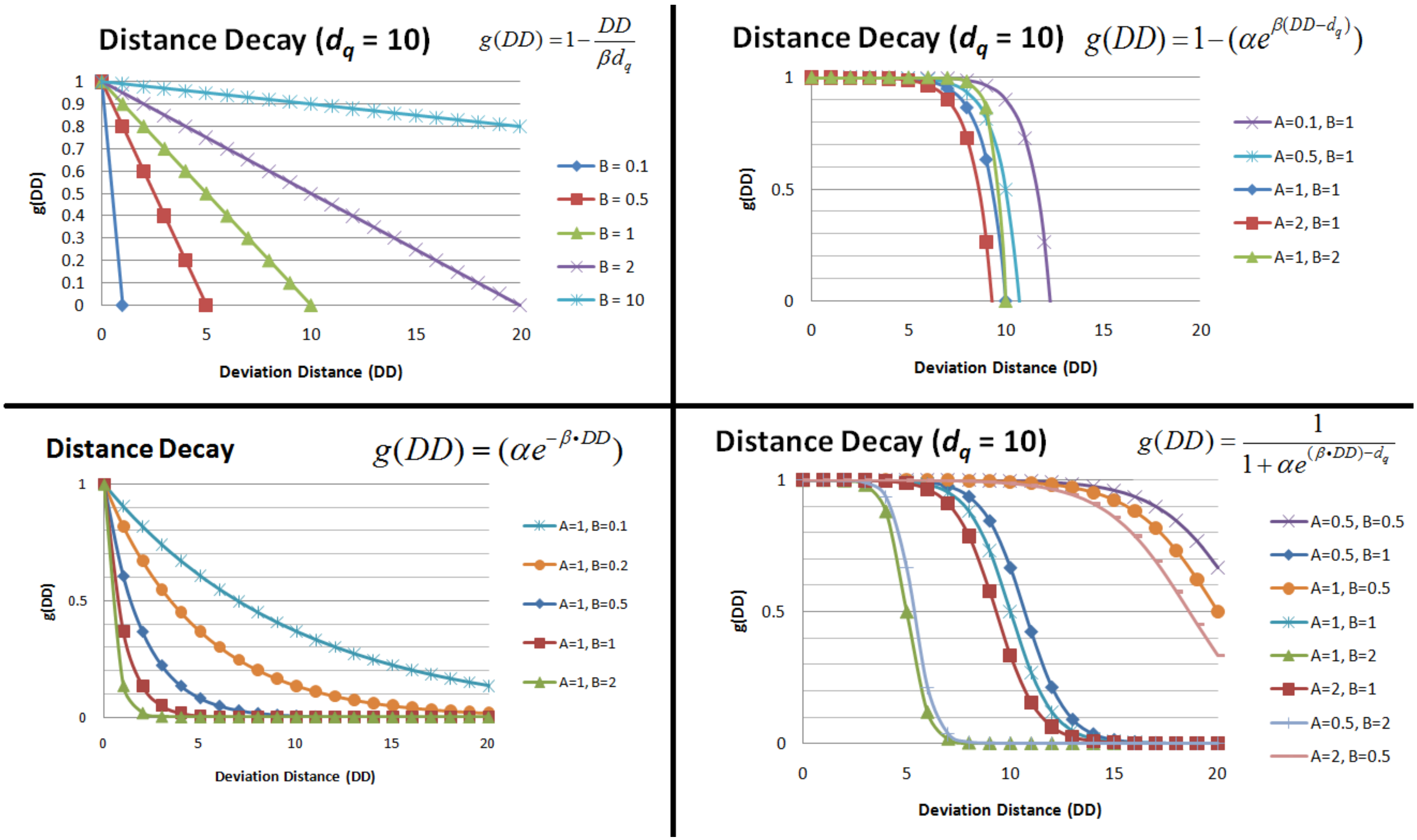

Figure 4.3 Example of Distance Decay Functions.

The fraction of flow volume on a deviation path with deviation distance of *DD* is expressed as a function of reference distance d_q and deviation distance *DD*. By specifying parameters (α or β), the shape of the function is determined. Figure 4.3 shows four classes of graphs depicting deviation function shapes with reference distance of 10 and different parameters. These illustrative graphics are provided to aid users' specification of distance decay function.

The reference distance, in combination with the other specified parameters, defines the bandwidth. For example, the distance decay functions in the example use reference distance d_q of 10. A large reference distance implies that the spatial extent of distance decay is large, which will result in smooth distance decay, whereas a small reference distance will result in a rapidly decreasing weighting. It can be specified as fixed, or it can be derived individually from each OD path (i.e., shortest path distance). When the shortest distance is specified for it, different impedance functions for each OD path will be "adaptively" generated. If a fixed distance is used, on the other hand, one distance decay model will be globally applied.

4.4.3 *Evaluating Feasibility of Deviation Path*

The MILP formulation of the DFRLM requires generation of the valid set of facilities *h* for each deviation path *r* (See section 4.3. constraints (16)). The formal algorithm for this task is presented in Kuby and Lim (2005) in detail. The difference is that for the DFRLM, the set *H* is generated over all the deviation paths rather than all the shortest paths. The algorithm reads in the vehicle range and the sequence of nodes on a deviation path for an OD. The remaining range in a vehicle is set to half the vehicle range unless there is a station at the starting node. It moves to the next node in the sequence while subtracting the link distance traveled from the vehicle's remaining range. The remaining range is assumed to be full when the visiting node already has a facility. If the round-trip taking the deviation path of the OD pair successfully ends without running out of fuel, the deviation path is considered feasible with the given set of facilities. The algorithm runs for all deviation paths and the outputs the list of *r* and its corresponding *h*. Because this algorithm assumes that drivers refuel whenever there is a station, it works regardless of the number of loops in the deviation paths as long as the path is feasible.

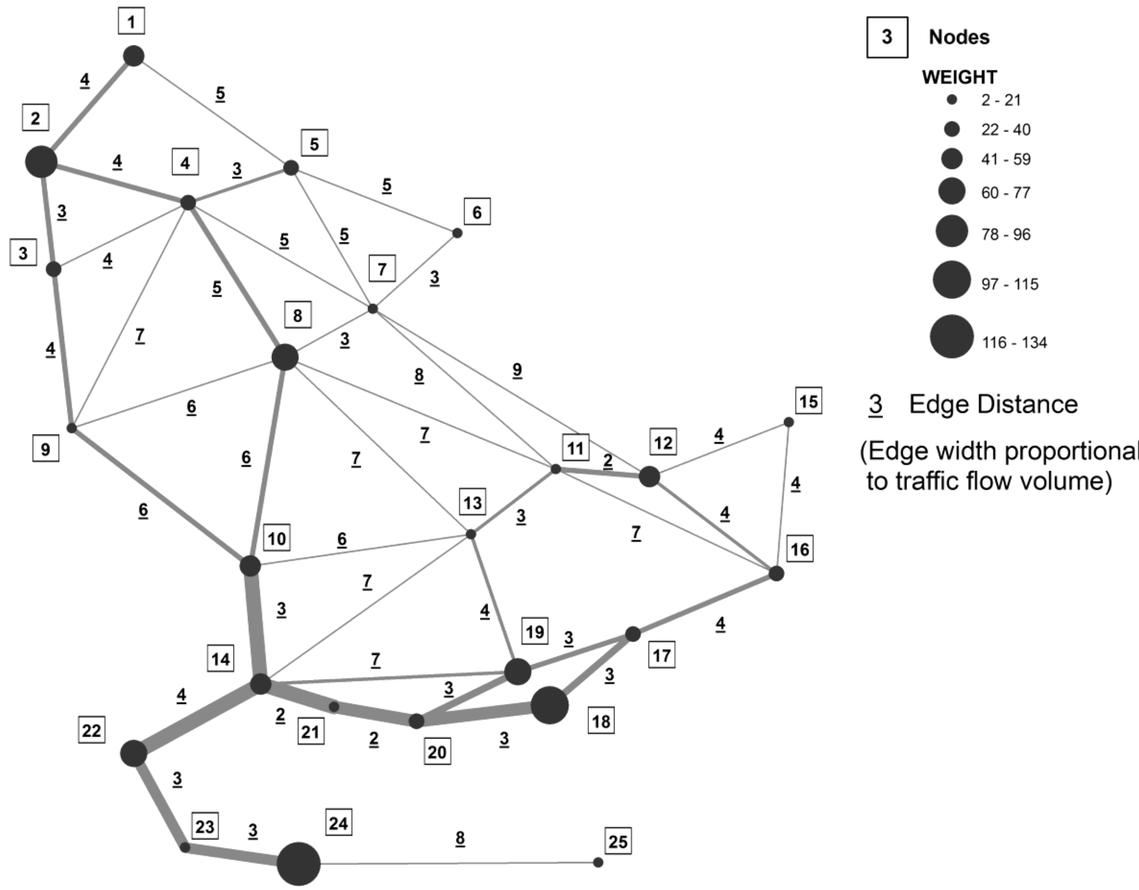

Figure 4.4 25-Node Test Network.

4.5 Analysis on a Test Network

This section provides the experimental design to test the DFRLM. The test network[5] has 25 nodes, 43 edges, and 300 OD pairs with their flow volumes estimated using a gravity model, and assigned to their shortest paths (Figure 4.4). Each node is both an OD node and a candidate site.

The MILP of the DFRLM was built in and solved optimally by using Xpress-MP 7.0 software, and the input for the model was generated by an application coded in C# language, which was described above (Section 4.4). For the upper limit of deviation distances,[6] three values were used: 0%, 10%, and 50% of shortest path distance. To account for the fraction of flows on deviation paths, $g(DD)_{\text{No Decay}}$ and $g(DD)_{\text{linear}}$ were used. In the linear function, bandwidth is the shortest distance of each OD pair, and therefore, the fraction of flows becomes 0% when deviation distance equals shortest path distance ($DD = d_q$). Three different vehicle ranges (4, 8, and 12) were used. All the problem instances were solved by a computer with four 2.4GHz cores and 4GB memory.

Problem size is highly dependent on the number of deviation paths $|R|$, which is mainly determined by the maximum deviation distance allowed (DD_{max}).

---

[5] This test network was used by Berman and Simchi-Levi (1988), Hodgson (1990), and Kuby and Lim (2005).

[6] A cautionary choice of upper limit deviation distance is required. For example, given that the farthest OD pair is 1-25, whose shortest path length is 38, 100% of deviation means drivers are willing to deviate up to 38 distance units on this OD pair. With this deviation distance, the number of possible deviation paths is enormous, and thus the upper limit should not be very high. In fact, Xpress-MP returned a “not enough memory” error for the instance of DFRLM with range 8 and upper limit of 100% of the shortest path.

It is also dependent on vehicle range that will determine the size of the set of potential facility combinations $|H|$. For instance, when vehicle range is 4 and no deviation is allowed, there are 395 deviation-flow coverage variables Y_r; 109 facility combination variables V_h; 67 contributing deviation-path choice constraints (15); 119 refueling constraints (16); 396 combination constraints (17). On the other hand, if the DD_{max} is allowed up to 50% of shortest path distance and vehicle range is set 12, the number of variables and constraints increase substantially: 15,344 Y_r; 13,883 V_h; and 90,992 total constraints.[7]

4.6 Numerical Experiments

4.6.1 *Computation Time*

Computation times for each test problem are summarized in Table 4.2. In general, as the maximum deviation distance gets higher, more time is required to generate deviation paths. The branch-and-bound solution time is shorter when linear distance decay function was used. It is also faster when the maximum deviation distance is lower, or the vehicle's range is shorter. In an attempt to solve the problems faster, only X_k is forced to be binary and other decision variables (Y_r , V_h) are relaxed to be continuous. Because the MILP formulation of DFRLM is "integer friendly," as is the FRLM (Kuby and Lim 2005), this relaxation will not affect the global optimality but will result in reduced number of binary variables, which in turn is expected to solve faster than all-integer version of the problems. Given that the test network has 25 nodes, applicability of the MILP for the

[7] This research develops heuristic algorithms for DFRLM, see next chapter (5.3) for their discussion and performance comparison.

DFRLM to a real-world network may be limited to very small networks. This points to the need for efficient heuristic methods, which are developed later in this dissertation.

Table 4.2 Computation Time for Test Problems for p =1 to 25 (CPU seconds[a])

Vehicle Range	Procedure	No Deviation: One SP	No Deviation: Multi-SP	Distance Decay Function: Linear: *DDmax*: 10% of SP	Distance Decay Function: Linear: *DDmax*: 50% of SP	Distance Decay Function: No Decay: *DDmax*: 10% of SP	Distance Decay Function: No Decay: *DDmax*: 50% of SP
4	B-B	0.921	1.39	1.72	11.95	1.594	13.567
	Data Generation	N/A	0.47	0.54	59.71	0.533	59.302
	Total	0.92+	1.85	2.25	71.66	2.127	72.869
8	B-B	5.6	6.88	14.60	1279.20	12.551	1441.618
	Data Generation	N/A	0.53	0.66	159.70	0.647	163.91
	Total	5.60+	7.41	15.26	1438.90	13.198	1605.528
12	B-B	8.72	11.341	23.22	2511.14	22.424	2166.406
	Data Generation	N/A	0.623	0.83	493.57	0.82	494.132
	Total	8.72+	11.964	24.05	3004.70	23.244	2660.538

[a] Based on mixed integer variable formulation of DFRLM.

4.6.2 *Effects of Vehicle Range and Lack of Convexity*

As is observed in Kuby and Lim (2005), full refueling of all OD pairs is not possible even with facilities open for all candidate node locations when vehicle range is too small (range = 4 or 8). This is because both DFRLM and the original FRLM are restricted to consider nodal points as candidate sites, where a link might be longer than the vehicle's range so that no flows taking the link can be refueled even if stations are located at both nodes. This still applies to these deviation cases. When the range is 12, however, the total flows can be refueled with 15 stations if all the drivers are assumed to willingly deviate up to 50% of their shortest path distances.

The trade-off curves in Figures 5-7 are not convex even though they are non-decreasing. As stations are added to the solution, the marginal coverage enabled by the added station does not necessarily decrease from that of the previously added station because there are cases where the addition of one station enables a combination of facilities to refuel some flows that would not be feasible otherwise. This is also an expected property of the nodes-only version of the FRLM and its extensions (Kuby and Lim 2005; 2007).

4.6.3 *Effects of Deviation Distance and Distance Decay Function*

Tables 4.3-4.6 summarize the test results. By looking at how much the objective value improves compared with the base value obtained from the no-deviation case, it is clear that as the deviation distance increases, the same number of stations covers more flows (Figure 4.5). The percentage improvement ranges from 0.07% up to 14.79%. The most improvement was obtained when the stations' coverage is between 60% and 80%. We can interpret this range as providing more alternative paths with combinations of built stations. When stations are scarce, refueling trips would require a long deviation, which however may not be feasible because of unavailability of stations. As the stations are more available but not so many to cover the most of the flows on the shortest paths, drivers will still need to deviate to refuel and there could be feasible combinations of open stations that enable the O-D flows. These deviation-flows are not necessary when the refueling network becomes mature and most flows can be refueled on their shortest paths.

Table 4.6 contrasts different assumptions of drivers' sensitivity to their deviation distance. When drivers are indifferent to deviation distance up to 50% of SP and the range is 8, a full coverage of the flows is possible with 19 stations, whereas the sensitive flows cannot be fully refueled even with 25 stations when restricted to their shortest paths (labeled One SP in Table 4.6). Similarly, 15 stations can cover the full demand with a range of 12 while the full coverage of these sensitive flows requires 17 stations. This complementary information about sensitivity to deviation distance will be useful for the alt-fuel infrastructure service providers to strategically determine the level of coverage and the number of stations to construct. Table 4.6 and Figure 4.5 reveals an interesting point that smaller number of stations can refuel more indifferent flows of range 8 than sensitive flows of range 12 in as many as 12 out of 19 *p* values.

Figure 4.6 shows a typical difference in the solutions of DFRLM and FRLM; where both located 3 facilities for vehicles of range twelve. The DFRLM solution refuels more OD pairs by serving the flows on deviation paths. The additional gain is 8.12% point (Table 5). When the stations are at nodes 10, 20, and 22, the OD pair of 8-17 can be refueled by the open facilities if drivers are taking a deviation path: 8-10-14-21-20-18(19)-17, of which the distance is 19. Because the shortest path should visit 8-13-19-17 and its length is 14, the deviation distance (19-14 = 5) is less than 50% of the shortest path length. Therefore, DFRLM considers that all the flows of the OD pair will be covered by the solution. There are more such OD pairs that FRLM solution cannot take into account. The OD pair 13-14 is another example.

Figures 4.7-4.8 show the effect of the allowed maximum deviation distances and distance-decay functions. Obviously, deviation distance has direct impact on the coverage level (Figure 4.7). Increase of deviation distance results in higher objective values. In addition, deviation flows estimated by applying a $g(DD)_{NoDecay}$ yielded a higher objective value than by $g(DD)_{linear}$ (Figure 4.8).

Table 4.3 Optimal Coverage Gain with Range of 4

p	Percentage of Flows Refueled with No Deviation[a]	Distance Decay Function: Linear		Distance Decay Function: No Decay	
		DDmax: 10% of SP[b]	*DDmax*: 50% of SP[b]	*DDmax*: 10% of SP[b]	*DDmax*: 50% of SP[b]
1	4.92	-	-	-	-
2	6.31	-	-	-	-
3	11.81	0.68	0.68	0.68	0.68
4	20.38	-	-	-	-
5	25.88	1.66	1.66	1.66	1.66
6	31.26	2.75	2.75	2.75	2.75
7	37.77	3.64	3.64	3.64	3.64
8	41.31	3.95	3.95	3.95	3.95
9	48.76	4.84	4.84	4.84	4.84
10	50.72	5.25	5.35	5.25	5.36
11	54.57	5.25	7.03	5.25	7.80
12	56.26	5.42	7.33	5.44	8.15
13	57.47	5.25	7.03	5.25	7.80
14	59.87	5.25	7.03	5.25	7.80
15	62.64	5.25	7.03	5.25	7.80
16	64.33	5.42	7.33	5.44	8.15
17	65.87	5.42	7.33	5.44	8.15
18	66.50	5.47	**<u>7.49</u>**	5.49	**<u>8.34</u>**
19	67.94	5.57	7.00	5.59	7.52
20	68.58	**<u>5.62</u>**	7.16	**<u>5.64</u>**	7.70
21	68.58	**<u>5.62</u>**	7.16	**<u>5.64</u>**	7.70
22	69.04	**<u>5.62</u>**	7.16	**<u>5.64</u>**	7.70
23	69.14	**<u>5.62</u>**	7.16	**<u>5.64</u>**	7.70
24	69.14	**<u>5.62</u>**	7.16	**<u>5.64</u>**	7.70
25	69.14	**<u>5.62</u>**	7.16	**<u>5.64</u>**	7.70

Note: "-" means no improvement compared with the solution of the FRLM with no deviations.
[a] percent, [b] gained percent point relative to the FRLM with no deviations.

Table 4.4 Optimal Coverage Gain with Range of 8

p	Percentage of Flows Refueled with no Deviation[a]	Distance Decay Function: Linear		Distance Decay Function: No Decay	
		DDmax: 10% of SP[b]	*DDmax*: 50% of SP[b]	*DDmax*: 10% of SP[b]	*DDmax*: 50% of SP[b]
1	13.37	3.76	3.76	3.76	3.76
2	27.08	5.50	5.50	5.50	5.50
3	39.72	4.69	4.69	4.69	4.69
4	51.00	4.97	5.06	4.97	5.08
5	58.56	4.97	5.06	4.97	5.50
6	63.97	4.11	6.52	4.11	7.64
7	68.54	3.79	5.36	3.79	6.78
8	72.32	5.33	9.43	5.54	12.24
9	77.39	5.25	**11.66**	5.38	**14.79**
10	82.81	**7.04**	11.42	**7.25**	13.18
11	88.75	5.66	8.43	5.66	9.50
12	94.26	2.54	3.68	2.54	4.50
13	95.75	2.02	2.76	2.02	3.27
14	96.73	1.69	2.27	1.70	2.72
15	97.24	1.48	2.03	1.50	2.47
16	97.36	2.32	2.40	2.35	2.45
17	98.05	1.69	1.75	1.72	1.81
18	98.18	1.65	1.73	1.68	1.78
19	98.21	1.69	1.75	1.72	1.79
20	98.33	1.56	1.63	1.59	1.67
21	98.33	1.56	1.63	1.59	1.67
22	98.33	1.56	1.63	1.59	1.67
23	98.33	1.56	1.63	1.59	1.67
24	98.33	1.56	1.63	1.59	1.67
25	98.33	1.56	1.63	1.59	1.67

[a] percent, [b] gained percent point relative to the FRLM with no deviations.

Table 4.5 Optimal Coverage Gain with Range of 12

p	Percentage of Flows Refueled with no Deviation[a]	Distance Decay Function: Linear		Distance Decay Function: No Decay	
		DDmax: 10% of SP[b]	*DDmax*: 50% of SP[b]	*DDmax*: 10% of SP[b]	*DDmax*: 50% of SP[b]
1	13.76	4.46	4.46	4.46	4.46
2	29.51	4.83	4.83	4.83	4.83
3	40.92	**6.98**	7.68	**6.98**	8.12
4	52.76	5.24	8.47	5.38	9.89
5	61.61	5.96	9.36	6.09	10.85
6	71.27	3.52	8.06	3.73	10.53
7	79.04	3.43	**9.73**	3.65	**12.42**
8	85.49	3.12	7.37	3.34	10.12
9	90.03	2.80	6.10	2.89	7.56
10	93.99	2.84	4.27	2.84	4.98
11	95.78	2.03	3.24	2.03	3.76
12	97.19	1.47	2.32	1.47	2.61
13	98.32	0.98	1.37	0.98	1.53
14	99.30	0.55	0.55	0.55	0.66
15	99.85	-	-	-	0.15
16	99.93	0.07	0.07	0.07	0.07
17	100.00	-	-	-	-
18	100.00	-	-	-	-
19	100.00	-	-	-	-
20	100.00	-	-	-	-
21	100.00	-	-	-	-
22	100.00	-	-	-	-
23	100.00	-	-	-	-
24	100.00	-	-	-	-
25	100.00	-	-	-	-

Note: "-" means no improvement compared with the solution of the FRLM with no deviations.
[a] percent, [b] gained percent point relative to the FRLM with no deviations.

Table 4.6 Optimal Coverage Gain by Indifference to Deviation Distance

	Range 4		Range 8		Range 12	
p	One SP[a*]	No Decay, 50% SP[b]	One SP[a]	No Decay, 50% SP[b]	One SP[a]	No Decay, 50% SP[b]
1	4.92	-	13.37	3.76	13.76	4.46
2	6.31	-	27.08	5.50	29.51	4.83
3	11.81	0.68	39.72	4.69	40.92	8.12
4	20.38	-	51.00	5.08	52.76	9.89
5	25.88	1.66	58.56	5.50	61.61	10.85
6	31.26	2.75	63.97	7.64	71.27	10.53
7	37.77	3.64	68.54	6.78	79.04	**12.42**
8	41.31	3.95	72.32	12.24	85.49	10.12
9	48.76	4.84	77.39	**14.79**	90.03	7.56
10	50.72	5.36	82.81	13.18	93.99	4.98
11	54.57	7.80	88.75	9.50	95.78	3.76
12	56.26	8.15	94.26	4.50	97.19	2.61
13	57.47	7.80	95.75	3.27	98.32	1.53
14	59.87	7.80	96.73	2.72	99.30	0.66
15	62.64	7.80	97.24	2.47	99.85	**0.15**
16	64.33	8.15	97.36	2.45	99.93	0.07
17	65.87	8.15	98.05	1.81	100.00	-
18	66.50	**8.34**	98.18	1.78	100.00	-
19	67.94	7.52	98.21	**1.79**	100.00	-
20	68.58	7.70	98.33	1.67	100.00	-
21	68.58	7.70	98.33	1.67	100.00	-
22	69.04	7.70	98.33	1.67	100.00	-
23	69.14	7.70	98.33	1.67	100.00	-
24	69.14	7.70	98.33	1.67	100.00	-
25	69.14	7.70	98.33	1.67	100.00	-

Note: "-" means no improvement compared with the solution of the FRLM with no deviations.
[a] percent, [b] gained percent point relative to the FRLM with no deviations.

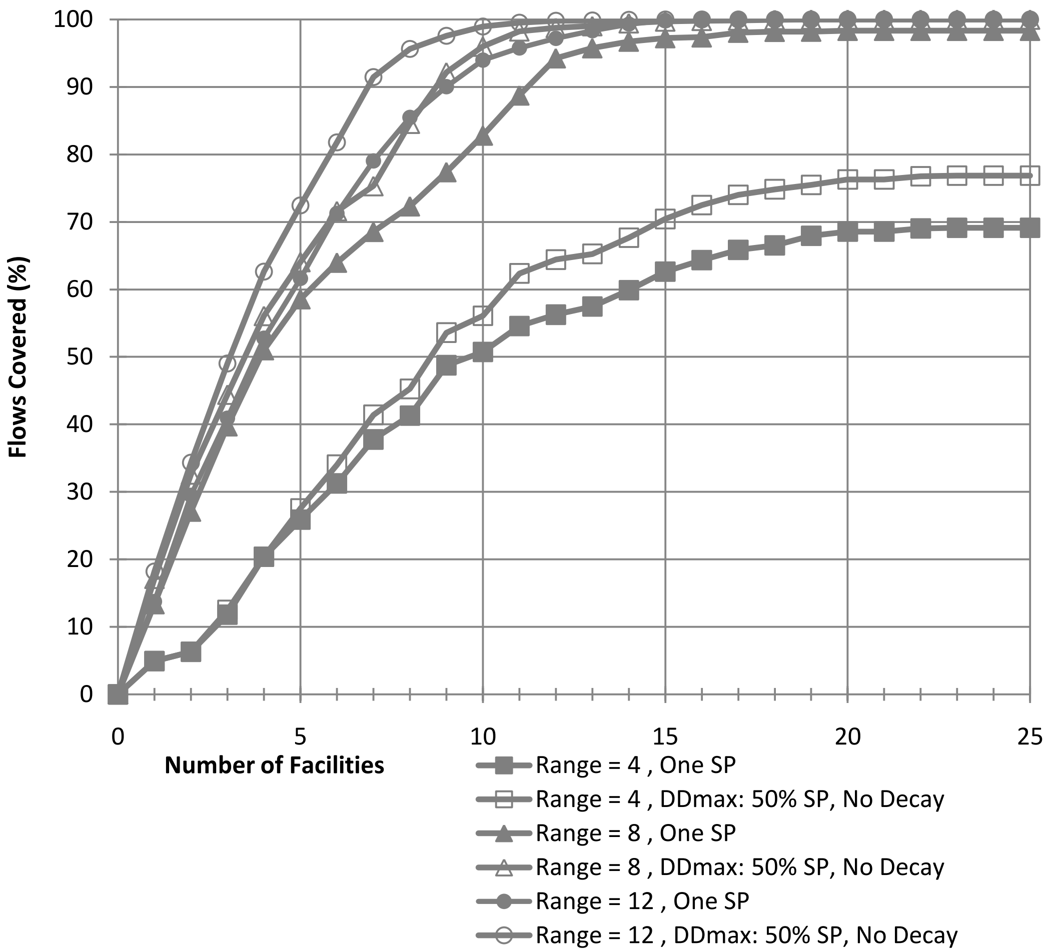

Figure 4.5 Tradeoff Curves for Contrasting Sensitive to Deviation.

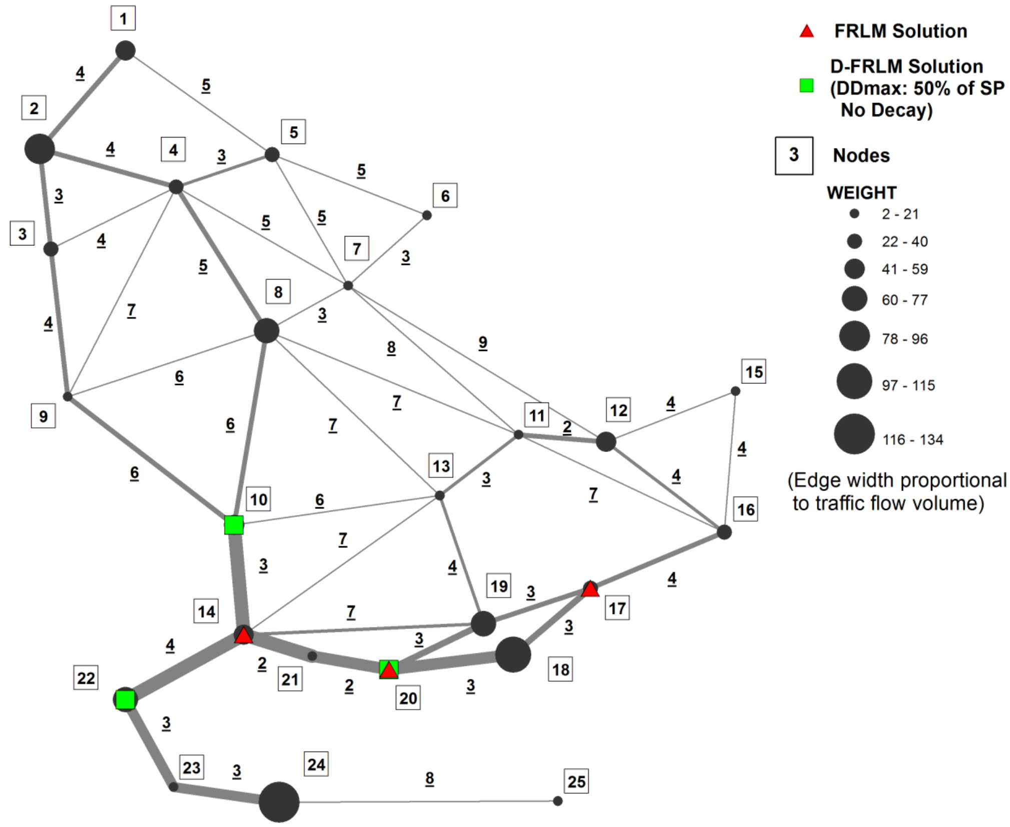

Figure 4.6 Optimal Solutions of DFRLM and FRLM for p = 3, Range = 12.

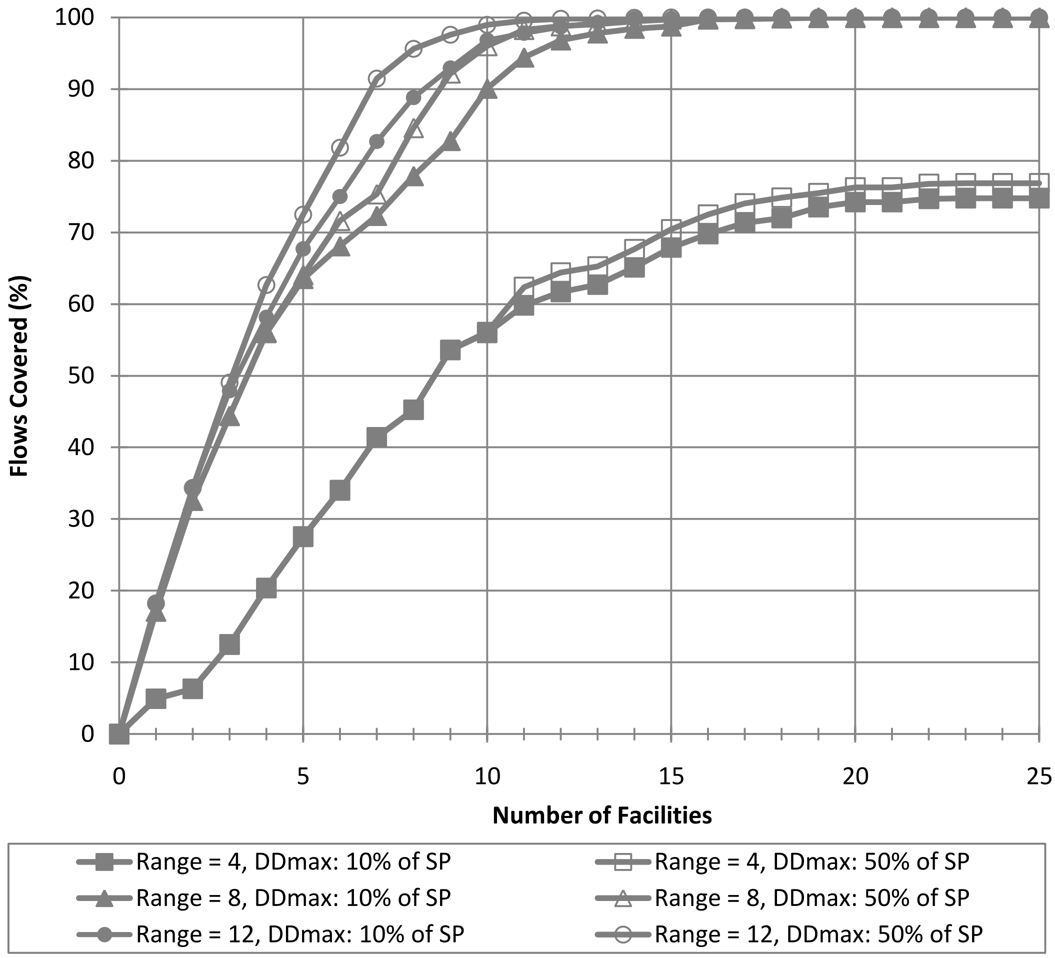

Figure 4.7 Tradeoff Curves for Different Deviation Distances.

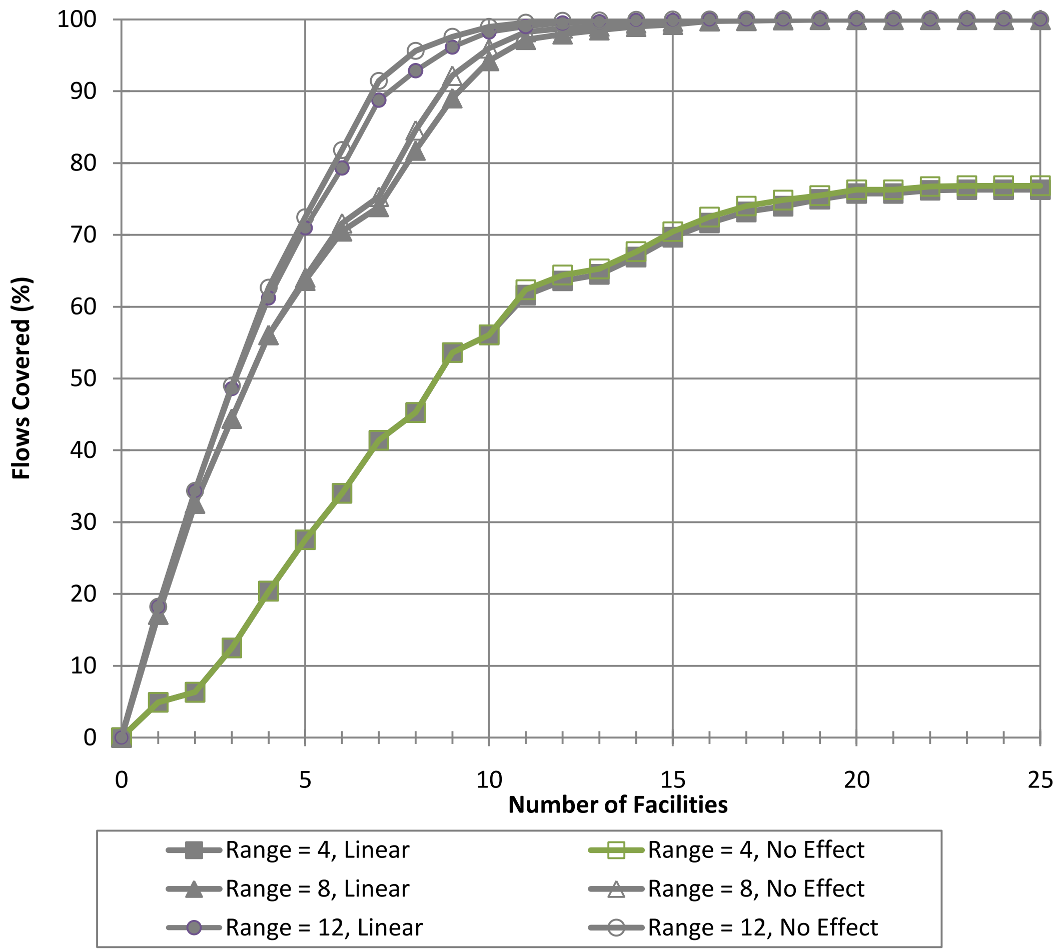

Figure 4.8 Tradeoff Curves of Different Distance Decay Functions.

4.6.4 *Effects of Multiple Shortest Paths*

By specifying *DDmax* = 0 (zero), the DFRLM becomes the FRLM with multiple shortest paths (FRLM-MSP). Note that in Table 4.2 the column of no deviation with one shortest path indicates the result of the FRLM (FRLM-SSP) and multiple shortest paths column is for DFRLM with zero deviation distance. One obvious difference of FRLM-MSP solutions is that the computation times are longer than for the FRLM-SSP, which is mainly because of the increased problem size. Specifically, even if no deviation is allowed, the use of a KSP algorithm in generating all deviation paths results in multiple alternative shortest paths for each OD pair that have the same distance (Section 4.4.1). As a result, the number of paths $|R|$ has increased, which in turn may increase the number of facility combinations $|H|$.

These changes often result in FRLM-MSP reporting higher objective value even with the same solution as from the FRLM-SSP. A set of facilities may not provide a feasible combination to refuel one shortest path but this does not necessarily mean that the same set cannot refuel another possible shortest path of the OD pair. Of course, the solution from FRLM-MSP could be different from the solution of FRLM-SSP. In all cases, FRLM-MSP estimated objective values better than FRLM-SSP (Figure 4.9). The gap ranges from 0.07% to 6.98% point. An example is the p = 3 solution for a range of four (Table 4.7). FRLM-SSP found 14, 18, and 20 as the solution whereas FRLM-MSP located facilities at 18, 19, and 20 with the higher objective value. The OD pair of 18-19 can be traversed by nodes 18-17-19 (A) or 18-20-19 (B). Depending on the choice of shortest path generation algorithm and implementation details, FRLM-SSP fixes one from the two paths and generates feasible facility combinations H from it. If the algorithm chose (A) as *the* path, which is the case here, the objective value from the solution of 18, 19, and 20 would be underestimated by not counting in the flows on the path (B) that is exactly as good as (A). That is the reason why FRLM-SSP had to move on to choose 14 whereas FRLM-MSP was able to consider both paths.

Table 4.7 Optimal Coverage Gain by Multiple Shortest Paths

	Range 4		Range 8		Range 12	
p	One SP*	Multi SP**	One SP*	Multi SP**	One SP*	Multi SP**
1	4.92	-	27.08	3.76	29.51	4.46
2	6.31	-	39.72	5.50	40.92	4.83
3	11.81	0.68	51.00	4.69	52.76	**6.98**
4	20.38	-	58.56	4.97	61.61	4.71
5	25.88	1.66	63.97	4.97	71.27	4.57
6	31.26	2.75	68.54	4.11	79.04	1.26
7	37.77	3.64	72.32	3.79	85.49	1.17
8	41.31	3.95	77.39	3.07	90.03	1.17
9	48.76	4.84	82.81	4.97	93.99	2.67
10	50.72	5.25	88.75	4.78	95.78	2.84
11	54.57	5.25	94.26	**5.66**	97.19	2.03
12	56.26	5.25	95.75	2.54	98.32	1.47
13	57.47	5.25	96.73	2.02	99.30	0.98
14	59.87	5.25	97.24	1.63	99.85	0.55
15	62.64	5.25	97.36	1.24	99.93	-
16	64.33	5.25	98.05	1.81	100.00	0.07
17	65.87	5.25	98.18	1.18	100.00	-
18	66.50	5.30	98.21	1.14	100.00	-
19	67.94	**5.40**	98.33	1.18	100.00	-
20	68.58	**5.40**	98.33	1.05	100.00	-
21	68.58	**5.40**	98.33	1.05	100.00	-
22	69.04	**5.40**	98.33	1.05	100.00	-
23	69.14	**5.40**	98.33	1.05	100.00	-
24	69.14	**5.40**	98.33	1.05	100.00	-
25	69.14	**5.40**	98.33	1.05	100.00	-

Note: "-" means no improvement compared with the solution of the FRLM with no deviations.
[a] percent, [b] gained percent point relative to the FRLM with no deviations.

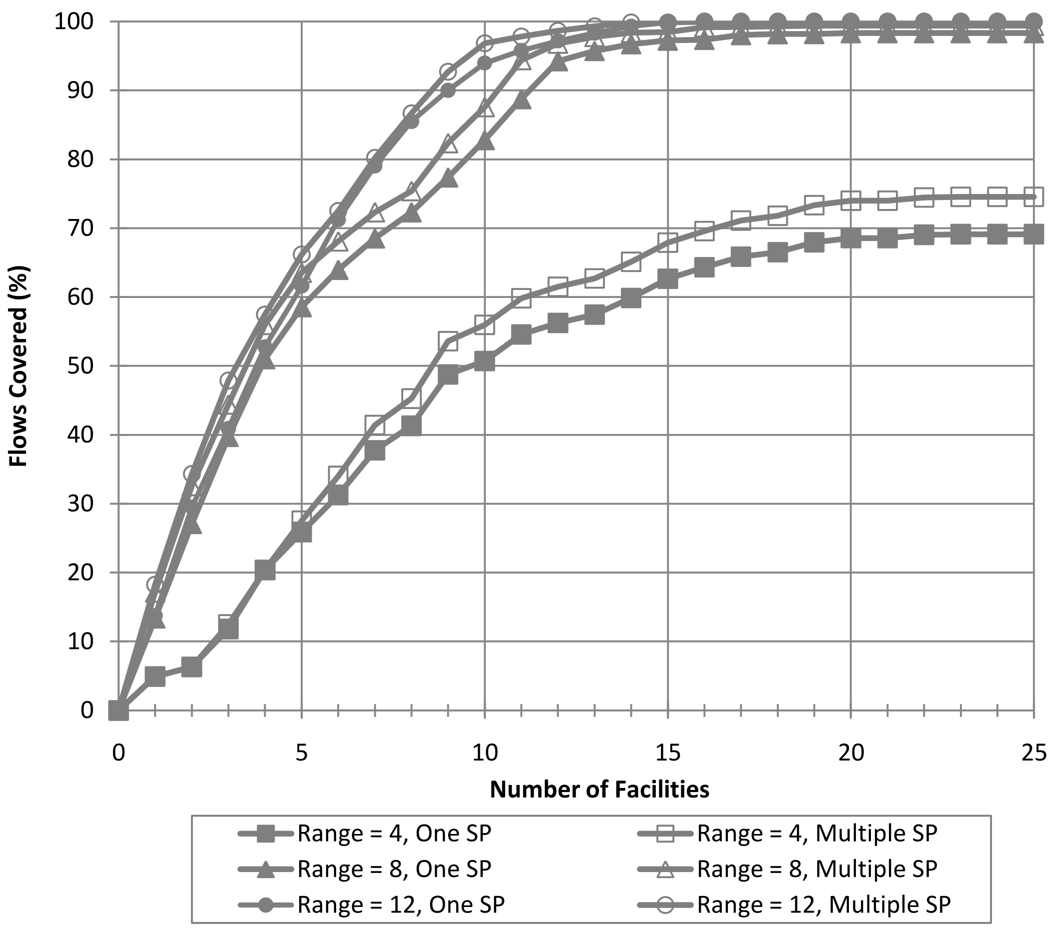

Figure 4.9 Tradeoff Curves for the Same Problems with Different Formulations. (FRLM: One SP / DFRLM: Multiple SP)

4.7 Conclusions and Future Research

In this chapter, the FRLM was relaxed to consider the need of consumers to deviate from their shortest paths to visit a service facility. The number of drivers to visit a facility off of their pre-planned paths was assumed to be decreasing as the required deviation increases. The new model (DFRLM) provides a more realistic representation of refueling behavior especially when the

AFV infrastructure is in its infancy. A mixed-integer linear programming formulation was presented and the procedures to generate input data for the model were given. Drivers' sensitivity to deviation can be modeled by one of the procedures. The problem instances were solved to the optimality and the results were discussed.

In general, the results of DFRLM were consistent with the node-only version of FRLM. The consideration of deviations in DFRLM resulted in an increase of the objective function even with the same set of facilities as FRLM and this implies higher utilization of facilities and more accurate projection of covered demands. The increase of the objective was consistently observed as the vehicle range or deviation increases given that the objective gain is a composite product of deviation and vehicle range. Depending on the specification of the deviation function, the spatial pattern of optimal stations and the required number of stations to meet a certain level of coverage changed. The MILP formulation of the DFRLM and the procedures for input data generation could be used to solve FRLM problems and more importantly it could enhance the results by eliminating the possibility of coverage underestimation.

Enhancement in reliability required tradeoff in tractability mainly by needing more time to solve more complex problems. Therefore, improvements in deviation path generation algorithm or development of more flexible feasibility evaluation algorithm will be interesting future research topics. More runs with different deviation behavior models or calibration of parameters with empirical data will provide realism to the D-FRLM.

5 HEURISTIC SOLUTION APPROACH FOR THE DFRLM

One of the innovative elements of this research is a development of heuristic algorithms to solve the DFRLM. The procedure to solve DFRLM using a MILP was discussed in the previous chapter. There were three computationally intensive tasks to carry out: generating the deviation paths r for each O-D flow q; making all valid combinations of facilities h for each deviation path; and making the matrix g_{qr} that represent the fraction of path q customers who take deviation path r based on a user-specified distance decay function. The first two tasks require extensive computation and may not be as applicable for acquiring solutions for real-world size networks as is the FRLM (Lim and Kuby 2010).

This research develops greedy-adding and greedy-adding with substitution algorithms to solve DFRLM problems. Previous development of greedy algorithms for the FRLM *without* deviations, by Lim and Kuby (2010) provides a starting point. In addition, the greedy heuristic developed for the FCLM with deviation (Berman, Bertsimas, and Larson 1995) gives perspectives on the ways to deal with deviation cases in general. The new heuristic algorithms evaluate whether facilities are adequately spaced to refuel deviation paths for each O-D pair during the run-time without needing to pre-generate all possible deviation paths and all combinations of facilities that can refuel the each deviation path.

This section first introduces a conceptual refueling network, which uses only a subset of the nodes of the network such that refueling is by definition feasible using the selected nodes. It is followed by implementation details on how to construct and manage the feasible network. Details and implementation considerations on greedy-adding and greedy-adding with substitution algorithms are then discussed in the next subsections.

5.1 Feasible Network: Concept and Management

5.1.1 *Concept of Feasible Network*

The primary goal of the heuristic algorithms is to evaluate covered flows by a temporary solution set, where the contributing flows are either on the shortest distance path or shortest distance deviation path[8] of each *OD* pair. This research introduces a conceptual network to represent the feasibility of refueling among *OD* pairs. Assume an undirected weighted network $G = (N, A)$ where N is the set of nodes with cardinality $|N| = n$ and A is the set of arcs. This is referred to as the physical network in that it depicts physical properties of a road network of interest. Assume an undirected weighted network $G_f = (V, E)$ where V is the union of *OD* nodes in G and the set of temporarily selected facilities; E is the set of shortest *paths* among the nodes in G that are feasible given the provision of V and the assumed vehicle driving range. This is referred to as feasible network. Note that in the feasible network, the shortest path distance between any *OD* pair represents either the shortest path distance (if feasible) or shortest feasible deviation path distance of the physical network. It is also possible that there will be no feasible path between an O and D.

[8] Note that if there is no deviation path between an OD pair, its shortest distance deviation path is the same as the shortest distance path.

In determining feasibility of refueling between an *OD* pair with the facility set *V*, important properties that are drawn from observation of the FRLM solutions are exploited (Section 4.4.3 and Kuby and Lim, 2005). These properties determine refueling feasibility considering node type, link length, and vehicle range. They are as follows:

- If any end of a link is an *OD* node, and a facility is at either end, and the length of the link is equal to or shorter than half the vehicle range, then the link is feasible.
- If facilities are at both ends of a link and the length of the link is equal to or shorter than the vehicle range, the link is feasible.

To illustrate the logic of feasible network, let us use the 7-node network in Figure 5.1. In addition, let us distinguish OD nodes and junctions so that junctions indicate nodes that are neither at the origin nor the destination. With this distinction, first consider a case where there is a facility at node 3 and the vehicle range is 6 (Figure 5.2). With a facility located at 3, links 1-3 and 2-3 become feasible, and therefore G_f is by definition a graph with $V = \{1,2,3,4,6,7\}$ and $E = \{1,3\}$ and $\{2,3\}$. Note that G_f may include vertices that are not connected via links, some of which would be members of OD pairs that are not feasible. With the two links added into G_f, the whole flow volumes between the OD pair 1-3 (30 trips) are covered. In addition, a deviation path 1-3-2 for an OD pair 1-2 is also feasible, and a reduced fraction of its flow (< 20) will also be covered by the facility at 3. Note that path 1-3-2 is the shortest deviation path for the pair 1-2 that can be obtained from the current feasible network G_f. Flows between 1 and 2 will not be fully covered (that is, with no deviation necessary) until there are stations at *both* ends of link 1-2. The fraction of flows on the deviation path can be specified and is assumed to be a decreasing function of deviation distance (Section 4.2.2).

It is worth noting that the feasibility evaluation proposed above only considers link lengths, and thus the shortest feasible link does not necessarily represent the least time path in the physical network. It is easily understood if one imagines the case where traveling on a shorter local road takes more time than taking a slightly longer highway section. This restriction can be partially alleviated by using two types of weight (distance and something else such as time or travel cost) for physical links and checking the distance of the least cost path over vehicle range. In fact, the implemented program for this research can take in both weight types. However, even this approach may underestimate the flows on the feasible link when in a rare instance the shortest feasible link does not corresponds to the least-cost or least-time path, and therefore some penalty could be applied to the flows. We could use length as the sole weight under a strict assumption that drivers are taking the shortest paths not the least cost path. Alternatively, we could use two different types of weight and acknowledge the possible underestimation of the flows refueled. This research used the former approach for testing on the 25-node and took the latter approach for testing on the real-world network.

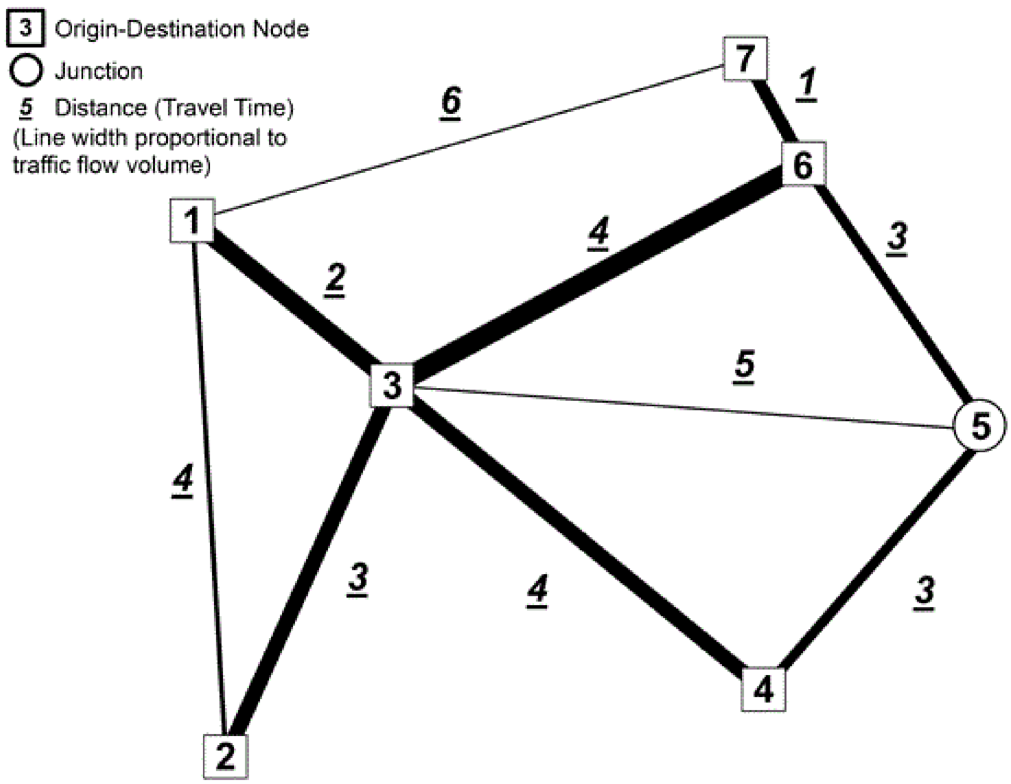

O-D Flow Volume						
	1	**2**	**3**	**4**	**6**	**7**
1		20	30		30	
2	20			25		25
3	30			20	10	10
4		25	20		23	
6	30		10	23		
7		25	10			

Figure 5.1 A 7-Node Network and Its OD Flow Volume.

(The OD flow volumes shown are the full volume assuming the trip can be made on the shortest path. If a deviation to refuel is necessary, these volumes are reduced.)

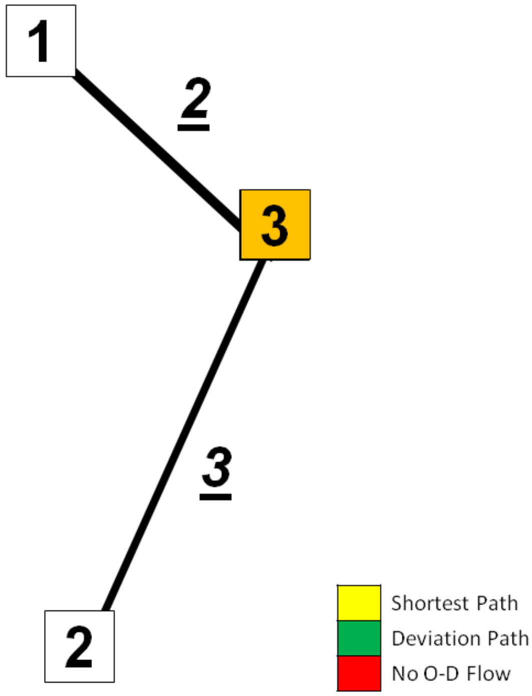

Artificial Feasible Network

	1	2	3	4	6	7
1	∞	5	2	∞	∞	∞
2	5	∞	3	∞	∞	∞
3	2	3	∞	∞	∞	∞
4	∞	∞	∞	∞	∞	∞
6	∞	∞	∞	∞	∞	∞
7	∞	∞	∞	∞	∞	∞

O-D Flow Volume

	1	2	3	4	6	7
1		20	30		30	
2	20			25		25
3	30			20	10	10
4		25	20		23	
6	30		10	23		
7		25	10			

Figure 5.2 The Feasible Network with a Facility at Node 3 (Range of 6)

5.1.2 *Adding a Candidate Node to Feasible Network*

This section presents greedy heuristics that add a node at a time to the temporary solution to maximize additional flows covered. Adding a node to the solution is essentially an update of V of feasible network G_f, which requires subsequent updates of E and of the associated costs of all edges. In doing so, feasibility of each element of E must be evaluated with a given vehicle range. The following is an algorithm that adds a candidate node and updates the feasible network.

Algorithm 5.1 Adding a Candidate Node and Updating Feasible Network

Input: k, $Range$, G_f^{+}, S

$G_f^{*} = G_f^{+}$

$V^{*} = OD \cup S \cup \{k\}$

For all $j \in V^{*}, j \neq k$

  if $(j \in OD)$ **or** $(k \in OD)$

    if $(d_{kj} \leq \frac{1}{2}\, Range)$

    GOTO: Update Feasible Network

  if $(j \in S)$

    if $(d_{kj} \leq Range)$

    GOTO: Update Feasible Network

: Update Feasible Network

  Add k, j **to** G_f^{*}

  if $edge(k, j) \notin G_f^{*}$

    Add $edge(k, j)$ **to** G_f^{*}

    cost$(k, j) = d_{kj}$

Return G_f^{*}

Where

- G_f^{+} : current feasible network
- G_f^{*} : temporary feasible network
- V^{*} : set of vertices for temporary feasible network
- j : index of set V
- OD : set of origin-destination nodes
- S : set of selected facilities
- k : index of candidate node set K
- d_{kj} : shortest distance between nodes k and j in the physical network
- $Range$: range of vehicle

This algorithm takes the current feasible network G_f^+, its link weights, a new node (the candidate site being evaluated), and the vehicle range as input. It returns the updated temporary feasible network G_f^*, from which deviation paths among all OD pairs will be generated later. It first makes G_f^* by cloning G_f^+ and adds *k* to it. Making a copy of G_f^+ is required for later purpose because the flows coverage by G_f^* may not be higher than that of G_f^+. In those cases, G_f^+ must remain unchanged to be provided as a base in evaluating the next candidate node; otherwise *k* would have to be removed. Removing *k* requires re-evaluation of *E,* as adding *k* to *V* required subsequent updates of *E* and their associated costs. We cannot simply remove *k* and its adjacent edges because there may be edges that were included in the G_f^+ by facilities not necessarily being located at *k*. Removal of *k* and re-evaluting *E* could be achieved either by restoring a backup G_f^+ or by running algorithm 5.1 for each element of V^+. Given that cloning does not involve assessing the feasibility of links, the former should be less computationally complex than the latter. After adding a node to G_f^*, the algorithm determines feasibility of links between all pairs of *V* utilizing the property described in the previous section. When all vertices are evaluated, the algorithm returns updated G_f^*.

This section illustrated that the concept of feasible network is valid as a framework for solving a DFRLM problem. In addition, construction and management of a feasible network inevitably requires evaluation of links' feasibility. The next section provides overview and details of the implemented heuristic algorithms.

5.2 Heuristic Algorithms for DFRLM

Greedy-adding and greedy-adding with substitution algorithms were implemented to solve DFRLM problems. These algorithms were effective in solving instances of FILM, FILM with deviation cases, and FRLM (Lim and Kuby 2010; Hodgson 1990; Berman, Bertsimas, and Larson 1995). Both heuristics for the DFRLM include the all-pairs shortest path problem as a sub-problem (Algorithm 5.4). The concept of a feasible network is used in the implementation of the heuristics to account for the need of generating deviation paths while simultaneously considering vehicle range efficiently. Nevertheless, given that generation of shortest paths is computationally complex, the implemented shortest path algorithm (SP) is the main component that drives the overall efficiency of the heuristics. Implementing all available SP algorithms in the heuristics and comparing their performance was beyond the scope of this research. This research, however, employs a more efficient network storage structure than naïve structure and advanced queue storage whenever available, which were identified as efficient by Zhan(1997) and Zhan and Noon (1998).

To account for the users' need to force some facility locations into the solution, both algorithms can read in a list of forced or "fixed" locations (Algorithm 5.2). These facilities are added in the initialization stage of the algorithms.

5.2.1 *Greedy-adding Algorithm*

The greedy-adding algorithm first initializes inputs, and then adds all fixed facilities F to the current feasible network G_f^+ using algorithm 5.1. After initialization and addition of F to G_f^+, this algorithm selects an element k from candidate set K that maximizes additional flows covered. This selection procedure continues until the cardinality of solution set $|S|$ reaches the user-specified p number of facilities to build or until there are no remaining elements in K. The selection procedure consists of three main sub-procedures: adding a node to the feasible network (Algorithm 5.1 discussed in section 5.1.2), computing the shortest deviation-path distances (Algorithm 5.4 discussed in section 5.2.3), and computing the fraction of flows on deviation paths (Algorithm 5.5 discussed in sections 5.2.4 and 4.2.2). The outline of the greedy-adding algorithm can be sketched as follows:

Where w_{ij} : weight of arc(i,j)

NS : set of non-selected facility location

F : set of fixed facility location

SPD : i by j matrix of shortest path distances

DPD : $|OD|$ by $|OD|$ matrix of deviation path distances

OBJ^+ : current maximum objective value

OBJ^* : calculated temporary objective value

x : index of facility location maximizing additional flows covered

SP_DIJKSTRA(i,j,G)

: Dijkstra's shortest path algorithm that returns shortest distance from i to j on network G

Algorithm 5.2 Greedy-adding

I. Initialization

$G(N, A)$

for all $(i, j) \in A$

$w_{ij} = d_{ij}$

$K = N, S = \varnothing, NS = K, G_f^+ = \varnothing$

$S = S \cup F, NS = K - F$

for all $i, j \in N$

$SPD[i, j]$ = **SP_DIJKSTRA**(i, j, G)

II. Computation for fixed facilities

$if\ |S| > 0$

for all $s \in S$

G_f^+ =**Algorithm5.1**$(s, Range, G_f^+, S)$

next s

$DPD[o, d]$ = **Algorithm5.4**(OD, G_f^+)

OBJ^+ = **Algorithm5.5**$(DPD[o, d], SPD[i, j], DevDistDecayModel)$

III. Computation for selecting new facilities

while $(|S| < numberOfFacilties)$ **and** $(K \neq \varnothing)$ **do**

for all $k \in NS$

$G_f^* =$ **Algorithm5.1**$(k, Range, G_f^+, S)$

$DPD^*[o, d]$ = **Algorithm5.4**(OD, G_f^+)

OBJ^* = **Algorithm5.5**$(DPD[o, d], SPD[i, j], DevDistDecayModel)$

if **(**$OBJ^* > OBJ^+$)

$x = k$

$G_f^* = \varnothing$

next k

$NS = NS - \{x\}$

$S = S \cup \{x\}$

G_f^+ = **Algorithm5.1**$(x, Range, G_f^+, S)$

$DPD^+[o, d]$ = **Algorithm5.4**(OD, G_f^+)

$OBJ^+ =$ **Algorithm5.5**$(DPD[o, d], SPD[i, j], DevDistDecayModel)$

end while

return S, G_f^+, OBJ^+

5.2.2 *Greedy-adding with Substitution Algorithm*

The myopic characteristic of the greedy-adding algorithm can lead to suboptimal solutions because there is no element of looking-ahead or back-tracking. The greedy-adding with substitution algorithm, however, substitutes one of the facilities from the non-selected set *NS* for one of the facilities in solution set *S*. If such substitution improves the objective value, the algorithm keeps the substitution until the user specified number of substitution iteration is reached. If substitution does not improve objective value, substitution stops. The greedy substitution algorithm makes it possible to escape from some local maxima, though it does not guarantee it.

The foundation of the greedy-adding with substitution algorithm is the greedy-adding algorithm (Section 5.2.1). After the greedy-adding algorithm selects a new facility, a substitution procedure runs. The selection of the substituting facility uses the same selection procedure as depicted in the previous section. The only difference is the set of vertices in the feasible network excludes the newly selected facility that was chosen from the last selection procedure. This is because we know already that there is no other facility that can perform better than the newly selected facility. Below is the outline of the implemented greedy-adding with substitution algorithm.

Where OBJ^s : current maximum objective value obtained from substitution

r : index of solution set that can be substituted

NSS : set of nodes that should not be substituted

nss : index of set NSS

sx : index of solution facility that is selected by substitution

Algorithm 5.3 Greedy-adding with Substitution

```
I. Initialization                                  // See Algorithm 5.2
II. Computation for fixed facilities                // See Algorithm 5.2
III. Computation for selecting new facilities  // Same as Algorithm 5.2. before 'end while' line
III-1. Substitution                               // Runs whenever a new facility is selected
  OBJ^s = 0
  for z = 0 to numberOfIterations do
      for all r ∈ S, r ≠ x, r ∉ F do
          NSS = S − {x}, G_f^s = ∅
          for all nss ∈ NSS
              G_f^s = Algorithm 5.1(nss, Range, G_f^s, NSS)
          next nss
          for all m ∈ NS
              G_f^* = Algorithm 5.1(m, Range, G_f^s, NSS)
              DPD^*[o, d] = Algorithm 5.4(OD, G_f^s)
              OBJ^* = Algorithm 5.5(DPD[o, d], SPD[i, j], DevDistDecayModel)
              if (OBJ^* > OBJ^s)
                  OBJ^s = OBJ^*, sx = m
                  store r
              G_f^* = ∅
          next m
      next r
      if (OBJ^s > OBJ^+)
          OBJ^+ = OBJ^s, x = sx, S = S − {r} ∪ {sx}
          G_f^+ = ∅
          for all s ∈ S
              G_f^+ = Algorithm 5.1(s, Range, G_f^+, S)
          next s
      else
          break
  next z                  // End of III-1. Substitution
                          // Goes back to the first line of III.Selection
end while                 // End of III.Computation for selecting new facilities. See Algorithm 5.2.
return S, G_f^+, OBJ^+
```

5.2.3 *Calculating Deviation Path Distance on Feasible Network*

Once a temporary feasible network is updated with a candidate node (Algorithm 5.2), the next step is to generate deviation paths among OD pairs. Because each link in a feasible network not only represents the shortest path between nodes in the physical network G by design, but also its refueling feasibility is already verified while constructing the G_f, the shortest path between a pair of nodes in G_f is in effect the shortest feasible path. As is illustrated above (Section 5.1.1), the shortest feasible path could be a deviation path if the temporary solution set cannot cover flows on the physically shortest but infeasible-for-refueling-purposes path. By running an all-pairs shortest path algorithm on G_f, we can compute shortest feasible path distances among all OD pairs, and they are at the same time shortest deviation path distances.

Given that generation of shortest paths is computationally complex and the heuristics need to generate all-pairs shortest paths many times, the efficiency of the implemented shortest path algorithm (SP) is the main determinant of the overall efficiency of the heuristics. Critical implementation issues include design decisions on network storage structure and selection rule/node processing structure (Zhan 1997; Zhan and Noon 1998). This research implements Dijkstra's SP algorithm (Dijkstra 1959) and executes it to compute all OD paths from each node $v \in V$. Because the shortest feasible path must be an exact solution, heuristic SP algorithms such as A^* are not considered for implementation. Forward star structure is used for the network data storage structure, and both physical and feasible networks are modeled as weighted undirected graphs. It conforms to the round-trip assumption of the DFRLM and requires less memory space for the network. Candidate nodes are stored in a Fibonacci heap to improve the efficiency of the operations required for the SP algorithm and they are being searched by the best-first-search strategy.

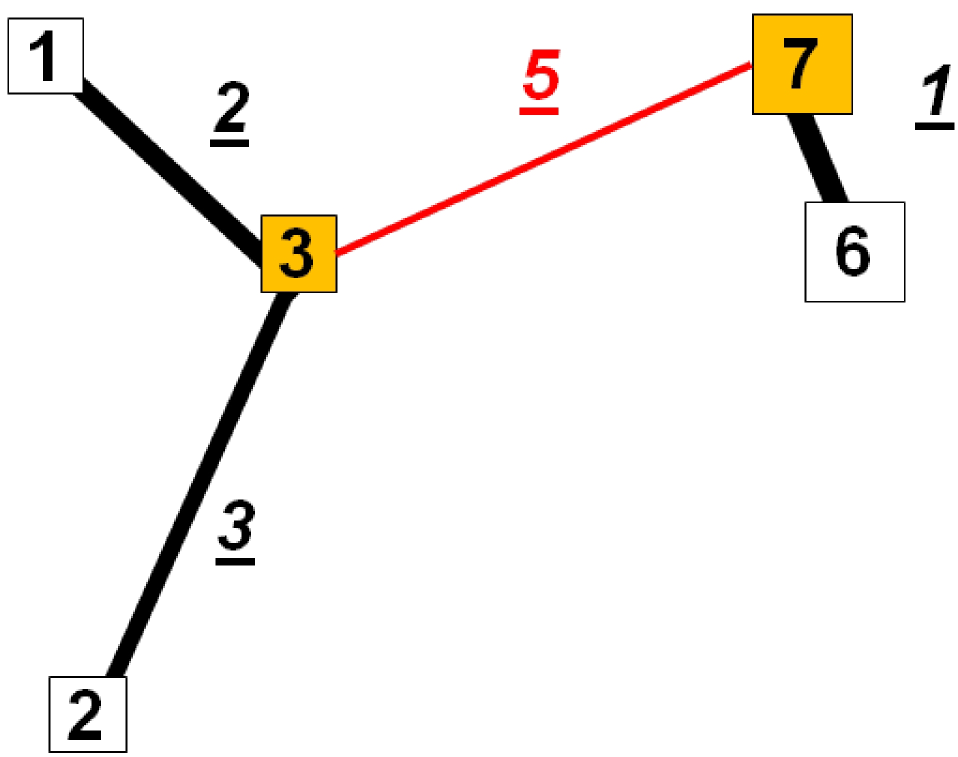

Figure 5.3 Multiple Cycles Exist in the Deviation Path for the OD pair 3-6.

After a deviation path is generated, the algorithm determines whether the path contains multiple cycles at the origin or destination and then makes sure at most one cycle exists at either ends of the path. Figure 5.3 illustrates this case with a deviation path for the OD pair 3-6. Consider that node 3 was already included in the solution and we need to evaluate the candidate node k = 7 in a feasible network with a vehicle range of 6. According to the Algorithm 5.1, an artificial shortest feasible link (colored red in the Figure) was added between node 3 and 7 because the length of the shortest path from stations 3 to7 is less than the vehicle range. Node 6 and its link to node 7 are also added to the feasible network because the length of the shortest path from station 7 to destination node 6 is less than half of the vehicle range. Note that there is no feasible link between node 3 and 6 because its length (4) is longer than half the vehicle range (6 / 2 = 3). The feasible link 3-7 actually represents the path 3-6-7 in the physical network. If we recall that DFRLM must ensure the feasibility of a round trip between an OD (Section 4.2.3), the deviation path of the OD 3-6 is 3-7-6-7-3 in the feasible network. In the physical network this translates into a path with two cycles at the destination node: 3-6-7-6-7-6-3. The first occurrence of the cycle (6-7) on the way to the destination is inevitable because there is no facility at node 6 but no one would want to make unnecessary trip to node 7 on the way back to the origin. Therefore we need to remove the redundant cycle (6-7) at the destination (i.e. the second visit to node 7). The possible cycles at the intermediate nodes of a path are not violating the assumptions of DFRLM and FRLM. Below is the outline of the implemented algorithm that generates deviation paths among all OD pairs.

Algorithm 5.4 All-Pairs Shortest Deviation Paths on Feasible Network

```
Input: OD, G_f(V, E)
For all  o ∈ V, o ∈ OD
    For all  d ∈ V, d ∈ OD
        if (o < d)
            DPD[o, d] = SP_DIJKSTRA(o, d, G_f)
            if (DPD[o, d] > SPD[o, d]) & (DD max > 0)
                DPD[o, d] = Remove Multiple Cycles(o, d, G_f)
    next d
next o
Return DPD[o, d]
```

The greedy-adding heuristic needs to run Algorithm 5.4 $\sum_{i=1}^{p}\left(|V| - i + 1\right)$ times to obtain p facilities. In the greedy-adding with substitution algorithm, the number increases up to $\sum_{i=1}^{p}\left[\left(|V| - i + 1\right) + \left\{z \times (i-1) \times (|V| - i - 1)\right\}\right]$, where z (> 1) is the number of substitution iterations. The complexity[9] of the algorithm 5.4 depends on the density of $G_f^{\ *}(V, E)$ at each iteration, which is affected by the structure of G, the deviation penalty function, the vehicle range, and the current feasible solution. Empirical results in a test setting (Section 5.3) show that the algorithm took 10 milliseconds for a temporary feasible graph $G_f^{\ *}(V, E)$ when $|V|$ = 12 and $|E|$ = 11, whereas it took 44 milliseconds[10] for $G_f^{\ *}(V, E)$ when $|V|$ = 59 and $|E|$ = 188.

---

[9] Theoretically, a Fibonacci heap implementation of Dijkstra's SP algorithm has the complexity of $O(|E| + |V| \log |V|)$.

[10] Average of 10 runs. Both have $|OD|$ of 74

5.2.4 *Computing the Fraction of Flows on Deviation Paths*

This algorithm requires as inputs the deviation path distance matrix, shortest distance matrix, upper limit of deviation distance, and deviation function model as inputs. It then computes the fraction of flows on each deviation path and outputs the $|OD|$ by $|OD|$ fraction matrix, g_{qr}. The fraction of flows is calculated from the specified distance decay function, which is modeled using user's input parameter. See above sections (4.2.2 and 4.4.2) for detailed discussion on assumptions and function types. One difference of this algorithm is that only one *shortest* deviation path is considered in the calculation for an OD pair. This became possible because we have already obtained the shortest feasible deviation path from the Algorithm 5.4. The output of the algorithm will be used to obtain the objective function value by summing the multiplication of each element of *GDD[o,d]* and f_q. Below is the general structure of Algorithm 5.5.

Where *DD* : deviation distance

DD^{max} : upper limit of deviation distance

DevDistDecayModel : a set of parameters required in defining distance decay model

CAL_GDD : a procedure that executes the distance decay model

Algorithm 5.5 Computing the Fraction of Flows on Deviation Paths

Input: $DPD[o, d]$, $SPD[i, j]$, DD^{max}, $DevDistDecayModel$

For all $o \in OD$

  For all $d \in OD$

    if $(o < d)$

      $DD = DPD[o, d]$ **-** $SPD[o, d]$

      if ($DD =< DD^{max}$)

        CAL_GDD(DD, $DevDistDecayModel$**)**

  next d

next o

Return $GDD[o, d]$

5.2.5 *Summary of the Heuristics*

Considering all above aspects, the solution approach is based on greedy adding and greedy adding with substitution heuristics that constructs a temporary "artificial refuelable network" and finds all-pairs shortest paths in each iteration. Each temporary feasible network will consist of all O-D nodes, the set of facilities chosen at previous round, and one candidate site that is under evaluation. The feasible links will represent shortest *paths* among the nodes in the actual network. The feasibility of the feasible links in the network will be determined by the property described above. In other words, the network will include only feasible links (representing paths in the physical network) that are feasible given the range. Initially distances among all O-D pairs are set to infinity and then, on each iteration, the algorithm attempts to add or substitutes a candidate facility that can maximize the flows on the feasible network that can be refueled using this facility and others already located. When evaluating each candidate facility in each iteration, creation of a new feasible network and solution of an all-pairs shortest path problem will be required to generate deviation paths. For each constructed deviation path, the detection and removal of multiple cycles at the origin or destination is required. The evaluation of each candidate needs to be done for all potential facility locations. This process will continue until the number of facilities reaches *p*.

5.3 Numerical Experiments

This section provides the experimental design and results to test the performance of the heuristics for the DFRLM using two test networks. The first test is on the 25-node network that was used above (Section 4.5). The second uses an aggregated road network for the state of Florida (Lines et al. 2007; Kuby et al. 2009), which has 302 nodes, 495 edges, 74 OD nodes, and 2,701 OD pairs with their flow volumes estimated using a gravity model (Figure 5.4). The 25-node network is small enough to obtain optimal solutions[11] and compare them with heuristics, but for the Florida network, the greedy-adding heuristic algorithm is compared with the greedy-adding with substitution heuristic.

For both networks, solutions for p = 1 to 25 were obtained while measuring the computation time of the algorithms. The upper limits of deviation distance were 10% and 50% of shortest distance; $g(DD)_{NoDecay}$ was used to model

[11] Note, however, that it took about 2,100 seconds for the branch-and-bound algorithm to generate an optimal solution for a D-FRLM problem (see section 4.6.1) with *DDmax* = 50% of shortest path and constant was used for distance decay function. In another case, Xpress-MP returned “not enough memory” error for the instance of D-FRLM with range = 8 and *DDmax* = 100% of shortest path.

the fraction of flows on deviation. For the 25-node network, three different vehicle ranges (4, 8, and 12) were used, and for the Florida state network, 100 miles was specified for the vehicle range. For the smaller 25-node test network, optimal solutions were obtained using XpressMP 7.0 software with the MILP formulation (Section 4.6). The heuristic algorithms were implemented using C# language, and ESRI ArcGIS 10.0 was used as a platform to process data, to visualize the results, and to hold the implemented component of heuristics. All the problem instances were solved on a computer with four 2.4GHz cores and 4GB memory.

It is important to clarify how the term *deviation* will be used in the experiment. The term deviation so far has been defined as the additional *distance* incurred when a customer deviates from the pre-planned trip. It should, however, be understood in a broader context so that other types of weight such as travel time can also be used to represent deviation. As was discussed earlier, this research employed two types of weight (distance and travel time). Even though a feasible network must be constructed using distance as weight because fuel is largely consumed in proportion to distance, a different type of weight (other than distance) can be used in computing the least cost paths among all OD pairs and applying penalty to the deviation flows. For the 25-node network distance was the only available weight. However, for the Florida state network, distance was used only for constructing a feasible network and travel time (measured in minutes) was used as the weight for other required computation.

In an attempt to decide a realistic deviation *time*, the flow volume data of the Florida state network were analyzed and an aspect of the travel time structure was identified. A small number (45 out of 2701) of short paths between nearby nodes account for about 75% of the total flow volumes, of which the origin and destination nodes are clustered around four metropolitan areas: Miami, Orlando, Tampa, and Jacksonville. Table 8 shows a travel time characteristic of those high-volume paths, where the travel-time on high-volume paths is on average 30 minutes. In identifying the effect of specifying different distance-decay functions, two different scenarios were devised and their solutions were compared for the Florida state network. For the penalty functions, one problem set applied $g(DD)_{NoDecay}$ to the flows whereas a linear function $g(DD)_{linear}$ with beta of 1 was applied to the other problem set.

Table 5.1 Travel Time Characteristics of High-Volume Paths in the Florida Network

Count	Travel Time (minutes)			
	Minimum	Maximum	Average	Standard Deviation
49	6.5	60.0	29.6	12.85

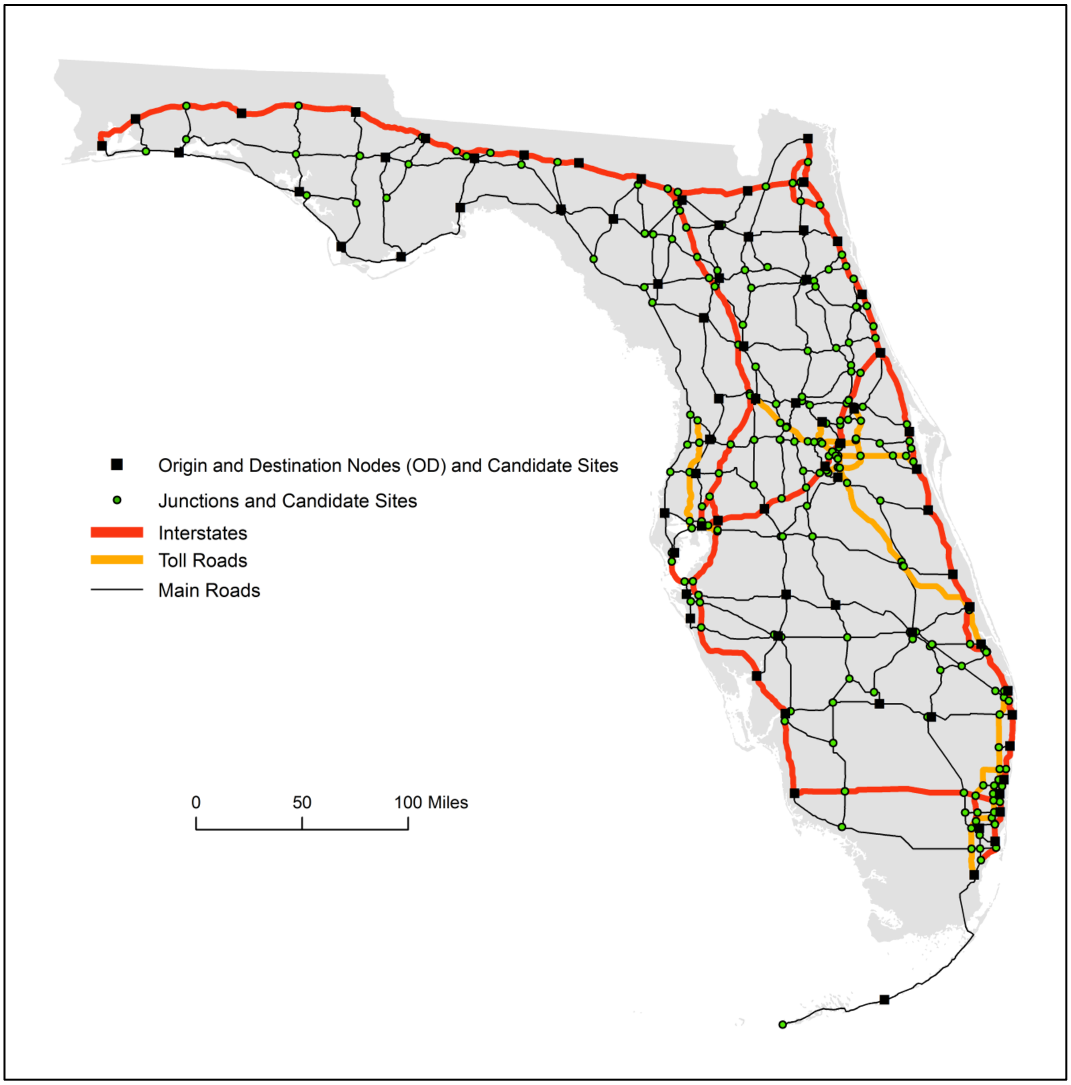

Figure 5.4 Florida State Network.

5.3.1 *Test on the 25 Node Network*

5.3.1.1 Solution Time

The greedy-adding heuristic was, as expected much faster than greedy with substitutions in all instances. Note that greedy with substitution heuristics output in a similar time regardless of the number of substitution iterations. This can be interpreted that only one iteration of substitution was mostly enough to reach the maximum possible improvement given that the substitution is not replacing multiple facilities at a time. Exact solutions were found fairly quickly for smaller problems (23.24 seconds for *DDmax* = 10% of SP). However, as the problem size increased the exact solution time increased substantially (2,661 seconds for *DDmax* = 50% of SP), and considering the small size of the test network, this result suggests the necessity of using the heuristics for bigger problems.

Table 5.2 Computation Time for 25-Node Network

Range	*DDmax*, Distance Decay Function	Computation Time (CPU seconds)					
		Optimal	Greedy	Greedy Sub 1 Iteration	Greedy Sub 2 Iterations	Greedy Sub 3 Iterations	Greedy Sub 4 Iterations
4	10% of SP, No Decay	2.13	< 1	3	4	4	4
	50% of SP, No Decay	72.87	< 1	3	4	4	4
8	10% of SP, No Decay	13.20	< 1	7	8	8	8
	50% of SP, No Decay	1605.53	< 1	7	8	8	8
12	10% of SP, No Decay	23.24	1	9	10	10	11
	50% of SP, No Decay	2660.54	1	9	10	10	11

5.3.1.2 Optimality Gap

The objective values of optimal solutions were compared with the results from heuristics and are summarized in Tables 5.3-5.7. The greedy-adding heuristic (GRD) obtained the optimal solutions three times when the vehicle range is small. The maximum gap of 61.92% was observed when vehicle range is four and p is small (p =< 4). As the vehicle range becomes longer, the GRD performed well for solving the problems by providing high objective function values. Specifically, with vehicle range of 8, it found more optimal solutions (72% of time when DDmax = 10% SP, 52% of the time for DDmax = 50% SP) than it did when the range was 12 (52% of time when DDmax = 10% SP, 64% of the time for DDmax = 50% SP). The average optimality gap for range = 4 is 28% but it drops dramatically for vehicle ranges of eight and twelve (0.25% ~ 0.92%).

The optimality gap decreased as the number of substitution iterations increased. It was clearly illustrated in the results that substitutions enhanced the objective. For example, with *DDmax* = 10% of SP and vehicle range = 8, the solutions of exact and greedy-adding with substitution heuristic (GRD-Sub) were the same until p = 7. When selecting 8 facilities, the exact algorithm added nodes 4, 8, and 10 replacing 12 and 13. On the other hand, GRD-Sub added 8 and replaced 2 with 4. It found the optimal solution by adding 10 for p = 9.

As the substitution iterations increase, the GRD-Sub algorithm performed well even for solving problems of range = 4. The poor performance of the GRD algorithm especially for problem instances of vehicle range = 4 is mainly because there is no swapping or replacing procedure after a facility is selected, and therefore a facility or a set of facilities that performed well previously may not be the best one to provide larger coverage in combination with facilities that are selected later. The GRD-Sub was expected to address this problem and in fact the result shows that the GRD-Sub algorithm (especially with 3 and 4 iterations) found optimal solutions 17 out of 22 times ($p > 3$). The GRD-Sub algorithm, however, did not always find optimal solution because the substitution was carried out one facility at a time, whereas the exact algorithm explorers the entire branch and bound tree.

We can observe a special case with the range = 12 (Table 5.5 and 5.8), where the solutions of heuristics had higher objective values than exact solution. The reason for this abnormality lies in the difference of input data. The KSP algorithm implemented to generate paths for the Xpress model generates a large number of paths, but did not generate *all* possible deviation paths. For example, in the case of *DDmax* = 50% of SP, both exact and heuristic algorithms had the same solution $S = \{4, 10, 12, 14, 17, 20\}$ for $p = 6$, but there were some paths only the heuristic identified as feasible. By the solution set *S*, OD pair 9-11 whose shortest path is 9-8-11 is actually feasible by taking deviation path 9-10-13-11-12-11. This path, *which contains a cycle*, was not generated by the KSP algorithm used in this research. As a result the exact algorithm chose another facility, which resulted in an inferior solution.

Table 5.3 Optimal Objective Value and Optimality Gap (*DDmax:* 10% of SP, $g(DD)_{NoDecay}$, Range = 4)

p	Optimal Objective Function Value (%)	Optimality Gap (%)				
		Greedy	Greedy Sub 1 Iteration	Greedy Sub 2 Iterations	Greedy Sub 3 Iterations	Greedy Sub 4 Iterations
1	4.92	-	-	-	-	-
2	6.31	0.63	0.63	0.63	0.63	0.63
3	12.49	48.20	48.20	48.20	48.20	48.20
4	20.38	61.92	46.47	5.54	-	-
5	27.54	53.01	-	-	-	-
6	34.01	32.70	12.85	12.85	-	-
7	41.41	24.34	19.13	19.13	-	-
8	45.26	26.16	22.27	22.27	3.62	3.62
9	53.60	33.40	33.40	33.40	11.42	11.42
10	55.97	33.18	33.18	33.18	12.02	12.02
11	59.82	37.48	35.49	34.37	-	-
12	61.69	34.67	31.87	29.89	-	-
13	62.72	31.92	30.21	28.59	0.89	0.89
14	65.12	30.18	30.18	30.16	1.84	1.84
15	67.89	30.76	30.76	30.76	-	-
16	69.77	31.63	31.63	31.63	-	-
17	71.30	33.10	33.10	33.10	-	-
18	71.99	33.70	33.09	33.09	-	-
19	73.53	34.37	34.37	34.37	-	-
20	74.22	34.98	26.57	16.15	-	-
21	74.22	26.57	14.08	-	-	-
22	74.68	16.54	-	-	-	-
23	74.78	14.59	-	-	-	-
24	74.78	-	-	-	-	-
25	74.78	-	-	-	-	-

Table 5.4 Optimal Objective Value and Optimality Gap (*DDmax:* 10% of SP, $g(DD)_{NoDecay}$, Range = 8)

p	Optimal Objective Function Value (%)	Optimality Gap (%)				
		Greedy	Greedy Sub 1 Iteration	Greedy Sub 2 Iterations	Greedy Sub 3 Iterations	Greedy Sub 4 Iterations
1	17.13	-	-	-	-	-
2	32.58	-	-	-	-	-
3	44.41	-	-	-	-	-
4	55.97	-	-	-	-	-
5	63.52	-	-	-	-	-
6	68.08	-	-	-	-	-
7	72.32	-	-	-	-	-
8	77.87	3.98	3.12	3.12	3.12	3.12
9	82.77	1.21	-	-	-	-
10	90.06	-	-	-	-	-
11	94.41	-	-	-	-	-
12	96.80	-	-	-	-	-
13	97.78	-	-	-	-	-
14	98.43	-	-	-	-	-
15	98.74	-	-	-	-	-
16	99.71	-	-	-	-	-
17	99.77	-	-	-	-	-
18	99.86	0.09	0.09	0.09	0.09	0.09
19	99.92	0.15	0.15	0.15	0.15	0.15
20	99.92	0.15	0.15	0.15	0.15	0.15
21	99.92	0.15	0.15	0.15	0.15	0.15
22	99.92	0.15	0.15	0.15	0.15	0.15
23	99.92	0.15	0.15	0.15	0.15	0.15
24	99.92	0.15	-	-	-	-
25	99.92	-	-	-	-	-

Table 5.5 Optimal Objective Value and Optimality Gap (*DDmax*: 10% of SP, $g(DD)_{NoDecay}$, Range = 12)

p	Optimal Objective Function Value (%)	Optimality Gap (%)				
		Greedy	Greedy Sub 1 Iteration	Greedy Sub 2 Iterations	Greedy Sub 3 Iterations	Greedy Sub 4 Iterations
1	18.23	-	-	-	-	-
2	34.34	-	-	-	-	-
3	47.90	-	-	-	-	-
4	58.14	-	-	-	-	-
5	67.70	-	-	-	-	-
6	75.00	0.36	0.36	0.36	0.36	0.36
7	82.68	2.03	2.03	2.03	2.03	2.03
8	88.83	4.31	4.03	1.80	-	-
9	92.93	3.85	1.73	-	-	-
10	96.83	4.61	-	-	-	-
11	97.81	2.64	-	-	-	-
12	98.66	1.85	-	-	-	-
13	99.30	1.50	-	-	-	-
14	99.85	1.19	-	-	-	-
15	<u>99.85</u>	0.55	<u>-0.08</u>	<u>-0.08</u>	<u>-0.08</u>	<u>-0.08</u>
16	100.00	0.15	-	-	-	-
17	100.00	0.07	-	-	-	-
18	100.00	-	-	-	-	-
19	100.00	-	-	-	-	-
20	100.00	-	-	-	-	-
21	100.00	-	-	-	-	-
22	100.00	-	-	-	-	-
23	100.00	-	-	-	-	-
24	100.00	-	-	-	-	-
25	100.00	-	-	-	-	-

Table 5.6 Optimal Objective Value and Optimality Gap (*DDmax:* 50% of SP, $g(DD)_{NoDecay}$, Range = 4)

p	Optimal Objective Function Value (%)	Optimality Gap				
		Greedy	Greedy Sub 1 Iteration	Greedy Sub 2 Iterations	Greedy Sub 3 Iterations	Greedy Sub 4 Iterations
1	4.92	-	-	-	-	-
2	6.31	0.63	0.63	0.63	0.63	0.63
3	12.49	48.20	48.20	48.20	48.20	48.20
4	20.38	61.92	46.47	5.54	-	-
5	27.54	50.98	-	-	-	-
6	34.01	28.61	12.85	12.85	-	-
7	41.41	19.80	15.33	15.33	-	-
8	45.26	21.94	18.63	18.63	3.36	3.36
9	53.60	32.09	30.35	30.35	7.67	7.67
10	56.08	32.17	32.17	32.17	8.29	8.29
11	62.36	39.00	35.50	32.44	-	-
12	64.41	36.44	30.29	30.29	-	-
13	65.26	33.59	28.84	28.84	0.37	0.37
14	67.66	31.84	30.15	30.15	2.68	2.68
15	70.44	32.34	32.21	32.21	-	-
16	72.48	33.13	33.13	33.13	-	-
17	74.02	34.52	34.52	34.52	-	-
18	74.84	35.20	34.61	34.61	-	-
19	75.47	35.03	35.03	35.03	-	-
20	76.28	35.72	27.28	16.49	-	-
21	76.28	27.28	14.41	-	-	-
22	76.75	16.89	-	-	-	-
23	76.84	14.90	-	-	-	-
24	76.84	-	-	-	-	-
25	76.84	-	-	-	-	-

Table 5.7 Optimal Objective and Optimality Gap (*DDmax:* 50% of SP, $g(DD)_{NoDecay}$,, Range = 8)

p	Optimal Objective Function Value (%)	Optimality Gap (%)				
		Greedy	Greedy Sub 1 Iteration	Greedy Sub 2 Iterations	Greedy Sub 3 Iterations	Greedy Sub 4 Iterations
1	17.13	-	-	-	-	-
2	32.58	-	-	-	-	-
3	44.41	-	-	-	-	-
4	56.08	-	-	-	-	-
5	64.06	-	-	-	-	-
6	71.61	-	-	-	-	-
7	74.40	0.82	0.82	0.82	0.82	0.82
8	84.56	6.62	-	-	-	-
9	92.18	-	-	-	-	-
10	95.99	-	-	-	-	-
11	98.25	-	-	-	-	-
12	98.76	-	-	-	-	-
13	99.03	-	-	-	-	-
14	99.45	0.33	0.33	0.33	0.33	0.33
15	99.72	0.51	-	-	-	-
16	99.81	-	-	-	-	-
17	99.87	0.02	0.02	0.02	0.02	0.02
18	99.96	0.11	0.11	0.11	0.11	0.11
19	100.00	0.15	0.15	0.15	0.15	0.15
20	100.00	0.15	0.15	0.15	0.15	0.15
21	100.00	0.15	0.15	0.15	0.15	0.15
22	100.00	0.15	0.15	0.15	0.15	0.15
23	100.00	0.15	0.15	0.15	0.15	0.15
24	100.00	0.15	-	-	-	-
25	100.00	-	-	-	-	-

Table 5.8 Optimal Objective Value and Optimality Gap (*DDmax:* 50% of SP, $g(DD)_{NoDecay}$, Range = 12)

p	Optimal Objective Function Value (%)	Optimality Gap (%)				
		Greedy	Greedy Sub 1 Iteration	Greedy Sub 2 Iterations	Greedy Sub 3 Iterations	Greedy Sub 4 Iterations
1	18.23	-	-	-	-	-
2	34.34	-	-	-	-	-
3	49.04	-	-	-	-	-
4	62.64	-	-	-	-	-
5	72.46	-	-	-	-	-
6	81.80	-0.43	-0.43	-0.43	-0.43	-0.43
7	91.46	1.80	1.80	1.80	1.80	1.80
8	95.61	2.69	1.33	-0.36	-0.36	-0.36
9	97.59	2.35	-	-	-	-
10	98.97	2.08	0.16	0.16	0.16	0.16
11	99.54	1.50	-	-	-	-
12	99.80	0.99	-	-	-	-
13	99.85	0.31	-0.04	-0.04	-0.04	-0.04
14	99.95	0.15	-	-	-	-
15	100.00	0.11	-	-	-	-
16	100.00	0.05	-	-	-	-
17	100.00	-	-	-	-	-
18	100.00	-	-	-	-	-
19	100.00	-	-	-	-	-
20	100.00	-	-	-	-	-
21	100.00	-	-	-	-	-
22	100.00	-	-	-	-	-
23	100.00	-	-	-	-	-
24	100.00	-	-	-	-	-
25	100.00	-	-	-	-	-

5.3.2 *Test on the Florida State Network*

5.3.2.1 Tradeoff between Objective Gain and Time

Results for the Florida state network are summarized in Tables 5.9-5.10. The greedy-adding with substitution algorithms (GRD-Sub) produced better solutions with more coverage than greedy-adding heuristic (GRD) in most cases, yet with substantial increase of computation time. For example, compared with GRD, the GRD-Sub1 produced non-inferior solutions in 24 out of 25 (96%) of cases, but computation time increased in the order of 20 more times (see section 5.2.3 for a way to estimate solution time). When the *DDmax* was set at 10% of SP, the maximum substitutions in selecting a facility was 3, and therefore GRD-Sub3 and -Sub4 all yielded the same solutions in similar computation times. Likewise, in the case of *DDmax* = 50% of SP, up to three facilities were replaced within a given four iterations.

As the *DDmax* increased from 10% of SP to 50% of SP, the solution time increased 1.2~1.6 times (Tables 5.9-5.10). The objective gain from the increase in *DDmax* ranges between 0.67% and 6.74% with an average of 3.6%. The maximum gain was observed when the algorithms found a small number of facilities (p = 3 ~ 8). This result confirms that drivers will need more deviations (or need to be more tolerant to deviation) when there are fewer stations.

5.3.2.2 Inner Dynamics of Substitutions

The inner dynamics of how the substitution algorithm selects and replaces facilities is worth describing. Specified with *DDmax* = 50% of SP (See Table 5.10), the Grd-Sub1 improved the solution for p=3 by replacing one facility in iteration 3 and 4. But the solution for *p*=5 from GRD-Sub1 became inferior to GRD's because of the added facilities. At that moment, there were three different facilities between the two solutions and replacing one facility in the solution would not improve, and therefore GRD-Sub1 could not find the same set of facilities as GRD found. However, for the remainder of the iterations the GRD-Sub1 produced better solutions than GRD by adding facilities to the once-inferior set.

The optimal locations found by GRD-Sub1 and GRD-Sub-2 diverged at iteration 3, where GRD-Sub2 made 2 substitutions, and then the two algorithms converged back at the very next iteration 4, where both found the same set of facilities by GRD-Sub1's one-step late substitution of the same facility as GRD-Sub2 did at the previous iteration. The solution became different again at iteration 15, but GRD-Sub1 soon caught up GRD-Sub2 in iteration 17 by replacing three facilities in three iterations, which GRD-Sub2 did the same in two iterations. They finally ended up having the same set of facilities at p = 17. This catching-up of GRD-Sub by multiple-step substitution is observed in other cases.

Table 5.9 Greedy Results: *DDmax* = 10% of SP, Range = 100 mi.

p	Grdy (%)	Time (s)	Grdy Sub-1 (%)	Time (s)	Grdy Sub-2 (%)	Time (s)	Grdy Sub-3 (%)	Time (s)	Grdy Sub-4 (%)	Time (s)
1	30.90	<1.00	30.90	<1.00	30.90	<1.00	30.90	<1.00	30.90	<1.00
2	43.19	<1.00	43.19	1	43.19	1	43.19	1	43.19	1
3	52.81	1	***53.88***	3	***54.56***	4	***55.50***	6	55.50	7
4	62.09	2	61.15	6	61.09	8	***61.61***	10	61.61	11
5	68.21	3	68.21	12	67.20	13	66.86	16	66.86	17
6	72.19	4	72.19	19	***72.45***	21	70.84	25	70.84	24
7	76.10	5	76.10	29	***76.43***	31	76.43	53	76.43	51
8	79.25	7	79.25	41	***79.58***	43	79.58	66	79.58	62
9	81.22	9	81.22	55	***81.88***	58	81.88	81	81.88	77
10	82.84	10	***82.89***	71	***83.55***	93	83.55	116	83.55	110
11	84.39	12	***84.44***	91	***85.10***	115	85.10	138	85.10	131
12	85.76	14	***85.84***	116	***86.50***	141	86.50	165	86.50	156
13	87.07	16	***87.21***	145	***87.87***	173	87.87	196	87.87	187
14	88.39	18	***88.46***	177	***89.12***	207	89.12	230	89.12	220
15	89.60	21	***89.86***	215	***90.32***	325	90.32	350	90.32	335
16	91.04	23	***91.13***	277	***91.47***	405	91.47	431	91.47	414
17	92.19	27	***92.28***	364	***92.44***	493	92.44	520	92.44	501
18	93.12	32	***93.26***	459	***93.37***	682	93.37	713	93.37	687
19	93.78	38	***93.90***	560	***94.01***	785	94.01	817	94.01	788
20	94.42	45	***94.52***	685	***94.63***	913	94.63	946	94.63	914
21	95.04	52	***95.15***	818	***95.26***	1048	95.26	1082	95.26	1047
22	95.55	59	***95.70***	963	***95.80***	1195	95.80	1229	95.80	1191
23	95.94	66	***96.21***	1116	***96.31***	1350	96.31	1384	96.31	1343
24	96.31	73	***96.68***	1279	***96.69***	1513	96.69	1547	96.69	1503
25	96.67	80	***97.00***	1451	***97.01***	1685	97.01	1719	97.01	1672

Table 5.10   Greedy Results: *DDmax* = 50% of SP, Range = 100 mi.

p	Grdy (%)	Time (s)	Grdy Sub-1 (%)	Time (s)	Grdy Sub-2 (%)	Time (s)	Grdy Sub-3 (%)	Time (s)	Grdy Sub-4 (%)	Time (s)
1	31.57	<1.00	31.57	<1.00	31.57	<1.00	31.57	<1.00	31.57	<1.00
2	47.07	<1.00	47.07	1	47.07	1	47.07	1	47.07	1
3	56.69	1	***58.27***	3	***58.94***	5	58.94	6	58.94	6
4	65.30	2	***66.98***	7	66.98	9	66.98	10	66.98	10
5	73.34	3	72.33	13	72.33	15	72.33	16	72.33	16
6	77.36	4	***77.58***	20	77.58	22	77.58	23	77.58	23
7	80.92	6	***81.13***	30	81.13	32	81.13	32	81.13	33
8	83.53	7	***83.90***	42	83.90	56	83.90	55	83.90	57
9	85.50	9	***86.37***	58	86.37	72	86.37	70	86.37	74
10	87.00	10	***87.86***	78	87.86	92	87.86	90	87.86	95
11	88.49	13	***89.35***	112	89.35	159	89.35	155	89.35	161
12	89.95	15	***90.85***	156	90.85	203	90.85	199	90.85	205
13	91.10	19	***91.87***	217	91.87	264	91.87	258	91.87	266
14	92.17	23	***92.88***	287	92.88	334	92.88	328	92.88	337
15	93.14	28	***94.18***	367	***94.19***	493	***94.24***	562	94.24	655
16	94.47	34	***95.20***	464	***95.25***	684	95.25	660	95.25	754
17	95.30	40	***96.07***	579	96.07	801	96.07	776	96.07	871
18	95.97	47	***96.72***	705	96.72	927	96.72	901	96.72	998
19	96.62	54	***97.20***	843	97.20	1195	*97.20*	1166	97.20	1266
20	97.10	61	***97.58***	990	97.58	1341	97.58	1312	97.58	1412
21	97.48	68	***97.91***	1148	97.91	1499	97.91	1468	97.91	1570
22	97.86	75	***98.23***	1315	98.23	1827	98.23	1794	98.23	1898
23	98.22	83	***98.52***	1495	98.52	2175	98.52	2139	98.52	2245
24	98.48	90	***98.74***	1682	98.74	2362	98.74	2324	98.74	2434
25	98.70	98	***98.92***	1897	98.92	2577	98.92	2538	98.92	2648

5.3.2.3 Effects of Different Distance-Decay Functions

The choice of distance-decay function affects not only objective values but also spatial distribution of the solutions. The solutions for the function $g(DD)_{NoDecay}$ with *DDmax* set at 50% SP obviously provided more coverage than those for the function $g(DD)_{linear}$ in all cases. The biggest gap of the objective value (2.62%) was observed when $p = 4$, and the solutions are interestingly disjoint (Figure 5.5).

One sharp contrast in the results of the two penalty functions is that $g(DD)_{linear}$ introduces partial coverage of the flows. The yellow highlighted path on the left map (Figure 5.5) is the shortest-time path from Manatee to a destination node near Kennedy Space Center. The flows of this OD pair were estimated to be partially (85%) covered by the facilities at nodes 107 and 183. Note that the solution in the left map served 143 flows (shown in aqua) and 55 of them (61%) were partially covered, whereas all the served flows on the right map were fully covered.

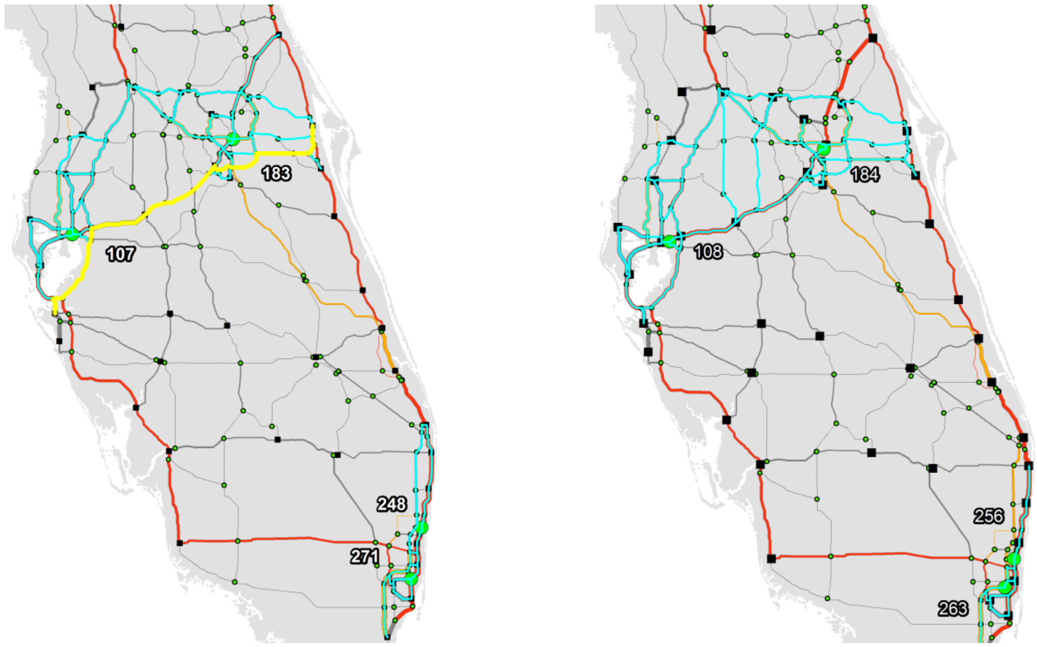

Figure 5.5 Disjoint solutions for $p = 4$; left: $g(DD)_{linear}$, right: $g(DD)_{NoDecay}$

These partially covered flows leave behind uncovered flows that need to be served by other facilities. The amount of these remaining flows depends on the specification of the deviation function and it will have some effect in determining spatial distribution of facilities. Let us illustrate this case using previous solutions. Suppose we force the heuristics to select three facilities (184, 256, 263) from the solution in the right map and then run the DFRLM GRD-Sub3 to select the fourth facility for $p = 4$ with $g(DD)_{linear}$. Basically this evaluates the incremental coverage gain by locating one additional facility at one of the remaining candidate nodes. The GRD-Sub3 added a facility at 107 (not 108) as the fourth facility and the objective became inferior to the optimal one in the left map by 3.57% point.

Another example can be presented. If a facility was built at one of the nodes the yellow path is made of, the fraction of the flows on a new (deviation) path would increase if $g(DD)_{linear}$ was used to estimate covered flows. But the contribution estimated by $g(DD)_{NoDecay}$ would remain the same since it is a binary function and all the flows were already counted towards the objective.

This result implies that a rollout plan for the refueling station network would benefit from a careful estimation of drivers' sensitivity to the required deviation at each development phase. Such practice is important not only because drivers' willingness to deviate may change as the refueling network and alt-fuel vehicle market become mature but because how the deviation behavior is modeled affects the optimal facility locations.

5.3.2.4 Comparison of DFRLM with FRLM

The results from DFRLM and FRLM[12] greedy heuristics were compared. In a previous section (4.6.4), the effects of multiple shortest paths on the exact solutions of FRLM were discussed where DFRLM was reduced to FRLM-MSP by specifying $DDmax = 0$. There is, however, extremely little chance that real-world network have multiple shortest-distance or shortest-time paths. It would be more of a matter of data precision. Therefore, a very small number (30 seconds) was set for *DDmax* so that anyone would regard it as negligible deviation. A linear function $g(DD)_{linear}$ was used for the deviation decay function in order to identify such an OD pair whose flows are partially covered.

---

[12] A more complete discussion on the FRLM results from various scenarios is detailed in Kuby et al. (2009).

Figure 5.6 shows the solutions for p = 2 from the heuristics[13], where both selected node 256 that refuels heavy flows with full coverage. FRLM GRD-Sub3 chose 270 as another facility but DFRLM GRD-Sub3 selected 271. Because the flows of the OD pair 266-270 were important to cover and its shortest travel-time path is 266-270, FRLM located a facility at 270 to fully cover its flows. DFRLM also served the flows but with partial coverage (99%) by assuming drivers would take the deviation path (266-271-270) that requires a little more time (< 16 seconds) to travel. Given that the shortest-travel time for the OD pair is 20 minutes, this deviation should be negligible. The facility at 271 also covered another heavy-traffic path of OD pair 257-266, which the FRLM solution could not cover. Instead, the FRLM solution covered flows on 270-273. There were other 20 OD pairs whose flows were fully covered by both solutions. By allowing 30 seconds of deviation, DFRLM provided a solution for p =2 that can provide more coverage (0.6% point) than FRLM.

[13] The greedy-adding with 3 substitutions was used for both sets of problem instances. The maximum number of substitutions was two and it was observed when solving p=17. Therefore there would be no further improvement in objective with more substitution iterations.

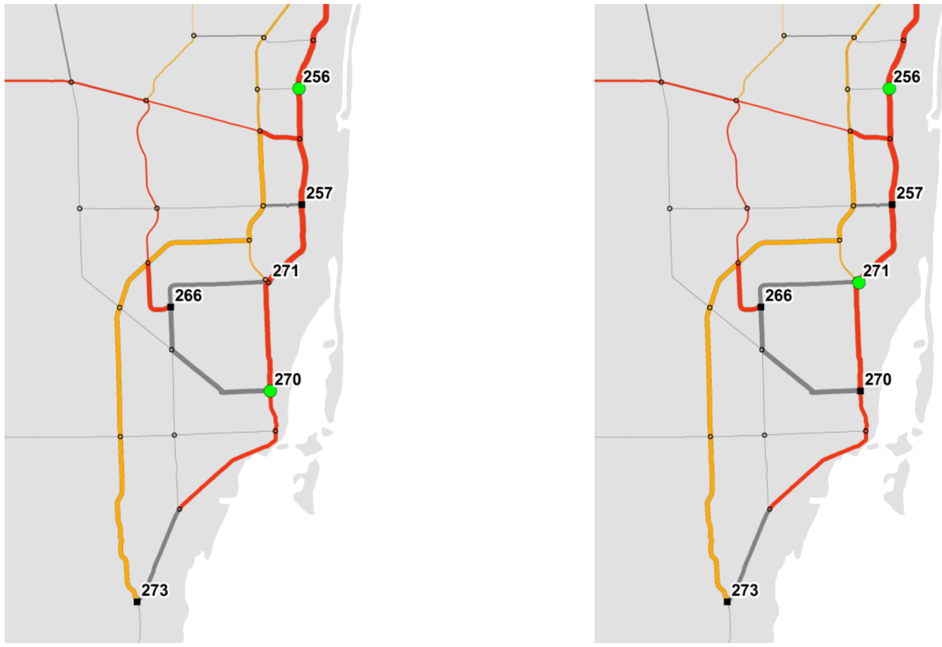

Figure 5.6 Different Solutions for p = 2 from FRLM (left) and DFRLM (right).

: Selected Sites

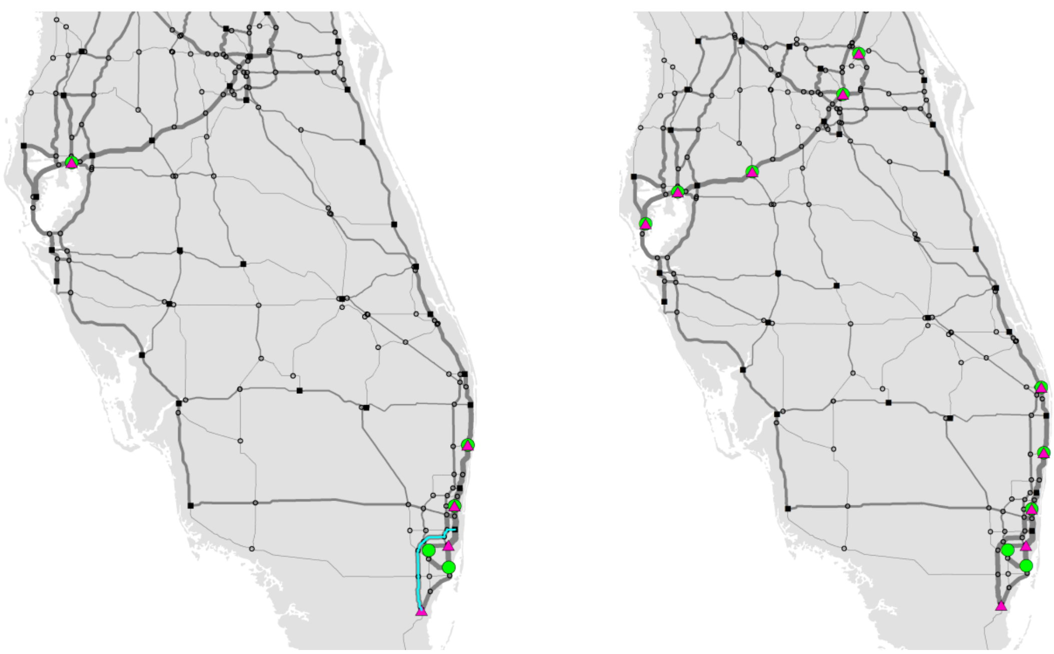

Figure 5.7 Different Solutions for p = 5 (left) and p = 10 (right).

: FRLM, : DFRLM

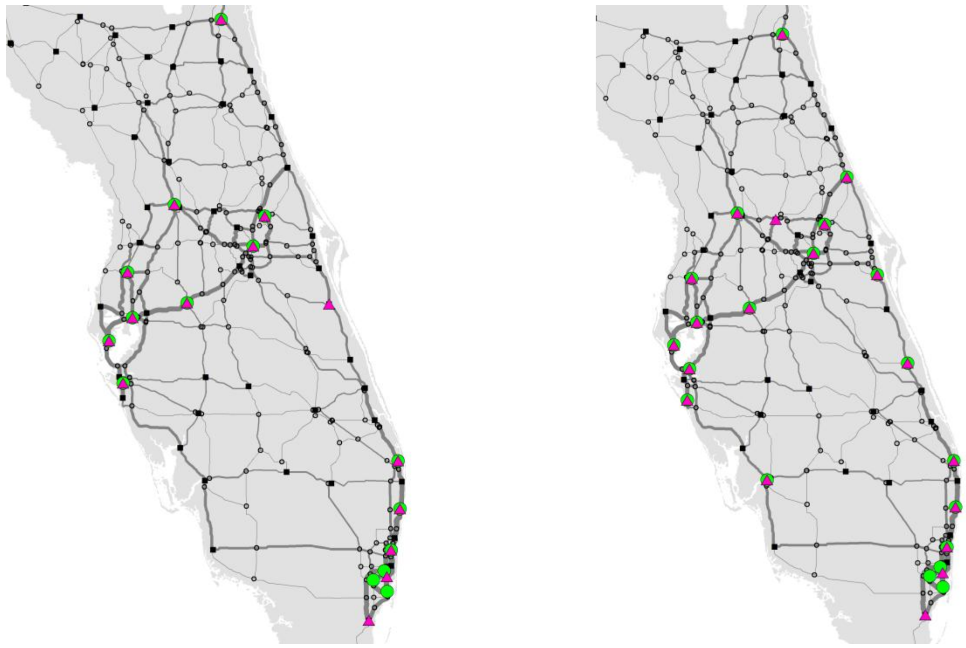

Figure 5.8 Different Solutions for *p* = 15 (left) and *p* = 20 (right).

: FRLM, : DFRLM

Figures 5.7-5.8 show optimal locations for *p* = 5, 10, 15 and 20 obtained from FRLM and DFRLM. For *p* = 5, both models located four facilities in the Miami metropolitan area and one in Tampa. Note that a subset of FRLM solution $\{266, 277\}$ and another subset of DFRLM solution $\{271, 273\}$ are disjoint (see Figure 5.6 for node number). Unlike the FRLM, which located the two facilities (266 and 270) in the central Miami to fully cover the heavy traffic among big population centers, DFRLM located a station further south along the coast (273) to cover additional flows of the OD pair 257-273[14] in addition to all the OD pairs

[14] The shortest-time path of this OD pair is highlighted in Figure 5.7. Note that this path does not pass one of the FRLM solution facilities.

that FRLM could. With this difference, the DFRLM solution refueled more flows. The two disjoint sets remain selected in the solutions all the way up to p = 20 (Figure 5.7-5.8). If we assume 30 seconds of deviation is acceptable to all the drivers, the latter subset of facilities from DFRLM is arguably superior to the former subset from FRLM because the objective function of DFRLM solutions were higher all the cases.

The solutions for p = 10 from the two models were the same except the disjoint two subsets. The added four facilities provided a corridor connecting Tampa-St. Petersburg and Orlando metropolitan areas. The difference in solutions for p = 15 is that DFRLM located a station in Brevard County near the east coast and this station made the long trip from Miami to Orlando feasible. On the other hand, FRLM located one more station in the Miami area. For 20 stations, DFRLM once again added a facility in Lake County northwest of Orlando that could provide additional service to the trips from the county to its near areas while the remaining stations could refuel the same flows as the solution from FRLM.

FRLM results have been compared with the results from DFRLM with negligible deviation. Overall the order and location of stations from the two models were similar. Nevertheless, the comparison showed that the introduction of deviations will have effect on the optimal station locations as well as on the objective function.

5.4 Conclusions and Future Research

Greedy-adding and greedy-adding with substitution heuristic algorithms are developed for solving real-world DFRLM problems. The heuristics are based on the concept of a feasible network, where traveling on its arcs is feasible by refueling at *p* facilities located at its nodes. The procedures in the heuristic efficiently generate all shortest deviation paths among all OD pairs given the vehicle range and probability of deviation while removing unrealistic multiple cycles at origins or destinations. Both heuristics are sub-optimal and the optimality gap decreases as substitution iteration number or vehicle range increases. Comparison of the two heuristics showed that substitutions enhance the objective with the cost of increased solution time, of which generation of all-pairs shortest paths on feasible network takes the most.

The choice of deviation decay function and maximum allowed deviation both have effects on solutions quality and optimal facility locations. Therefore, careful modeling of deviation behavior in practice is suggested. For example, the infrastructure developers and government agency will need to answer how sensitive potential (and actual) AFV drivers are to the required deviations. Such assessment may be required in every important phase of the infrastructure development.

More research is necessary to extend the reliability and usability of the DFRLM heuristics. Evaluation of refueling feasibility needs to take into account more diverse refueling behavior such as home-refueling, work-refueling, or refueling within a time window. It is expected that if candidates are not restricted at nodes and they are numerous “enough” relative to vehicle range, the optimality gap will decrease as in Kuby and Lim (2007). Future implementation of different algorithms for solving the most time-consuming sub-problem in the heuristics will reduce computational effort and may provide more competitive performance.

6 AN INTEGRATION OF POTENTIAL DEMAND FOR ALTERNATIVE-FUEL VEHICLES WITH O-D TRIP DATA

Geographically uneven demand for alternative-fuel vehicles (AFV) needs to be integrated into the flow-based location models to account for early AFV demand pattern. Melendez and Milbrandt (2006) were first to use GIS to model uneven hydrogen demands of United States using variables obtained by census boundary. Their method is based on a suitability analysis (McHarg 1969) and map algebra (Tomlin 1990). Since they converted nationwide census tracts into a raster format by applying a 20 by 20 mile grid, their approach is prone to the modifiable areal unit problem (Openshaw and Taylor 1981). The implicit assumption in doing so is that households are evenly distributed within each grid, which may not be the case considering the real world population distribution and the relatively large size of the grid. Instead, we suggest that using the smallest unit as consistently as possible in a vector format and apply an areal interpolation method if needed.

Given that flow-based location models require data on flow volumes of OD pairs, a method to weight the flow volumes to reflect estimated demand is needed. Such weighted flows can be used as input for the location models, and as a result refueling service can be provided at more convenient locations for the likely early AFV drivers. This research proposes and explores a method to integrate AFV demand and OD flow volume.

This chapter is comprised of detailed discussion of the methods and steps used in integrating AFV demand and OD flow volume. Section 6.1 reviews previous approaches to estimating AFV demand using GIS. Section 6.2 starts with description of the data used; discusses a modified method to estimate AFV demand; presents a framework to analyze the sensitivity of the estimation model; and proposes a process to integrate estimated demand density and trip flows. Section 6.3 describes results and it is followed by conclusions in section 6.4.

6.1 Geographically Uneven Demand for AFV

Without available data on flow volume of AFVs, previous research devised methods to estimated consumer demand for AFVs (see 2.2.1 for detail). Unlike most models that assume spatially uniform distribution of demand, Melendez and Milbrandt (2006) of the National Renewable Energy Laboratory (NREL) used GIS to estimate consumer demand for hydrogen (H2) vehicles across the US based on geographical distribution. The demand was assumed to be proportional to the estimated "composite score" of a spatial unit (Figure 6.1). To obtain the scores, they first identified key attributes affecting consumer acceptance of hydrogen vehicles. Such attributes include income, education level, the number of vehicles they own, and policy. Each attribute was standardized by assigning a classification rank score, and weights were assigned to each attribute to acquire composite score. The attributes/variables they used and the weights on the variables were based on the consensus judgments of a panel of experts convened by NREL for this purpose. This result of the linearly weighted sum was expected to represent relative likelihood of a consumer's purchasing a hydrogen vehicle.

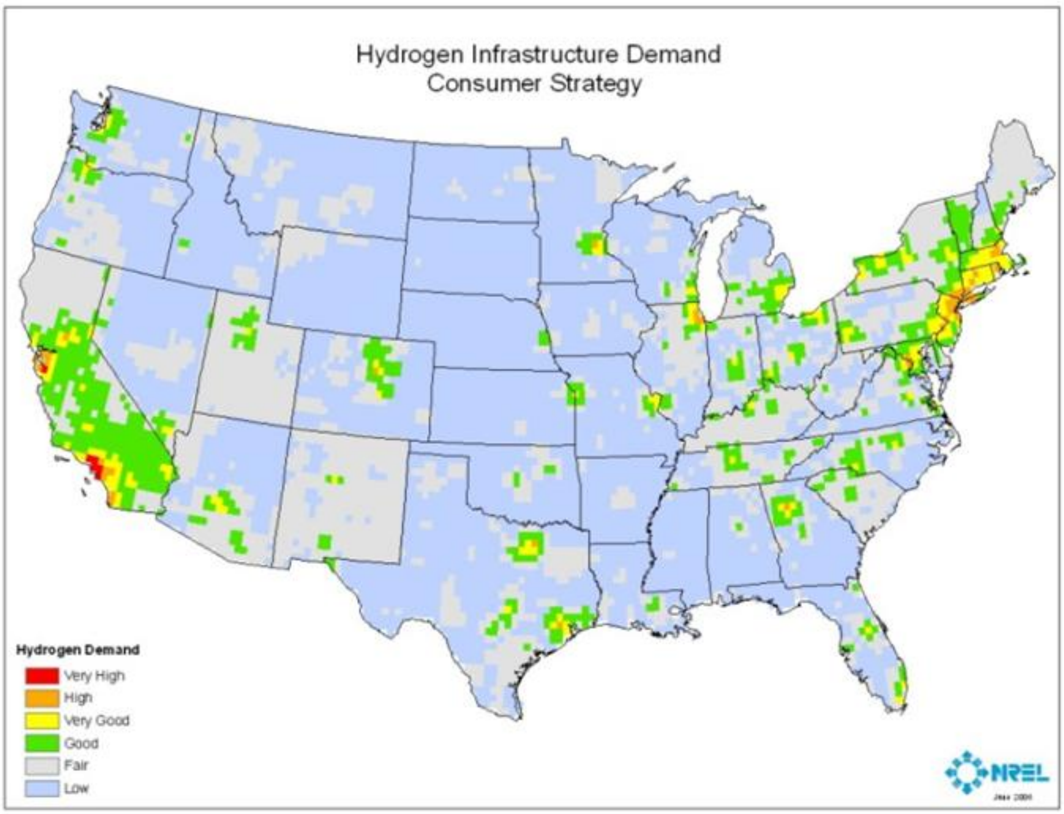

Figure 6.1 An Example of Geographically Uneven Demand for Alternative Fuel.

(Source: Melendez and Milbrandt. 2006. 8)

6.2 Methods

6.2.1 *Data*

This research used real-world road network and census data[15] for the Orlando metropolitan area (Lines et al. 2007; Kuby et al. 2009). Figure 6.2 shows the study area. The data used for building the network for Orlando and estimating the alt-fuel demand-weighted flows were collected from many sources including Florida DOT, US Census Bureau, and Department of Energy, and ESRI Inc. (Table 6.1). The raw street network data were investigated to ensure no topological error exists. Traffic Analysis Zones (TAZs) were aggregated into 102 areas and a single OD point was selected to represent each TAZ. The OD points were located at intersections of major roads or traffic-inducing business centers. Least-time paths for all OD pairs were generated using the posted speed limits of the network arcs as costs. TAZ trip flows obtained from FDOT travel demand models were aggregated and assigned to the least-cost paths assuming traffic flows occur on the shortest paths. Selection of the TAZs to be merged and location of OD centers involved extensive discussion among participant scientists of the FHI project and iterative calibration of data (Kuby et al. 2009). Demographic data of year 2000 collected by census block were obtained from US Bureau of Census.

[15] Originally these data were collected as a part of DOE funded project (Florida Hydrogen Initiative Project).

Table 6.1 Spatial Data Layers

Layer	Description
O-D Centers	Aggregated TAZ centers
Junctions	Defined by analysts at all intersections of arcs
Candidate Facilities	Combines the OD and junctions layer
Road Network	Florida Department of Transportation layers. Aggregated.
Shortest Path Routes	Least-cost paths were generated based on Dijkstra's algorithm. TAZs are the input nodes and maximum speed of arc is the cost.
Demographic Data	2000 US Census data collected by census tracts

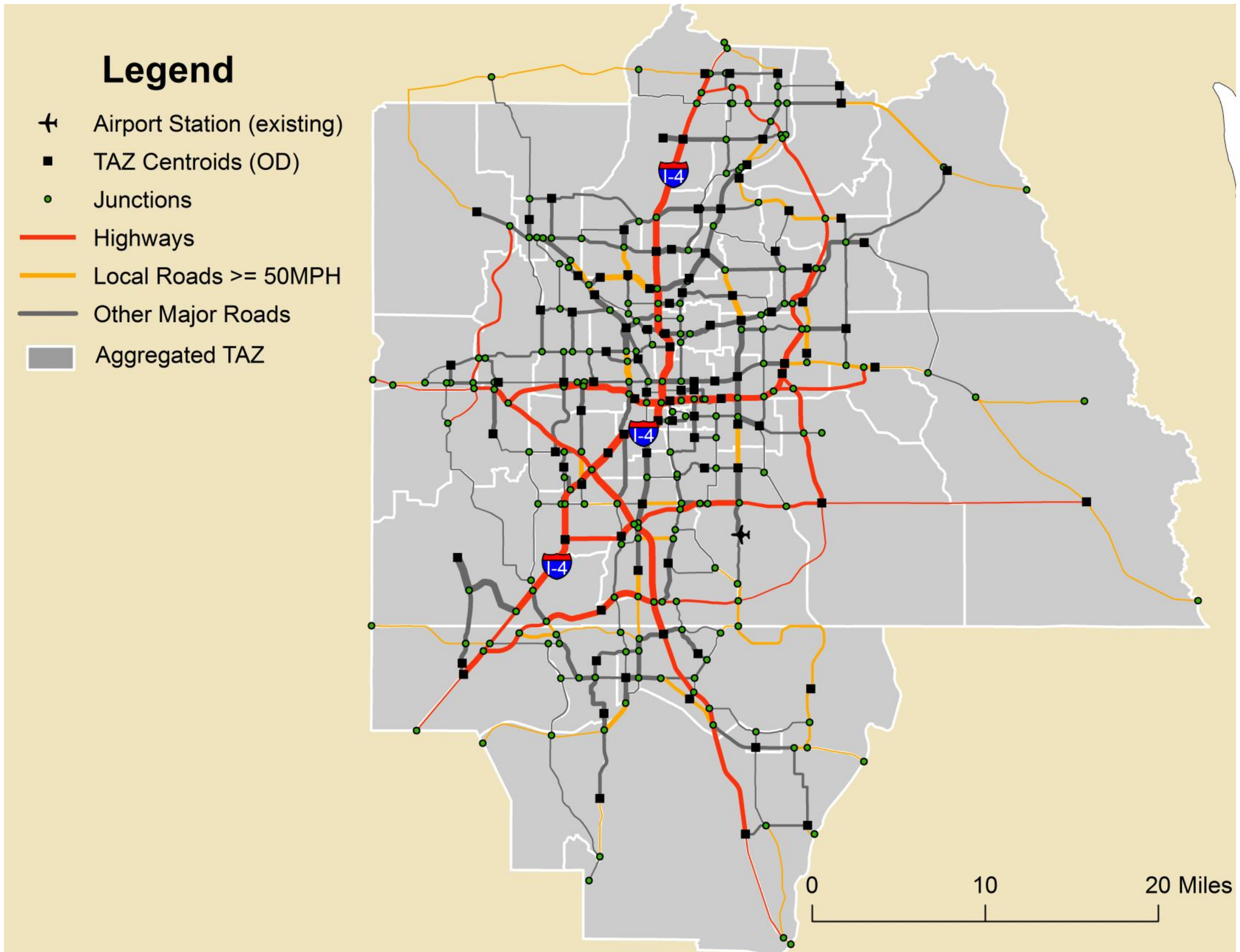

Figure 6.2 Orlando Metropolitan Area.

6.2.2 *Estimation of Alternative Fuel Demand*

Alt-fuel demand was estimated using geographic information system and multi attribute decision making analysis based on NREL's approach. But it was modified for flow-based models. Adapted and NREL's original GIS model are shown in Table 6.2. Specific differences are detailed as below.

The flow-based location models require flow volume between OD pairs, but the NREL method was developed to estimate the total demand in a zone, and therefore the estimates need to be revised on a per capita basis so that they can be multiplied by the total number of trips between two zones. For example, an extensive attribute "total number of people with bachelor's degree" was changed to be an intensive attribute "*percentage* of people with bachelor's degree." Some of NREL's attributes were state-level (state incentives, zero-emission vehicle mandates, and hybrid registration) or not applicable to state of Florida (there are no counties of non-attainment status for air quality). These attributes were not used and their weights were re-assigned to other attributes.

Equal-interval classification was used instead of natural break method in assigning a standardized rank score to each census tract. The range of values was the maximum and minimum of all the tracts in Florida rather than those in Orlando area. The range was divided equally into seven classes. Figure 6.3 shows spatial distribution of the rank scores of each attribute.

Once the rank score for each attribute was obtained, it was multiplied by the weight assigned for each attribute. The base case weighting scheme is shown in Table 6.2. Weighted rank scores were summed for all attributes to obtain a composite rank score for each tract. The next two sections present details of weighting scenarios and aggregation method.

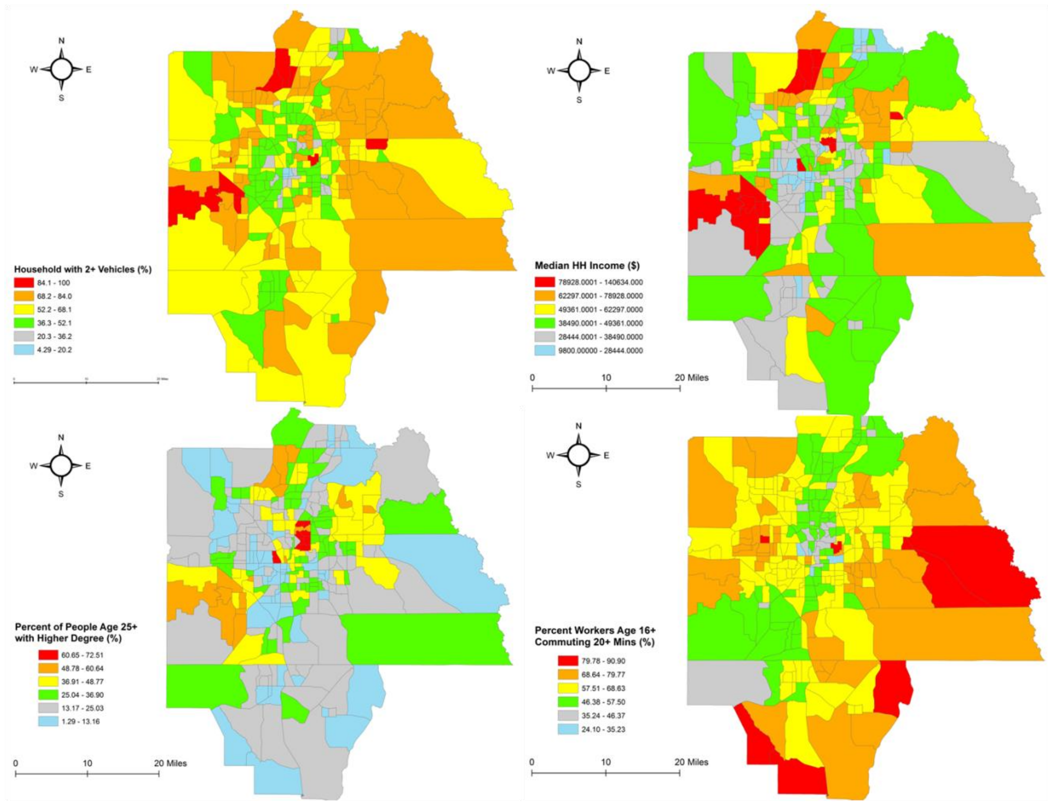

Figure 6.3 Spatial Distribution of Rank Scores

Table 6.2 Proposed Attributes Affecting AFV Demand and Rank Score Scheme

NREL Data Layer (weight - %)	NREL Classes	NREL Rank Score	Data Layer (base case weight - %)	Adapted Classes	Rank Score
Median Household Income (High - 15%)	54,955–86,901	7	Median Household Income (High - 23%)	172,515 – 200,001	7
	43,109–54,954	6		145,029 – 172,514	6
	36,152–43,108	5		117,542 – 145,028	5
	30,673–36,151	4		90,056 – 117,541	4
	24,748–30,672	3		62,569 – 90,055	3
	15,405–24,747	2		35,083 – 62,568	2
	0–15,404	1		0 – 35,082	1
Number of People with Bachelor's Degrees (Medium - 10%)	943,877–1,770,650	7	***Percentage*** of People with Bachelor's Degrees (Medium – 18%)	75.7 – 100	7
	415,521–943,876	7		63.1 – 75.6	6
	228,465–415,520	6		50.5 – 63.0	5
	123,779–228,464	5		38.0 – 50.4	4
	51,563–123,778	4		25.5 – 37.9	3
	14,107–51,562	3		12.84 – 25.4	2
	0–14,106	2		0 – 12.83	1
Number of Workers Age 16+ who commute more than 20 minutes (Medium - 10%)	908,659–1,572,668	7	***Percentage*** of Workers age 16+ who commute more than 20 minutes (Medium – 18%)	78.6 – 100	7
	418,740–908,658	7		66.3 – 78.5	6
	219,920–418,739	6		53.9 –66.2	5
	109,577–219,919	5		41.5 –53.8	4
	47,249–109,576	4		29.1 –41.4	3
	12,529–47,248	3		16.8 –29.0	2
	0–12,528	2		0 – 16.7	1
Number of Households with 2+ Vehicles (High – 15%)	179,419–312,470	7	***Percentage*** of Households with 2+ Vehicles (High – 23%)	80.8 – 100	7
	312,471–516,079	7		68.0 – 80.7	6
	118,941–179,418	6		55.2 – 67.9	5
	68,543–118,940	5		42.4 – 55.1	4
	30,240–68,542	4		29.6 – 42.3	3
	8,065–30,239	3		16.6 – 29.5	2
	0–8,064	2		0 – 16.5	1
Clean Cities Coalitions, by County (Medium – 10%)	Yes	7	Clean Cities Coalitions, by County (Medium – 18%)	Yes	7
	No	1		No	1
Air Quality (Medium – 10%)	Severe	7	Not applicable	Florida has no counties in non-attainment status for air quality	
	Moderate	6			
	Marginal	5			
	None	1			
State Incentives (Medium – 10%)	Yes	5-7	Not applicable	(State level attribute, Not used because it is the same for all TAZs)	
	None	1			
ZEV Sales Mandate (Medium – 10%)	Yes	7	Not applicable	(State level attribute, Not used because it is the same for all TAZs)	
	No	1			
Registered Hybrid Vehicles, by State (Medium – 10%)	1,551-2,875	7	Not applicable	(State level attribute, Not used because it is the same for all TAZs)	
	686-1,550	6			
	372-685	5			
	169-371	4			
	68-168	3			
	12-67	2			
	0-11	1			

Note: Modified from Melendez and Milbrandt (2006)

6.2.3 *Sensitivity Analysis on Demand Estimation Model*

Sensitivity analyses were conducted to explore the sensitivity of AFV demand estimates to changes in attribute weighting scheme. Five scenarios—base case, equal weighting, policy emphasis, demographic emphasis, and no policy—were created and Table 6.3 shows weighting scheme for each scenario. Spatial clusters of the resulting rank scores were visualized using Local Moran's *I* statistics. The percentage of population falling in each demand category was also identified.

Table 6.3 Five Scenarios and Weighting Scheme

	Base Case (%)	Equal Weighting (%)	Demographic Emphasis (%)	Policy Emphasis (%)	No Policy (%)
VEH[a]	23	20	21	23	25
INC[b]	23	20	21	18	25
EDU[c]	18	20	21	18	25
COMM[d]	18	20	21	18	25
POL[e]	18	20	16	23	0

[a] Percentage of Households with 2+ Vehicles

[b] Median House-hold Income

[c] Percent-age of people with bachelor's degrees

[d] Percentage of workers age 16+ who commute more than 20 minutes

[e] Clean Cities Coalitions, by County

6.2.4 *Aggregation of Demand Density*

The spatial units of original data sources were different, and thus areal interpolation was needed to aggregate composite rank scores of tracts to TAZ boundary. Population density was used as intermediate control value. Aggregation of demand density calculated on each tract into TAZ needed special attention in choosing the interpolation method. The census zoning system is different than the TAZ zoning system. The delineation of TAZ boundaries is not only based on the census boundaries but also on a transportation network. The cardinality of the relationship between TAZ and tracts is not one-to-one or one-to-many. It is many-to-many cardinality; most tracts fall in one TAZ, but in some cases one tract may fall in multiple TAZs. Most tracts fall in only one TAZ, thus aggregation for such tracts is relatively easier; each demand density can be weighted by the tract's weight variable and then the average of all the weighted values from the tracts is assigned to the covering TAZ. The weight variable could be a constant, population, area, or any variable that can represent the relative importance of each tract. We think population serves better than area as a weight variable for demand density aggregation.

6.2.5 *Weighting Flow Volume by Alternative Fuel Demand*

The next step was an integration of composite rank scores with the trips between an origin-destination pair to obtain alt-fuel demand weighted trips. Rank scores that were assigned for a pair of origin and destination were averaged. The average rank score for an origin-destination pair needed to be converted to a weighting factor between 0 and 1 using a transformation function (Figure 6.3).

The resulting value (AFV adoption rate) was a multiplier to the trips to acquire alternative fuel demand weighted trips. Two transformation functions (linear and sigmoid) were employed and the resulting link flow patterns were compared. Note, however, AFV adoption rate should be interpreted in relative terms. For instance, if an OD pair *A* that has an average composite score of 5, which translates to 0.67 by the linear transformation function. There may be another OD pair *B* with the composite score of 2, and thus 0.167 for AFV adoption rate. In this case, we are estimating that four times as many customers are likely to adopt AFV for trips on *A* than for the trips on *B*, but we do not claim to estimate that 67% or 16.7% of drivers will adopt AFVs.

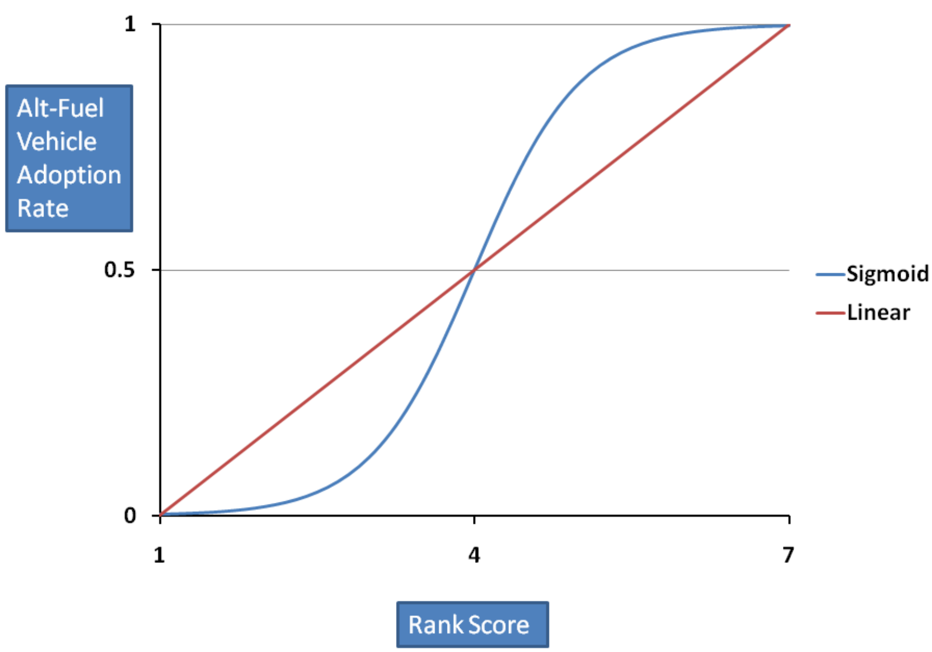

Figure 6.4 Transformation Function Curves.

6.2.6 *Solving the FRLM with AFV-Demand Weighted Scenarios*

For each demand density score from five attribute weighting scenarios, two sets of weighted trip flows (linearly weighted and sigmoid function weighted) for each OD pair were assigned to its shortest time path. The FRLM was solved using greedy algorithm with substitution (iteration #: 1) at a vehicle's range of 100 miles for p = 10 and p = 20 using the demand-weighted flows. Therefore, there were 10 demand-weighted flows (5 scenarios x 2 transformation functions) as input for the FRLM. Table 6.4 is an example of the weighted flows.

Table 6.4 Example of Demand-Weighted Flows

Q	O	D	OD TRIPS	Sigmoid Function Weighted Trips					Linearly Weighted Trips				
				BC[a]	NP[b]	EW[c]	PE[d]	DE[e]	BC[a]	NP[b]	EW[c]	PE[d]	DE[e]
1	1	2	1804	1533	673	1702	1924	879	1802	1517	1850	1915	1599
2	1	3	957	777	312	856	990	427	956	795	978	1017	844
3	1	4	597	432	161	486	573	234	590	485	606	631	521
4	1	5	1359	1120	463	1244	1423	626	1366	1141	1401	1453	1209
5	1	6	454	368	154	414	471	208	452	379	465	482	402

[a] Base Case

[b] No Policy

[c] Equal Weighting

[d] Policy Emphasis

[e] Demographic Emphasis

6.3 Results

6.3.1 *Spatial & Probability Distribution of AFV Demand Estimate*

Figure 6.14 shows the maps of composite rank scores from each scenario. In addition, breakdown of population by each demand score range is shown in Figure 6.6. Policy emphasis scenario resulted in more tracts with high rank scores. Specifically, about 49% of population falls in the tracts with high (> 4.6) scores. This contrasts to no policy scenario where the similar percentage of population falls in fair to high score ranges. This may be interpreted that policy could push up consumers to the next class in terms of demand density category.

Probability distribution of all scenarios had positive skewness (0.12 ~ 0.16). This suggests there are a small number of tracts with high rank scores, which will be good target areas. The composite rank scores showed high correlation (> 0.998) among different weighting scenarios, and thus to identify clusters this research mapped Local Moran's *I* of composite ranks scores (Figure 6.7). The LISA maps, for which a queen-type contiguity weight matrix was used for modeling neighbors, show that high- and low-value cluster pattern look about the same at all weighting scenarios. Three predominant areas were identified: north, northeast, and southwest of Orlando metropolitan.

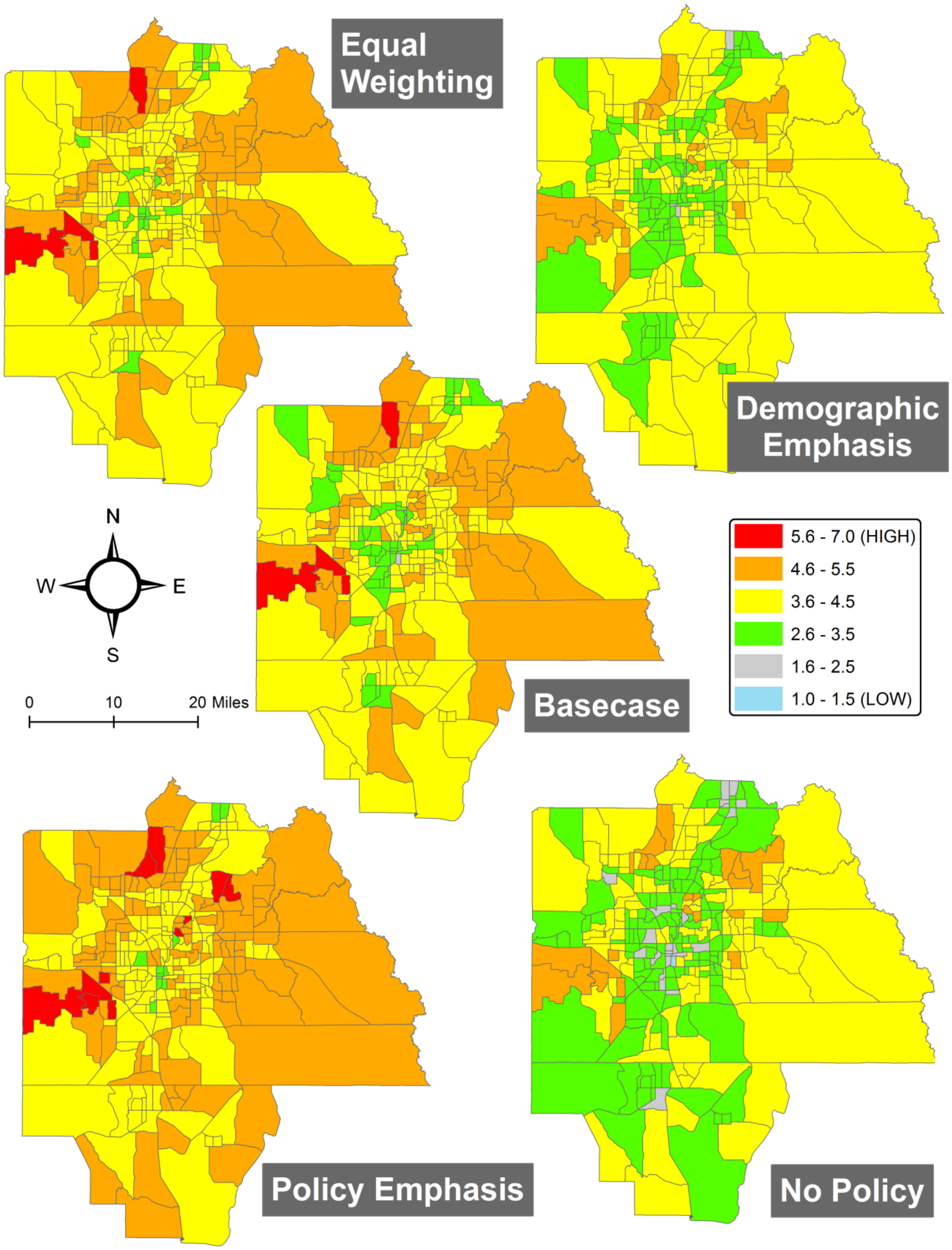

Figure 6.5 Composite Scores from Different Scenarios.

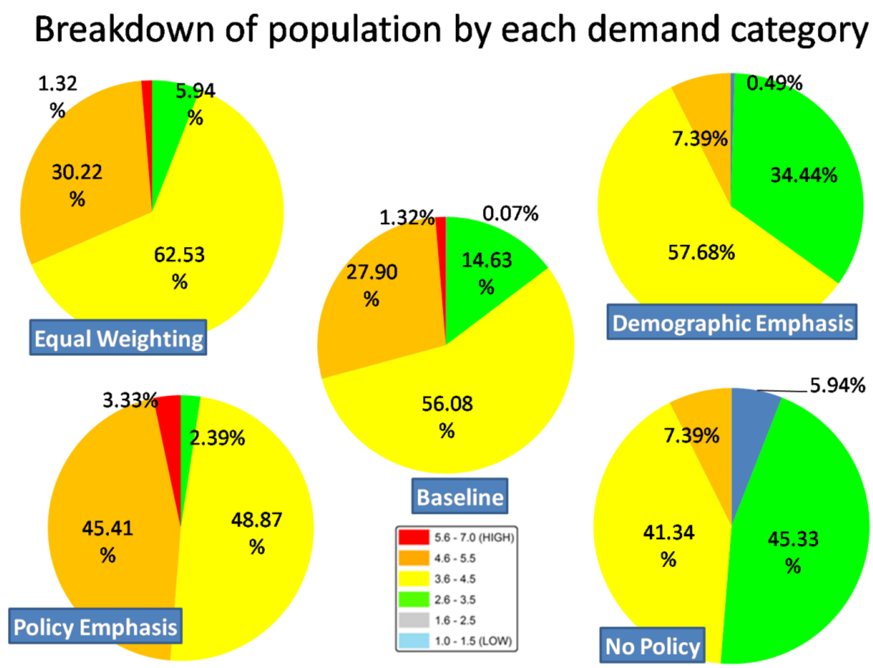

Figure 6.6 Breakdown of Population by Demand Score Range.

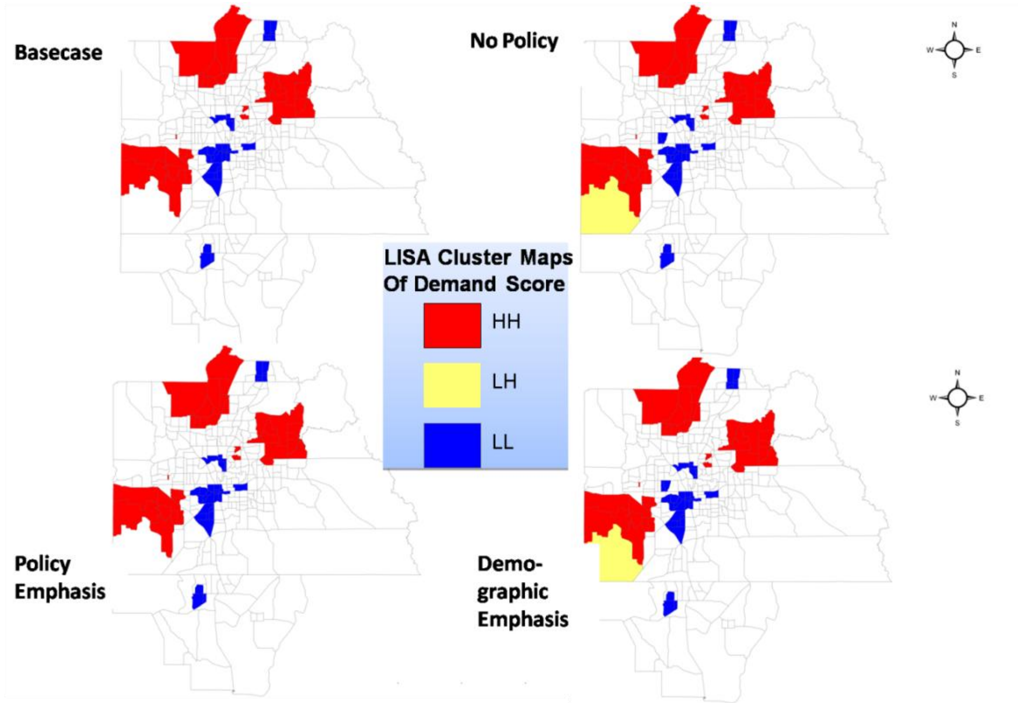

Figure 6.7 LISA Cluster Maps of Demand Scores.

6.3.2 *Effects of AFV Demand Estimate on Locating Refueling Facilities*

The dispersion of probability distribution of AFV adoption rate for 104 TAZs in Orlando area was shown in Table 6.5. The most dispersed adoption rate was observed when sigmoid function was used in transforming composite scores of no policy scenario (CV: 0.696), whereas the least dispersed one was linearly transformed scores of policy emphasis scenario (CV: 0.115). The former can be interpreted as a situation where market mostly drives AFV acceptance, and the latter simulates the case when the policy is actively involved in transitioning to an AFV transportation system.

Using the above two sets, demand-weighted flows were computed as inputs for the FRLM, and the problem instances were solved using the greedy algorithm with one substitution for p = 10 and p = 20. The solutions for linearly transformed scores of policy emphasis scenario (LWT-P) were the same as solutions for non-weighted flows (TRIPS), but with less coverage (Table 6.6). However, transformation of no policy scenario scores by a sigmoid function (SWT-NP) resulted in higher coverage (0.01~4.44%) than TRIPS and different facility locations (Table 6.6 and Figure 6.8). Note that total flows to cover were reduced for SWT-NP and LWT-P as a result of AFV demand weighting from 1,466,942 to 461,096 and 91,337,483 respectively.

Regarding facility locations, the six initial facilities were selected at the same locations even though there was slight difference in the order of stations added. The 10 facilities from TRIPS and LWT-P located mainly to cover north-south flows and to serve some flows on southwest and northeast regions. TRIPS and LWT-P selected 11th - 20th stations that can cover east-west flows. They selected stations for further southwest and northeast regions as well so that drivers could drive further to that direction. We observe different pattern of facilities selected by SWT-NP. When SWT-NP selected 10 facilities, it replaced two stations in south Orlando in areas with demand scores of 2.75 and 3 with the ones in west and east areas having 4.5 and 5.5 for the demand scores. For 11th -20th stations, it seemed to locate stations further to northeast, northwest, and southwest of Orlando, where high demand clusters exist. This suggests that optimal solutions for maximizing SWT-NP have reflected the modified structure of alt-fuel demand, which had more dispersed distribution of AFV-demand scores than LWT-P or TRIPS.

Table 6.5   Dispersion of AFV Adoption Rates

	Sigmoid Function Transformation					Linear Transformation				
	BC[a]	NP[b]	EW[c]	PE[d]	DE[e]	BC[a]	NP[b]	EW[c]	PE[d]	DE[e]
Mean	0.550	0.324	0.589	0.653	0.360	0.590	0.504	0.603	0.626	0.523
Standard Deviation	0.214	0.225	0.203	0.192	0.193	0.076	0.091	0.073	0.072	0.069
Coefficient of Variance	0.389	**<u>0.696</u>**	0.345	0.295	0.535	0.129	0.181	0.121	**<u>0.115</u>**	0.132

[a] Base Case

[b] No Policy

[c] Equal Weighting

[d] Policy Emphasis

[e] Demographic Emphasis

Table 6.6 Effect of AFV-Demand Weighting on Coverage

p	Percentage of Coverage: Non-Weighted Flows	Coverage Gain of Weighted Flows (% of Non-Weighted Flows Covered)	
		No Policy / Sigmoid Function Transformation	Policy Emphasis / Linear Transformation
1	14.23	-26.99	-5.62
2	21.12	-10.40	-4.23
3	26.53	-1.16	-3.06
4	31.45	**1.93**	-1.55
5	36.14	**4.33**	-0.91
6	40.50	**4.44**	**0.04**
7	44.70	**3.63**	-0.37
8	48.19	**2.26**	-0.09
9	51.62	**1.14**	-0.39
10	54.59	**0.60**	-0.49
11	57.52	**0.01**	-0.56
12	60.02	**0.16**	-0.48
13	62.21	**0.35**	-0.59
14	64.41	**0.50**	-0.79
15	66.54	**0.43**	-0.91
16	68.60	**0.46**	-0.93
17	70.38	**0.79**	-0.90
18	72.09	**1.13**	-0.78
19	73.72	**1.34**	-0.56
20	75.46	**1.16**	-0.51

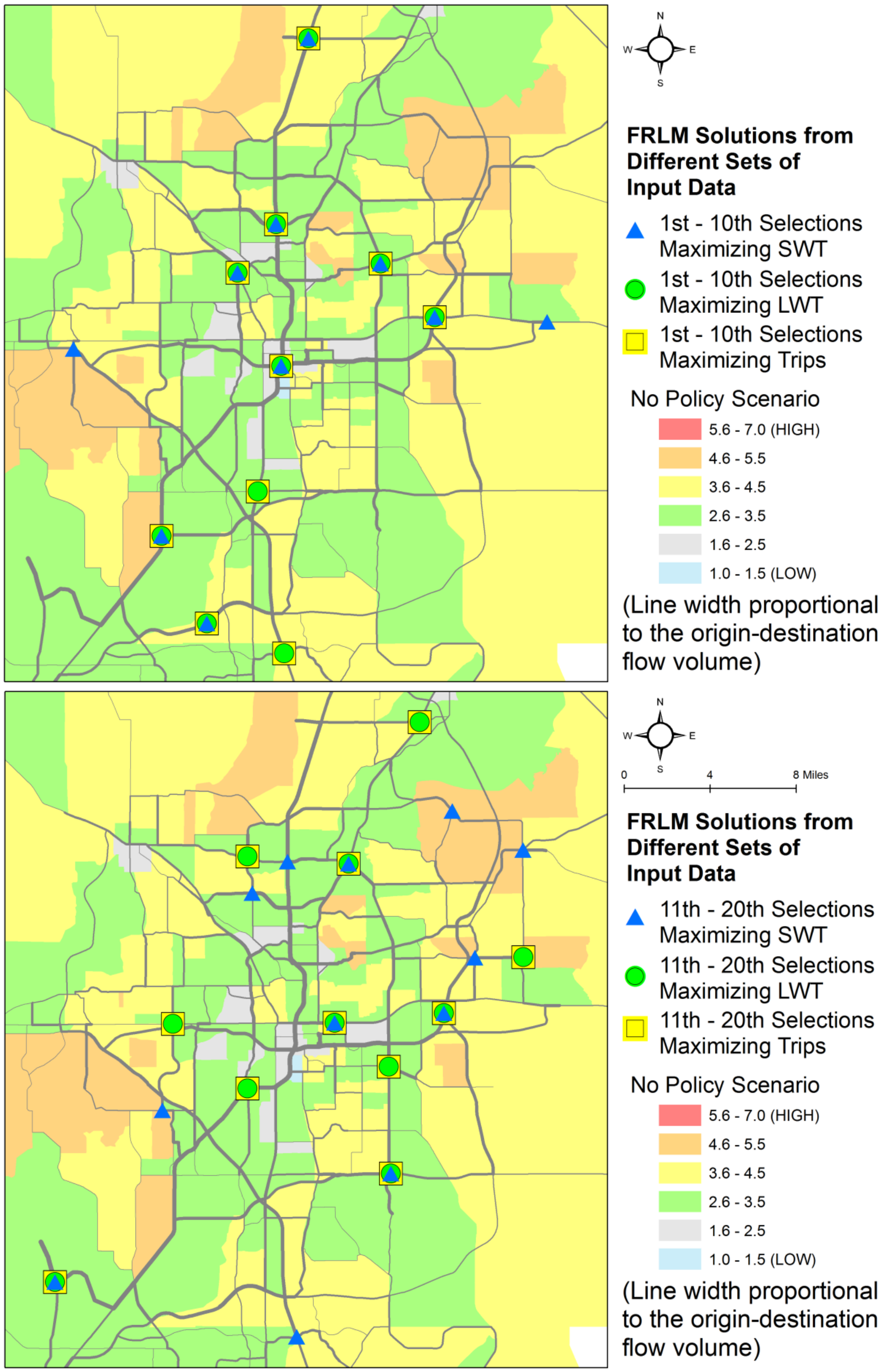

Figure 6.8 Different Selection of Facilities by the FRLM with AFV demand.

6.4 Summary and Conclusions

In summary, this chapter considered uneven distribution of AFV demand that is expected in the initial phases of AF station development. A method that incorporates NREL's raster-based AFV demand estimation model into the path-based FRLM was proposed and it was applied to the Orlando metropolitan data. Firstly, NREL's approach was enhanced by using census tracts, instead of raster-based data, as the basic spatial unit. Further, an areal interpolation was employed in aggregating the AFV estimates of tracts to TAZ boundaries. Lastly, AFV estimates of TAZs are averaged for each OD pair and transformed to represent the estimated proportion of AFV flow volumes traveling between the OD pair.

Results show that the weighted consumer demand has a minor effect on the optimal facility locations, which shift toward areas with high AFV purchase potentials. Even though this approach is straightforward and has the capability of providing enhanced representation of early consumer demand, the model's inherent uncertainties in the data, attribute ranking scheme, or scenario parameters raise questions about its applicability. Without empirical data to verify or evaluate the model's results, integration of the AFV estimation model into a framework where various scenarios can be generated and alternatives are efficiently compared would be valuable to the alt-fuel refueling network planners.

7 A PROTOTYPE SDSS FOR REFUELING SERVICE INFRASTRUCTURE PLANNING

As discussed in Chapter 2, an SDSS must provide components that facilitate and support decision-making processes. In particular, when the design is related to unknown phenomena such as the deviation of AFV drivers and unequal likelihood of AFV adoption rate, the capabilities of an SDSS to generate multiple scenarios and to explore those alternatives are important. Recognizing the absence of such a flexible SDSS, this research develops a prototype SDSS (DFRLM-SDSS) designed to support a planning decision of an AFV refueling facility network that explicitly considers uncertainties of drivers' deviation and AFV demands.

Section 7.1 discusses technical characteristics of the SDSS. In section 7.2 we detail the core functionalities highlighting the benefits of the SDSS. Section 7.3 discusses the application of the DFRLM-SDSS using a real-world network (statewide network of Florida). The final section summarizes and provides future research.

7.1 Technical Characteristics of DFRLM-SDSS

The DFRLM-SDSS integrates DFRLM, heuristic solution approach, and an AFV demand estimation model (Chapters 4-6) into a GIS. The components of DFRLM-SDSS are developed based on C# .NET language and uses ESRI ArcObjects when GIS components are needed. As a result, interoperability among the programming languages designed for the Common Language Infrastructure

(CLI) such as Visual Basic .NET and C++/CLI is naturally supported (Microsoft 2010). In other words, any part of the prototype SDSS components can be referenced and re-used in other CLI languages.

Two design objectives were pursued in designing the graphic user interface of the DFRLM-SDSS. The first is that the interface is divided into parts in such a way that each part contains all the required elements to perform a use case. Another consideration is to provide the user as much supplementary information as possible that explains the meaning and effects of the parameters. The former is expected to allow the user to focus on one task at a time and do not get overwhelmed by other tasks or by the number of parameters to set. The latter should provide the user with confidence in the results by removing ambiguity in the terms in the user interface.

Because location models represent real world entities in different ways under different assumptions on the process of phenomena, it is desirable for a SDSS to be extensible so that new or existing models can be added with little change. This quality is achieved in DFRLM-SDSS by following the object-oriented design approach. Specifically, the components of DFRLM-SDSS are modularized and grouped into five classes[16] that are interacting with each other: `DFRLM-ArcGIS-Command`, `DFRLM-Selection-Form`, `DFRLMData`, `Graph-Structure-Algorithm`, and `DFRLM-Greedy`.

[16] The classes provided by ArcObjects are not included.

`DFRLM-ArcGIS-Command` class provides a bridge between ArcGIS and DFRLM. This class creates a DFRLM-SDSS user interface. `DFRLM-Selection-Form` represents the graphic user interface that interacts with the user. This class is associated with all the other classes, and therefore it manages the interaction among the classes. `DFRLMData` reads in GIS data sources and converts them into network representation in memory. `Graph-Structure-Algorithm` is a set of classes that manage graph theory-based abstract data structures and algorithms (Microsoft 2008). `DFRLM-Greedy` class provides heuristic algorithms to solve a specific DFRLM problem of which the data and parameters are provided by other classes. Note that with the modularization in DFRLM-SDSS, classes that are not related with GIS operations can be reused as components of other applications.

7.2 Functional Components of the System

The DFRLM-SDSS is composed of several interacting functional components: data input, AFV demand estimation, deviation behavior modeling, optimization of the problem, and output generation. Figure 7.1 shows the functional framework of the system. The functional requirements for DFRLM-SDSS were obtained from examining the literature, the decision-making process, and evaluating the functionalities of previous systems. Discussions with refueling service providers provided insight into the functionalities for the proposed system.

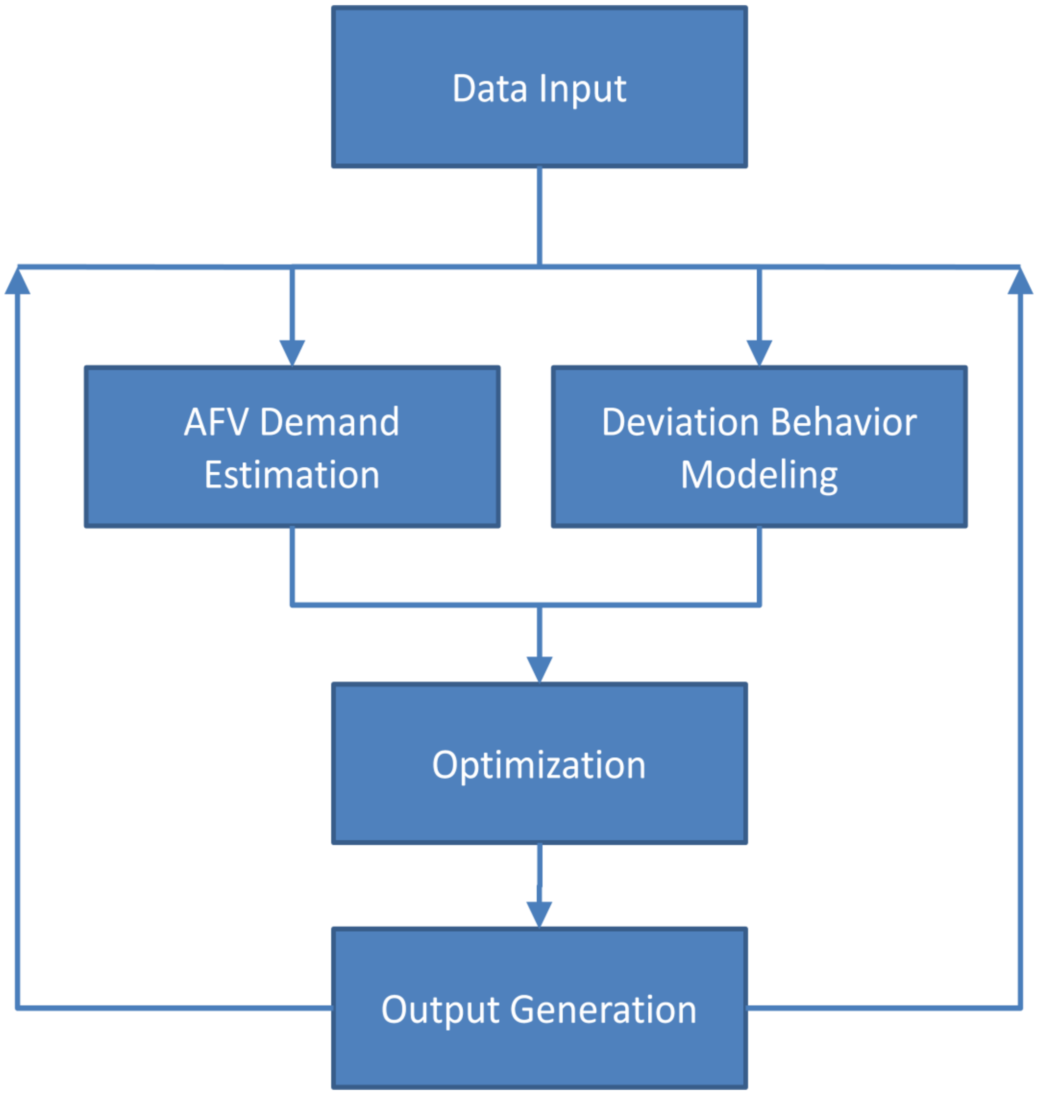

Figure 7.1 Functional Framework of the DFRLM-SDSS.

7.2.1 *Data Input*

The DFRLM-SDSS requires the users to provide network source data (node and edge) and associated flow data (OD nodes and OD flow). The SDSS reads in the list of layers added in its base GIS when it is initialized so that the user can specify the names of source layers and fields. Figure 7.2 shows the user interface for data input. The user can provide two types of edge weight, of which one must be distance because it is inevitable for solving the DFRLM problems (see Section 5.1). The other edge weight could be any user-specified impedance such as travel time.

Once all the required data are specified, the network is initialized and loaded into the memory with other data such as weights and OD flow volume. Maintaining all the source data in the memory is important because this allows the user to solve many problem instances on the same dataset while changing the assumptions in estimating AFV demand or in modeling drivers' deviation behavior. Otherwise, the user would have to repeatedly specify and load the data.

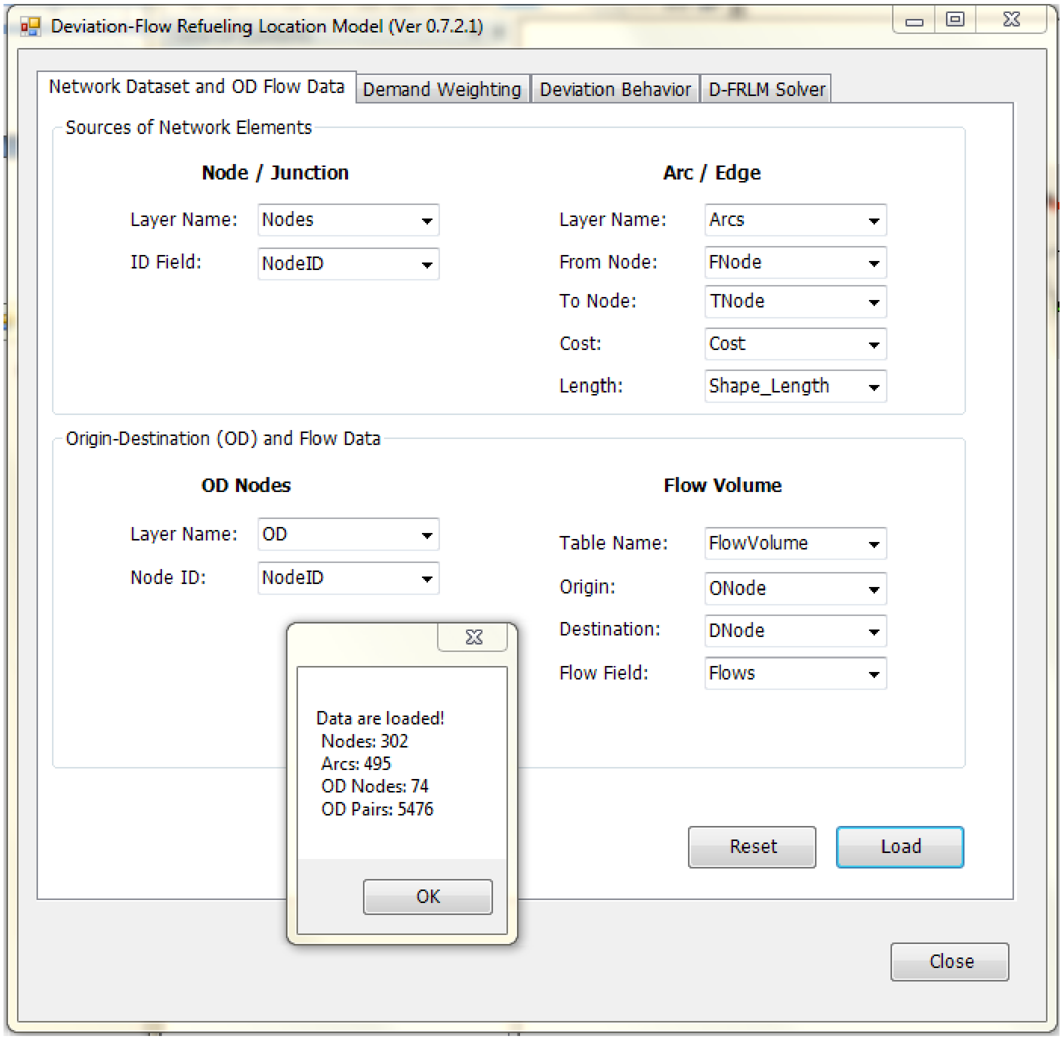

Figure 7.2 Data-Centric Part of the User Interface of DFRLM-SDSS.

7.2.2 *AFV Demand Estimation*

The user needs to estimate the AFV demand and apply it as weight for the flow volume because there are no available empirical data on the actual demand for AFV and the DFRLM requires OD flow volumes for its input. The prototype SDSS provides the user with a flexible GIS-based approach to account for regional variation of AFV purchase likelihood and a method to integrate the area-based demand estimates with the path-based flow volumes (see Section 6.2).

Figure 7.3 shows the user interface that can be used for AFV demand weighting. The user can specify penetration rate (% of AFV flows), key attributes affecting consumer acceptance, and their relative impact. By specifying a transformation curve, the user can model how consumers adopt new technology (AFV). This curve can be derived from the theory of innovation diffusion or be calibrated to empirical survey data if available.

Because all the inputs are parameterized the user is provided with a wide range of flexibility in estimation AFV demands. For example, by combining parameters in multiple ways, the user may focus on the amount of AFV flows served by the optimal stations, the effects of policy on the optimal station locations, or identification of strategic locations targeted to serve flows with high AFV-adoption potentials.

7.2.3 *Deviation Behavior Modeling*

Without available empirical data about how far drivers would deviate from their shortest paths and how many of them would take the deviation paths, the user needs to model deviation behavior. For example, the user may want to assume that all the drivers of an OD pair would deviate up to 3 minutes off their shortest time path to refuel their AFVs. On the other hand, one may want to assume that 90% of drivers would take deviations for refueling their AFVs if the additional time for the deviation is not longer than 5% of their total travel time, and that it would drop to 50% of drivers when they need 10% more time to reach the stations. As such, the SDSS provides a flexibility in dealing with this uncertainty in modeling drivers' deviation behaviors.

Figure 7.4 shows the user interface for modeling deviation behavior. Drivers are assumed to take the least cost deviation paths and the amount of flows on deviation paths is expected to decrease with the severity of the deviation (see Sections 4.2, 4.4, 5.2.4). The user can specify an upper bound of deviation in relative (e.g., 10% more than least travel time) or absolute (e.g., 3 minutes) terms. The deviation function can be specified to depict the drivers' likelihood to take a deviation path in relation to the incurred deviation distance. After the user modeled a specific deviation functional form, it will be applied to shortest paths and their flow volumes to derive the flow volumes on the deviation paths.

As the AFV refueling network becomes mature, drivers' deviation behavior may change; early adopters may take more deviations than laggards and even the same person would take less deviation when stations are more available. In addition, we demonstrated earlier that the specific deviation functional form chosen has measurable effects on the optimal facility locations (see Section 5.3). This implies that a rollout plan for the refueling station network would benefit from a careful estimation of drivers' sensitivity to the required deviation at each development phase. Therefore, the SDSS's feature that allows the user to model various deviation behaviors is valuable.

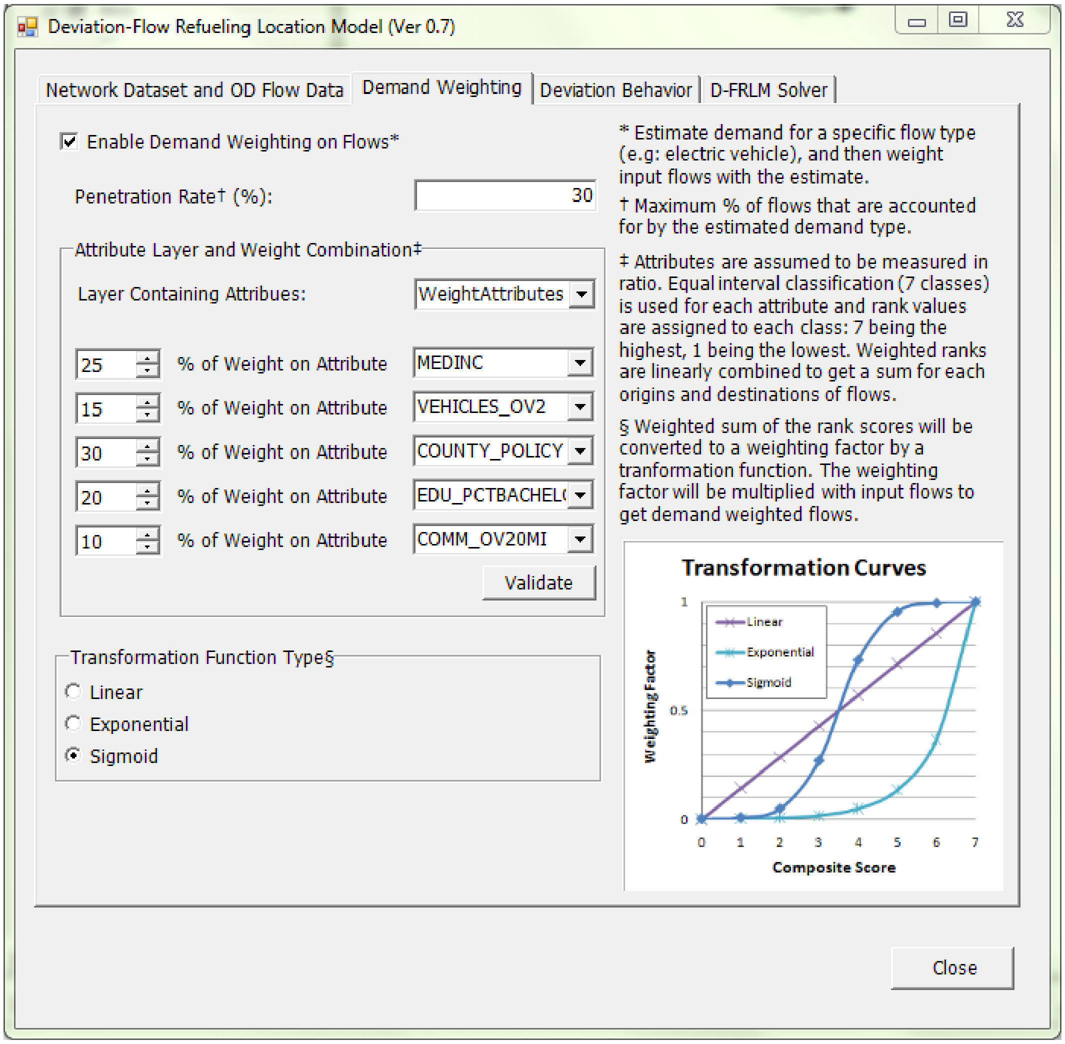

Figure 7.3 DFRLM-SDSS User Interface for AFV Demand Weighting.

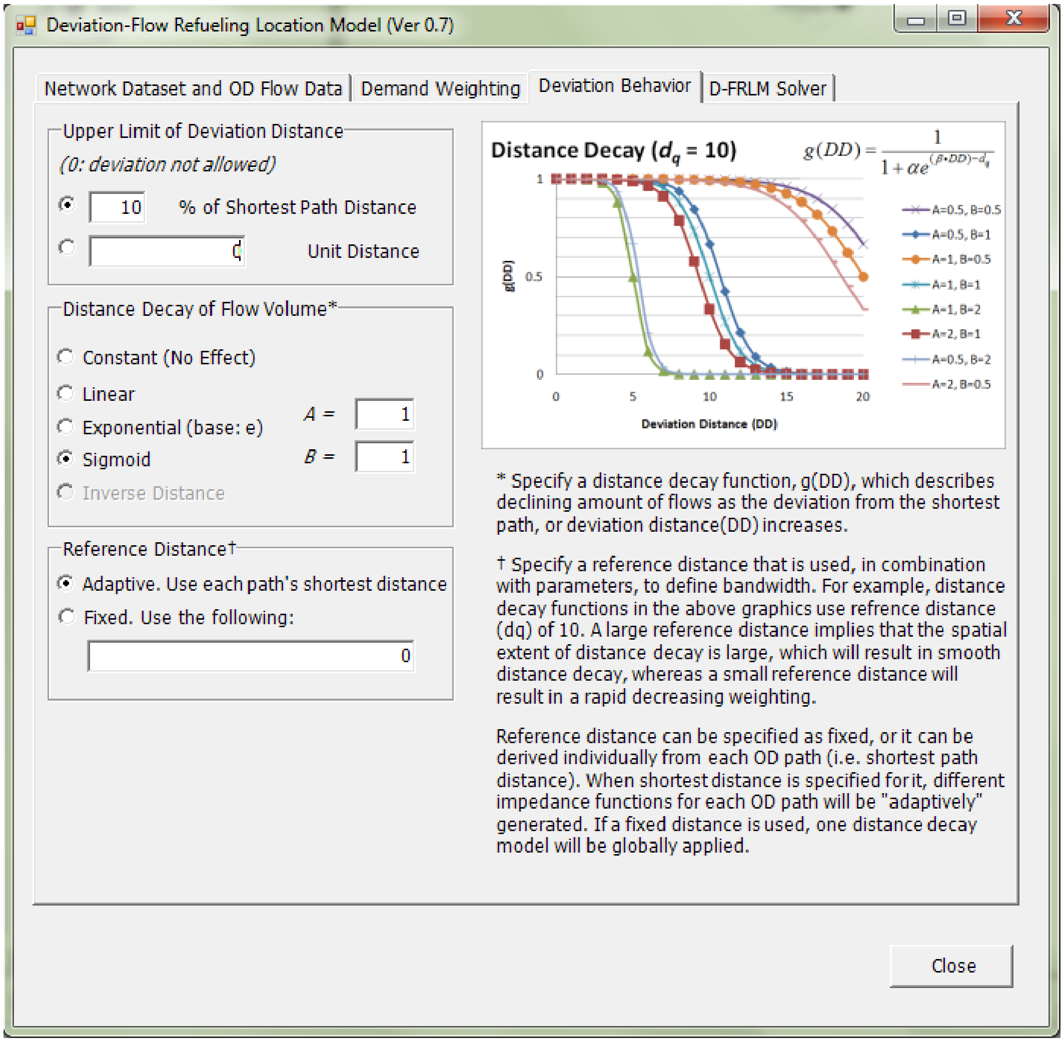

Figure 7.4 DFRLM-SDSS User Interface for Modeling Deviation Behavior.

7.2.4 *Optimization*

After all the inputs are specified, the user can solve the problem instance using heuristic algorithms for DFRLM (see Sections 5.1 and 5.2). The heuristic algorithms are implemented using C#.NET language and an open source QuickGraph library (Microsoft 2008). Figure 7.5 shows the user interface for specifying parameters for the heuristic algorithm. The user can choose solution algorithm (greedy or greedy with substitution), objective type (maximizing flows covered or maximizing vehicle distance traveled), vehicle range, and the number of facilities to locate. If the user chooses "Number of Trips" as the objective type, the model maximizes the flows refueled by the facilities, which are provided by the user and possibly weighted by AFV demand. On the other hand, if "Vehicle Distance Traveled" is selected, the model maximizes the total number of vehicle distances multiplied by the *demand-weighted* flows refueled with the solution facilities.

If the user provides the facility IDs that represent the existing facilities for "Fixed Facility IDs," those facilities are always included in the solution. The algorithm selects sites for the new facilities, of which the number is the difference between the number of facilities to build and fixed facilities. This is an important feature of the SDSS because this can be used in simulating multiple-phase development roll-out plans. For example, five stations could be built in phase 1 and the user may want to know optimal locations for additional 10 stations in phase 2. In this case, the five stations can be fixed while the number of station to select is 15.

Moreover, in conjunction with this, the user can specify different demand weighting scenarios and deviation behavior modeling as well to reflect changed market environment. Once parameters for the algorithm are all specified, the input network data, (AFV demand-weighted) OD flow volumes, deviation behavior model, DFRLM parameter set are cross-checked if they are valid. If all the inputs are valid, DFRLM heuristic is executed on the data with the parameters.

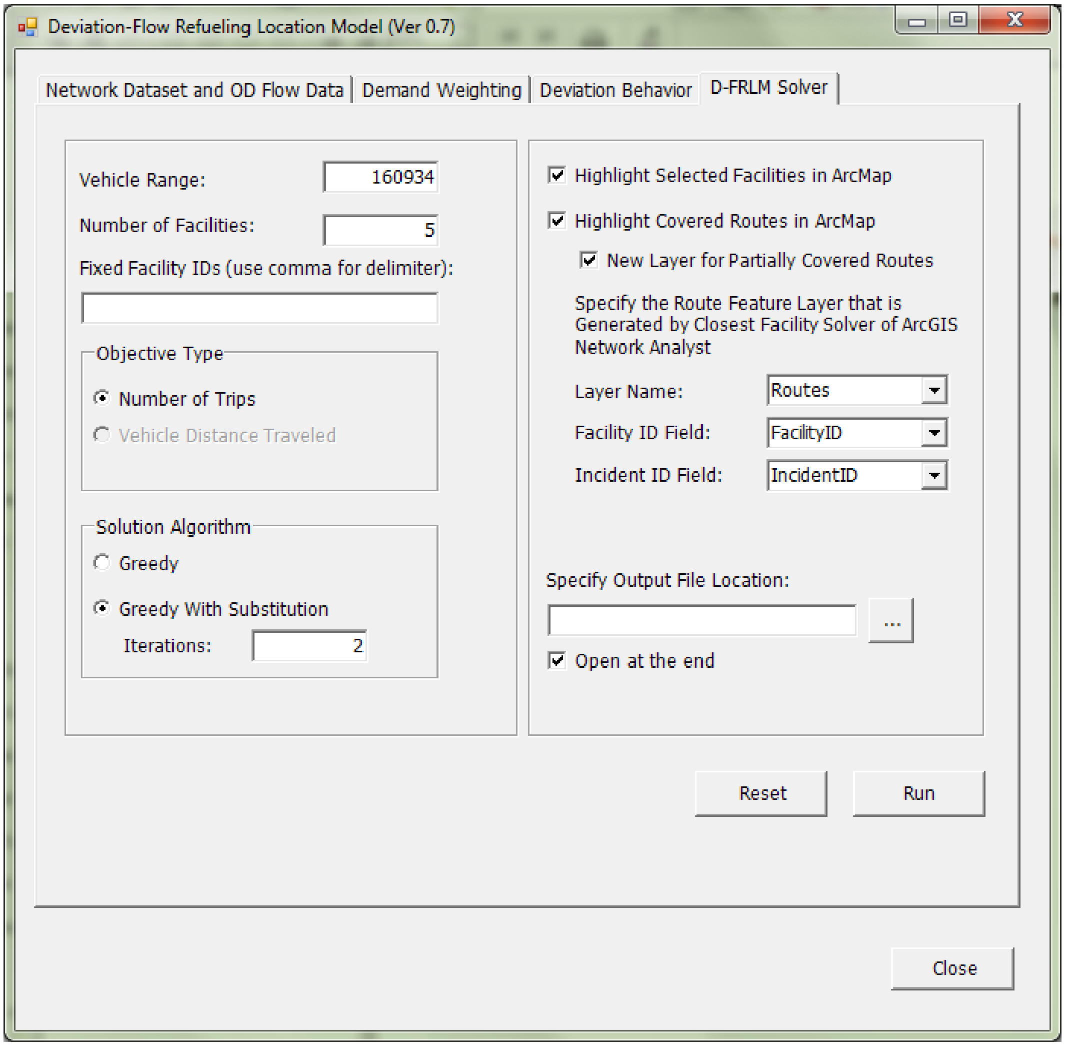

Figure 7.5 DFRLM-SDSS User Interface for Solving a DFRLM Problem and Specifying Outputs.

7.2.5 *Output Generation*

The problem solutions from the algorithm execution are presented in two forms: text file and map layer. Two output text files are generated at the user-specified path (Figure 7.5). One text file contains brief information: the number of facilities and the percentage covered. This file can easily be used in spreadsheet software to plot a tradeoff curve. More detailed information is stored in the other text file. It contains all the parameter values specified, selected facilities at each round, percentage refueled, list of OD pairs covered, the fraction of flows refueled, and computation time. Three map outputs are generated: selected facilities are highlighted in the node layer; covered routes are highlighted in the route layer; and partially covered routes are added to ArcGIS as a new layer. Figure 7.6 shows an example of outputs from the SDSS.

Given that the map outputs are standard GIS layers with spatial and attribute information, further analyses can easily be performed using ArcGIS's internal functionalities. For example, the user can obtain descriptive statistics of the flows refueled such as minimum, maximum, standard deviation, and frequency distribution. In addition, the user can export the results to physical files (shapefile or ESRI geodatabase feature class) for further comparison to other problem instance outputs.

It is worth noting that partially covered routes can easily be identified because they are highlighted in different colors on the map and they are easy to identify in the output text file as well. Identifying these partially covered routes is important in estimating stations' level of utilization more realistically. For example, imagine a case where 99% of a high-flow volume path is refueled by a solution when the maximum allowed deviation is only 30 seconds. This path would not have been refueled by the same solution if deviations were not allowed. However, in a practical setting, 30 seconds of deviation may be negligible and drivers would take the deviation. By looking at the OD pairs with high percentage of partial coverage, the user will be able to identify the effect of deviation model. The user may be more interested in the distribution of the deviation distances that drivers actually would have to take given the deviation model. Plotting the number of stations on the x-axis and the actual deviation distance on the y-axis will give the user some insight how the actual deviation changes as the refueling network grows.

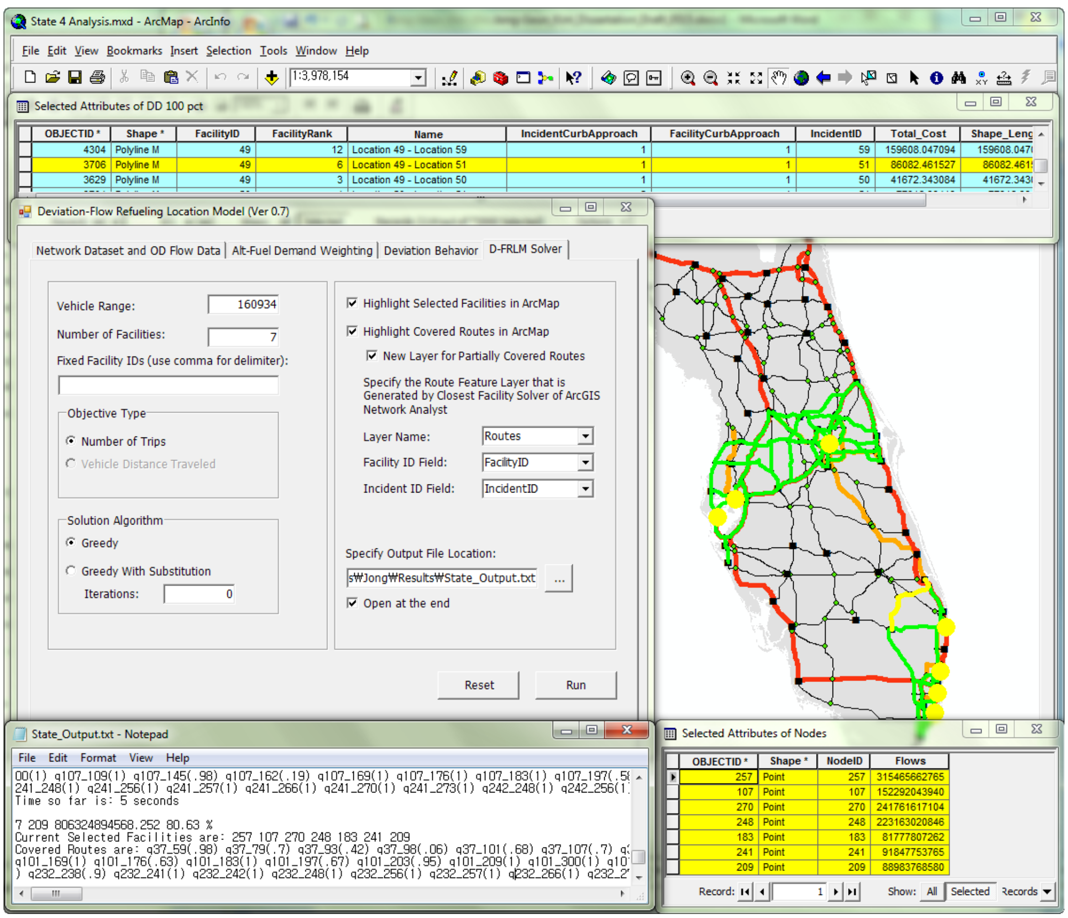

Figure 7.6 An Example of DFRLM-SDSS Results Output.

7.3 Application

In the previous sections, the functions and benefits of DFRLM-SDSS were illustrated using the data for the FHI project. The solution quality of implemented heuristics, effects of different decay functions to the solutions, and a comparison with FRLM were reported (See Sections 5.3 for experiment design, 5.3.2 for results, and 5.4 for conclusions). For the case of Orlando metropolitan data (Section 6.2.1 for details of data), the effects of demand weighting to the optimal solutions were reported (See Sections 6.3 and 6.4 for results and conclusions).

7.4 Summary and Future Research

The problem of optimally locating AFV refueling stations is a complex problem with a high degree of uncertainty. This research developed an extensible prototype SDSS that helps decision makers explore the effects of various AFV demand scenarios on the optimal station locations. The SDSS provides ample flexibility in combining different assumptions on AFV drivers' deviation behavior, spatial variation of AFV demand, vehicle range, and existing facilities. By tightly-coupling DFRLM with a powerful GIS, it provides multiple views of the results, including interactive maps and descriptive statistics while providing a best solution given the constraints. This implies that decision makers utilizing the DFRLM-SDSS would obtain a robust solution with reduced uncertainty.

The prototype SDSS can be enhanced by including tools that automate the generation of various AFV demand scenarios. These tools would enable the current system to transform itself into an anticipatory planning framework. In addition, the user would benefit from an inclusion of advanced visualization tools.

8 CONCLUSIONS AND FUTURE RESEARCH

8.1 Summary and Conclusions

Efficient methods that help optimize refueling infrastructure roll-out plans are essential in accelerating the advent of a new energy economy. Such methods should suggest strategic station locations and need to be based on realistic assumptions about drivers' refueling behavior and the characteristics of consumer demand for AFVs. The Flow Refueling Location Model (FRLM) models driver behavior realistically by basing it on drivers stopping along their way rather than making trips from home to station and back. This research departures from the FRLM to provide even more reality and applicability to the model. This research provides three approaches for the purpose. First, a new location model is developed extending the FRLM that simultaneously considers deviations and vehicle range. In addition, as a related and inevitable study, heuristic solution methods are developed to solve real-world problem instances of the model. Second, geographically uneven demands for AFV is considered. Third, a spatial decision support system (SDSS) is developed that integrates the location model, solution algorithms, and the demand estimation model with a GIS.

The new model (DFRLM) assumes that the number of drivers to visit a facility off of their pre-planned paths decreases as the required deviation increases. A mixed-integer linear programming (MILP) formulation was presented and the procedures to generate deviation paths and to model drivers' sensitivity to deviation were developed to provide input for the model. The results of DFRLM were generally consistent with the FRLM with no deviation. However, the results indicated that the specification of the maximum allowable deviation and specific deviation penalty functional form does have a measurable effect on the optimal locations of facilities and objective function values as well. Consideration of drivers' ability to deviate from their shortest paths to refuel enabled higher utilization of facilities and these facilities are expected to be more robust with their possibility of covering deviation flows.

In addition to optimally solving DFRLM problems, greedy-adding and greedy-adding with substitution heuristic algorithms were developed for solving real-world DFRLM problems. The heuristics are based on the concept of an artificial feasible network, where traveling on its arcs is feasible by refueling at *p* facilities located at its nodes. Both heuristics provided sub-optimal solutions and the optimality gap decreased as substitution iteration number or vehicle range increased. Comparison of the two heuristics showed that substitutions enhanced the objective with the cost of increased solution time, of which generation of all-pairs shortest paths on feasible network took the most.

Because the geographically uneven demand for AFVs has not been accounted for in optimization-based location models, a method that incorporates NREL's raster-based AFV demand estimation model into the path-based FRLM was proposed and it was applied to the Orlando metropolitan data. Results show that the weighted consumer demand has a minor effect on the optimal facility locations, which shift toward areas with high AFV purchase potential. Even though this approach is straightforward and has the capability of providing enhanced representation of early consumer demand, the model's inherent uncertainties raise questions about its applicability.

In supporting the decision process of refueling infrastructure development, a prototype location model-based SDSS was developed that integrates the DFLRM, heuristic algorithms, and AFV demand weighting into a GIS. The SDSS provides ample flexibility in combining different assumptions on AFV drivers' deviation behavior, spatial variation of AFV demand, vehicle range, and existing facilities. The DFRLM-SDSS helps identify robust locations for alt-fuel refueling stations.

8.2 Contributions

This research contributes to the literature of flow-based location models and to the literature of optimal location models for refueling stations with the consideration of deviation in modeling refueling flows. The structural characteristic of the DFRLM and the procedures for input data generation enhance the results of FRLM by eliminating coverage underestimation. This is achieved by the DFRLM's capability of considering multiple paths between an OD pair.

The heuristic algorithms developed here enable the application of DFRLM to solving real world problems. The heuristics dynamically generate deviation paths on a feasible network and feasibility of the paths is always guaranteed. Therefore the search space required for the heuristics is significantly smaller than that for pre-generation of *all* deviation paths in the original physical network.

We have not found other studies where geographically uneven alt-fuel vehicle demand estimates are incorporated into path-based origin-destination flow data. The method proposed here is straightforward and has the capability of providing enhanced representation of early consumer demand.

The developed DFRLM-SDSS broadens the literature of location model-based SDSS. The SDSS provides plenty of flexibility in combining different assumptions on various aspects of AFV demand and facility configuration. Besides, the user would benefit from the multiple views of the results, and therefore would be facilitated in obtaining robust solutions while reducing uncertainty.

This research provides an important implication for the development of alternative-fuel refueling infrastructure. The results of both exact and heuristic algorithms suggested that the choice of deviation decay function and maximum allowed deviation has a measurable effect on solutions quality and the optimal facility locations. Therefore, careful modeling of deviation behavior in practice is suggested. For example, the infrastructure developers and government agency will need to answer how sensitive potential (and actual) AFV drivers are to the required deviations. Such assessment may be needed in every important phase of the infrastructure development.

8.3 Direction for Future Research

There are future topics that are related to this research. First of all, empirical data that can tell us more about AFV drivers are needed. The data will be useful in gathering such important information about AFV drivers as deviation behavior, AFV purchase likelihood, socio-economic characteristics, refueling stops relative to drivers' home and work locations, typical refueling time of a day, or major usage of AFV. This information can be used to calibrate deviation decay model parameters and to realistically estimate geographic variation in AFV demands.

Second, the DFRLM assumes that each facility site is uncapacitated so that an unlimited number of flows can be refueled at a site. On the other hand, the CFRLM (Upchurch, Kuby, and Lim 2009) that accounts for the capacity of each facility assumes that drivers are always following the shortest path. Therefore, the development of a model that can simultaneously consider deviation and capacity is a promising future direction for research. In addition, given that the new model is oriented to be applied to real world problems, the development of efficient solution approaches for the integrated model is the logical next step.

Third, more research is necessary to extend the reliability and usability of the DFRLM heuristics. Specifically, the feasibility evaluation algorithm (or feasible network generation algorithm) in DFRLM heuristics needs to be more flexible so that it can take into account such diverse refueling (or, more specifically, electric vehicle recharging) behaviors as home-refueling, work-refueling, or refueling within a time window. Alternatively, a future implementation of DFRLM heuristics may focus on reducing the computation effort for the most time-consuming sub-problem, dynamic generation of all-pairs shortest paths in a feasible network. For instance, we could use *DDmax* in solving the sub-problem to filter out the nodes that are located farther than the *DDmax* from the shortest path of an OD pair.

Fourth, it is expected that if candidates are not restricted at nodes and they are numerous “enough” relative to vehicle range, the optimality gap of the solutions from DFRLM heuristics will decrease as in Kuby and Lim (2007). Even though the extension of DFRLM to include the augmented nodes from the added-node dispersion problem or mid-path segment methods seems readily possible, the application of the integrated model to a large network would require some efficient approaches. One obvious approach is to use improved heuristic algorithms for dynamic generation of deviation paths, as is suggested above. Another approach is to develop a new efficient formulation for the DFRLM as Capar, Kuby, and Rao (2010) efficiently reformulated the FRLM.

Fifth, research on the development of advanced visualization tools that help the user explore effects of various scenarios on the solution will be beneficial. Interactive and multi-dimensional views of the problem both in objective space and solution space may provide the user fundamental insight into the problem (Murray 2010) that might not have been revealed otherwise. In the context of SDSS literature, the usability of such tools would be maximized if they are accompanied with the tools that generate a variety of scenarios. Essentially integration of the tools would reduce the uncertainty in the problem.

REFERENCES

Abel, D. J., P. J. Kilby, and J. R. Davis. 1994. The Systems Integration Problem. *International Journal of Geographical Information Systems* 8 (1):1-12.

Ahearn, S., and J. Osleeb. 1993. Greenpoint/Williamsburg Environmental Benefits Program: Development of a Pilot Geographic Information System. *GIS/LIS Proceedings* 1 (November):10-18.

Anselin, L., and S. Bao. 1997. Exploratory spatial data analysis linking SpaceStat and ArcView. In *Recent developments in spatial analysis*, eds. M. M. Fischer and A. Getis. New York: Springer.

Anselin, L., R. F. Dobson, and S. Hudak. 1993. Linking GIS and Spatial Data Analysis in Practice. *Geographical Systems* 1:3-23.

Anselin, L., and A. Getis. 1992. Spatial Statistical Analysis and Geographic Information Systems. *Annals of Regional Science* 26 (1):19-33.

Argent, R. M. 2004. An overview of model integration for environmental applications--components, frameworks and semantics. *Environmental Modelling & Software* 19 (3):219-234.

Armstrong, M. P., and P. J. Densham. 2008. Cartographic support for locational problem-solving by groups. *International Journal of Geographical Information Science* 22 (7):721 - 749.

Balinski, M. L. 1965. Integer programming; Methods, uses, computation. *Management Science* 12:253-313.

Bankes, S. 1993. Exploratory Modeling for Policy Analysis. *Operations Research* 41 (3):435-449.

Bapna, R., L. S. Thakur, and S. K. Nair. 2002. Infrastructure development for conversion to environmentally friendly fuel. *European Journal of Operational Research* 142 (3):480-496.

Batty, M., and Y. Xie. 1994a. Modelling inside GIS: Part 1. Model structures, exploratory spatial data analysis and aggregation. *International Journal of Geographical Information Science* 8 (3):291-307.

———. 1994b. Modelling inside GIS: Part 2. Selecting and calibrating urban models using ARC-INFO. *International Journal of Geographical Information Science* 8 (5):451-470.

Bender, T., H. Hennes, J. Kalcsics, M. T. Melo, and S. Nickel. 2002. Location software and interface with GIS and supply chain management. In *Facility location: Applications and theory*, eds. Z. Drezner and H. Hamacher. New York: Springer.

Berman, O., D. Bertsimas, and R. C. Larson. 1995. Locating Discretionary Service Facilities, II: Maximizing Market Size, Minimizing Inconvenience. *Operations Research* 43 (4):623-632.

Berman, O., J. M. Hodgson, and D. Krass. 1995. Flow-interception problems. In *Facility location : a survey of applications and methods*, ed. Z. Drezner, 389-426. New York: Springer.

Berman, O., and D. Krass. 1998. Flow intercepting spatial interaction model: a new approach to optimal location of competitive facilities. *Location Science* 6 (1-4):41-65.

Berman, O., R. C. Larson, and N. Fouska. 1992. Optimal Location of Discretionary Service Facilities. *Transportation Science* 26 (3):201-211.

Berman, O., and D. Simchi-Devi. 1988. A heuristic algorithm for the traveling salesman location problem on networks. *Operations Research* 36:478-484.

Bersani, C., R. Minciardi, R. Sacile, and E. Trasforini. 2009. Network planning of fuelling service stations in a near-term competitive scenario of the hydrogen economy. *Socio-Economic Planning Sciences* 43 (1):55-71.

Bishr, Y. 1998. Overcoming the semantic and other barriers to GIS interoperability. *International Journal of Geographical Information Science* 12 (4):299-314.

Boccia, M., A. Sforza, and C. Sterle. 2009. Flow Intercepting Facility Location: Problems, Models and Heuristics. *Journal of Mathematical Modelling and Algorithms* 8 (1):35-79.

BTS. 2008. National Transportation Statistics: Bureau of Transportation Statistics, U.S. Department of Transportation (US DOT).

Burrough, P. A. 1992. Development of Intelligent Geographical Information Systems. *International Journal of Geographical Information Systems* 6 (1):1-11.

Burrough, P. A., and R. McDonnell. 1998. *Principles of geographical information systems*. New York: Oxford University Press.

Camm, J. D., T. E. Chorman, F. A. Dill, J. R. Evans, and D. J. Sweeney. 1997. Blending OR/MS, judgment, and GIS: Restructuring P&G's supply chain. *Interfaces* 27:128-142.

Capar, I., M. Kuby, and B. Rao. 2010. A New Formulation of the Flow-Refueling Location Model for Alternative-Fuel Stations. *IIE Transactions* Under Review

Chan, T. Y., V. Padmanabhan, and P. B. Seetharaman. 2007. An Econometric Model of Location and Pricing in the Gasoline Market. *Journal of Marketing Research (JMR)* 44 (4):622-635.

Church, R. L. 2002. Geographic information systems and location science. *Computers & Operations Research* 29:541-562.

Church, R. L., S. R. Loban, and K. Lombard. 1992. An interface for exploring spatial alternatives for a corridor location problem. *Computers & Geosciences* 18 (8):1095-1105.

Church, R. L., and M. E. Meadows. 1979. Location modeling utilizing maximum service distance criteria,. *Geographical Analysis* 11:358-373.

Church, R. L., and A. T. Murray. 2009. *Site selection, location analysis, and GIS*. Hoboken, NJ: John Wiley & Sons, Inc.

Church, R. L., and C. S. ReVelle. 1974. The maximum covering location problem. *Papers of Regional Science* 32:101-118.

Clarke, K. C. 2003. Geocomputation's future at the extremes: high performance computing and nanoclients. *Parallel Computing* 29 (10):1281-1295.

Cooper, L. 1963. Location-allocation problems. *Operations Research* 11:331-343.

———. 1967. Solutions of generalized locational equilibrium models. *Journal of Regional Science* 7:1-17.

Daskin, M. S. 2008. What you should know about location modeling. *Naval Research Logistics* 55 (4):283-294.

Densham, P., and G. Rushton. 1991. *Designing and Implementing Strategies for Solving Large Location- Allocation Problems with Heuristic Methods*: National Center for Geographic Information and Analysis.

Densham, P. J. 1991. Spatial Decision Support Systems. In *Geographical Information Systems: Principles and Applications*, eds. D. J. Maguire, M. F. Goodchild and D. W. Rhind, 403-412. New York: Willey & Sons.

———. 1994. Integrating GIS and spatial modelling: visual interactive modelling and location selection. *Geographical Systems* 1:203-219.

Densham, P. J., and G. Rushton. 1992. Strategies for solving large location-allocation problems by heuristic methods. *Environment and Planning A* 24:289-304.

Dijkstra, E. W. 1959. A Note on Two Problems in Connection with Graphs. *Numeriche Mathematik* 1:269-271.

DOE. 2002. *National Hydrogen Energy Roadmap: production, delivery, storage, conversion, applications, public education and outreach*.

———. *DOE Hydrogen Program: Annual Progress Reports* 2008 [cited November 7th, 2009. Available from http://www.hydrogen.energy.gov/annual_progress.html.

Dreyfus, S. E. 1969. An Appraisal of Some Shortest-Path Algorithms. *Operations Research* 17 (3):395-412.

Drezner, Z. 1995. *Facility location : a survey of applications and methods*. New York: Springer.

Drezner, Z., and H. Hamacher. 2002. *Facility location : applications and theory*. Berlin ; New York: Springer.

Duany, A., E. Plater-Zyberk, and J. Speck. 2000. *Suburban nation : the rise of sprawl and the decline of the American Dream*. 1st ed. New York: North Point Press.

EIA. 2009. Annual Energy Outlook 2009: With Projections to 2030. Washington, DC: Department of Energy, Energy Information Administration.

Eppstein, D. 1994. Finding the k shortest paths.

Erkut, E., and S. Neuman. 1989. Analytical models for locating undesirable facilities. *European Journal of Operational Research* 40:275-291.

Fedra, K. 1993. Environmental modeling and GIS. In *Environmental Modeling with GIS*, ed. M. Goodchild, B. Parks, and L. Steyaert, 35-50. Oxford: Oxford University Press.

———. 1994. Integrated Environmental Information and Decision-Support Systems. In *IFIP Transactions; Vol. B-16. Proceedings of the IFIP TC5/WG5.11 Working Conference on Computer Support for*

Environmental Impact Assessment, eds. G. Guariso and B. Page, 269-288: North-Holland Publishing Co. Amsterdam.

Fotheringham, A. S. 1998. Trends in quantitative methods II: stressing the computational. *Progress in Human Geography* 22 (2):283-292.

Fotheringham, A. S., and P. Rogerson. 1994. *Spatial analysis and GIS*. London ; Washington, DC: Taylor & Francis.

Gan, C.-T. 1994. A GIS-aided procedure for converting census data for transportation planning. *ITE Journal* 64 (Nov):34-40.

Gerrard, R. A., R. L. Church, D. M. Stoms, and F. W. Davis. 1997. Selecting conservation reserves using species covering models: Adapting the ARC/INFO GIS. *Transactions in GIS* 2:45-60.

Ghosh, A., S. McLafferty, and C. S. Craig. 1995. Multifacility retail networks. In *Facility location : a survey of applications and methods*, ed. Z. Drezner, 301-330. New York: Springer.

Goodchild, M., and V. Noronha. 1987. Location-allocation and impulsive shopping: the case of gasoline retailing. In *Spatial analysis and location-allocation models*, eds. A. Ghosh and G. Rushton. New York: Van Nostrand Reinhold.

Goodchild, M. F. 1979. The aggregation problem in location-allocation. *Geographical Analysis* 11:240-255.

———. 1987. A spatial analytic perspective on geographical information systems. *International Journal of Geographical Information Systems* 1:327-334.

———. 1990. Geographic Information Systems and environmental modeling. In *Seventh International Conference on Interactive Information and Processing Systems for Meteorology, Oceanography and Hydrology*, 5-10. Boston: AMS.

———. 1991. Integrating GIS and environmental modeling at global scales. In *GIS/LIS 91*, 117-127. Washington DC: ASPRS/ACSM/AAG/URISA/AMFM.

Goodchild, M. F., L. Anselin, and U. Deichmann. 1993. A framework for the areal interpolation of socioeconomic data. *Environment and Planning A* 25:383-397.

Goodchild, M. F., and S. Gopal eds. 1989. *Accuracy of Spatial Database*. London: Taylor and Francis.

Goodchild, M. F., R. P. Haining, S. Wise, and a. others. 1992. Integrating GIS and spatial data analysis: problems and possibilities. *International Journal of Geographical Information Systems* 6 (5):407-423.

Goodchild, M. F., and N. Lam. 1980. Areal interpolation: A variant of the traditional spatial problem. *Geoprocessing* 1:297-312.

Greene, D. L. 1996. Survey Evidence on the Importance of Fuel Availability to the Choice of Alternative Fuels and Vehicles. *Energy Studies Review* 8 (3):215-231.

———. 2001. TAFV Alternative Fuels and Vehicles Choice Model Documentation: Oak Ridge National Laboratory.

———. 2004. Transportation and Energy. In *The Geography of Urban Transportation*, eds. S. Hanson and G. Giuliano. New York: Guilford Press.

Greene, D. L., and D. Bowman. 2007. Integrated Analysis of Market Transformation Scenarios with HyTrans: Oak Ridge National Laboratory.

Greene, D. L., P. N. Leiby, B. James, J. Perez, M. Melendez, A. Milbrandt, S. Unnasch, D. Rutherford, and M. Hooks. 2008. Hydrogen Scenario Analysis Summary Report: Analysis of the Transition to Hydrogen Fuel Cell Vehicles and the Potential Hydrogen Energy Infrastructure Requirements.

Hakimi, S. L. 1964. Optimum Locations of Switching Centers and the Absolute Centers and Medians of a Graph. *Operations Research* 12 (3):450-459.

———. 1965. Optimum Distribution of Switching Centers in a Communication Network and Some Related Graph Theoretic Problems. *Operations Research* 13 (3):462-475.

Heuvelink, G. B. M. 1999. Propagation of error in spatial modelling with GIS. In *Geographical Information Systems*, eds. P. A. Longley, M. F. Goodchild, D. J. Maguire and D. W. Rhind, 207-217. New York: John Wiley and Sons.

Hodgson, M. J. 1981. The location of public facilities intermediate to the journey to work. *European Journal of Operational Research* 6 (2):199-204.

———. 1990. A flow-capturing location-allocation model. *Geographical Analysis* 22:270-279.

Hodgson, M. J., and O. Berman. 1997. A billboard location model. *Geographical and Environmental Modelling* 1:25-45.

Hodgson, M. J., K. E. Rosing, and J. Zhang. 1996. Locating vehicle inspection stations to protect a transportation network. *Geographical Analysis* 28 (4):299-314.

Hoffman, W., and R. Pavley. 1959. A Method for the Solution of the Nth Best Path Problem. *Journal of the ACM* 6 (4):506-514.

Hooker, J. N., R. S. Garfinkel, and C. K. Chen. 1991. Finite Dominating Sets for Network Location Problems. *Operations Research* 39 (1):100-118.

Huff, D. L. 1964. Defining and Estimating a Trade Area. *Journal of Marketing* 28:34-38.

Jankowski, P. 1995. Integrating Geographical Information Systems and Multiple Criteria Decision Making Methods. *International Journal of Geographical Information Systems* 9 (3):251-273.

Johnson, M. P. 2001. A spatial decision support system prototype for housing mobility program planning. *Journal of Geographical Systems* 3 (1):49-67.

Keles, D., M. Wietschel, D. Möst, and O. Rentz. 2008. Market penetration of fuel cell vehicles - Analysis based on agent behaviour. *International Journal of Hydrogen Energy* 33 (16):4444-4455.

Kim, K., and A. T. Murray. 2008. Enhancing spatial representation in primary and secondary coverage location modeling. *Journal of Regional Science* 48:745-768.

Kitamura, R., and D. Sperling. 1987. Refueling behavior of automobile drivers. *Transportation Research. Part A, Policy and practice* 21 (3):235-245.

Kuby, M. 1987. Programming models for facility dispersion: The p-dispersion and maxisum dispersion problems. *Geographical Analysis* 19:315-329.

Kuby, M., and S. Lim. 2005. The flow-refueling location problem for alternative-fuel vehicles. *Socio-Economic Planning Sciences* 39 (2):125-145.

———. 2007. Location of Alternative-Fuel Stations Using the Flow-Refueling Location Model and Dispersion of Candidate Sites on Arcs. *Networks & Spatial Economics* 7 (2):129-152.

Kuby, M., S. Lim, and C. Upchurch. 2005. Dispersion of nodes added to a network. *Geographical Analysis* 37 (4):383-409.

Kuby, M., L. Lines, R. Schultz, Z. Xie, J.-G. Kim, and S. Lim. 2009. Optimization of hydrogen stations in Florida using the Flow-Refueling Location Model. *International Journal of Hydrogen Energy* 34 (15):6045-6064.

Lempert, R. J., S. W. Popper, and S. C. Bankes. 2003. *Shaping the next one hundred years: New methods for quantitative, long-term policy analysis*. Santa Monica, CA: RAND.

Lim, S. 2007. Heuristic algorithms and a spatial decision support system for locating hydrogen-refueling stations. Ph.D. dissertation, School of Geographical Sciences, Arizona State University, United States.

Lim, S., and M. Kuby. 2010. Heuristic algorithms for siting alternative-fuel stations using the Flow-Refueling Location Model. *European Journal of Operational Research* 204 (1):51-61.

Lin, Z., J. Ogden, Y. Fan, and C.-W. Chen. 2008. The fuel-travel-back approach to hydrogen station siting. *International Journal of Hydrogen Energy* 33:3096-3101.

Lines, L., M. Kuby, R. Schultz, and Z. Xie. 2007. Location strategies for the initial hydrogen refueling infrastructure in Florida, Florida Hydrogen Initiative Final Report.

Liu, N., B. Huang, and M. Chandramouli. 2006. Optimal siting of fire stations using GIS and ANT algorithm. *Journal of Computing in Civil Engineering* 20:361-369.

Longley, P., and M. Batty. 1996. *Spatial analysis : modelling in a GIS environment*. Cambridge, New York: GeoInformation International.

Longley, P., M. F. Goodchild, D. J. Maguire, and D. W. Rhind. 2005. *Geographical information systems and science*. 2nd ed. Chichester: Wiley.

MacEachren, A. M. 1994. Visualization in modern cartography: Setting the agenda. In *Visualization in Modern Cartography*, eds. A. M. MacEachren and D. R. F. Taylor, 1-12. London: Pergamon Press.

———. 2001. Cartography and GIS: extending collaborative tools to support virtual teams. *Progress in Human Geography* 25 (3):431-444.

MacEachren, A. M., A. Robinson, S. Hopper, S. Gardner, R. Murray, M. Gahegan, and E. Hetzler. 2005. Visualizing Geospatial Information Uncertainty: What We Know and What We Need to Know. *Cartography and Geographic Information Science* 32 (3):139-160.

McFadden, D. 1974. Conditional Logit Analysis of Quantitative Choice Behavior. In *Frontiers in Economics,* ed. P. Zarembka. New York: Academic Press.

McHarg, I. 1969. *Design with nature*. New York: Natural History Press.

McQueen, B., and J. McQueen. 1999. *Intelligent transportation systems architectures*. Boston ; London: Artech House.

Melaina, M., and J. Bremson. 2008. Refueling availability for alternative fuel vehicle markets: Sufficient urban station coverage. *Energy Policy* 36 (8):3233-3241.

Melaina, M. W. 2003. Initiating hydrogen infrastructures: preliminary analysis of a sufficient number of initial hydrogen stations in the US. *International Journal of Hydrogen Energy* 28 (7):743-755.

———. 2005. Estimating Relative Station Sizes in Early Hydrogen Station Networks. In *National Hydrogen Association Annual Conference*: National Hydrogen Association.

Melaina, M. W., and J. Bremson. 2006. Regularities in Early Hydrogen Station Size Distributions. In *Proceeding of the 26th United States Association for Energy Economics*. International Association for Energy Economics North American Conference. Ann Arbor, Michigan.

Melendez, M. 2006. *Transitioning to a Hydrogen Future: Learning from the Alternative Fuels Experience*.

Melendez, M., and A. Milbrandt. 2005. Analysis of the Hydrogen Infrastructure Needed to Enable Commercial Introduction of Hydrogen-Fueled Vehicles: Preprint, Size: 23 pp. pages; Format: Adobe PDF Document with Extractable Text.

———. 2006. Geographically Based Hydrogen Consumer Demand and Infrastructure Analysis: Final Report, Size: 35 pp.

Microsoft. *QuickGraph, Graph Data Structures And Algorithms for .Net* 2008 [cited 29 November 2010. Available from http://quickgraph.codeplex.com/.

———. 2010. *C# Programming Guide* 2010 [cited 11/2/2010 2010]. Available from http://msdn.microsoft.com/en-us/library/67ef8sbd.aspx.

Miller, H. J. 1996. GIS and geometric representation in facility location problems. *International Journal of Geographical Information Science* 10:791-816.

Miller, H. J., and S.-L. Shaw. 2001. *Geographic Information Systems for Transportation: Principles and Applications*: Oxford University Press.

Mirchandani, P., P. Rebello, and A. Agnetis. 1995. The Inspection Station Location Problem in Hazardous Material Transportation: Some Heuristics and Bounds. *INFOR* 33 (2):100-113.

Murawski, L., and R. L. Church. 2009. Improving accessibility to rural health services: The maximal covering network improvement problem. *Socio-Economic Planning Sciences* 43:102-110.

Murray, A. T. 2003. Site placement uncertainty in location analysis. *Computers, Environment and Urban Systems* 27 (2):205-221.

———. 2005. Geography in Coverage Modeling: Exploiting Spatial Structure to Address Complementary Partial Service of Areas. *Annals of the Association of American Geographers* 95 (4):761-772.

———. 2010. Advances in location modeling: GIS linkages and contributions. *Journal of Geographical Systems* 12 (3):335-354.

Murray, A. T., and H. Kim. 2008. Efficient identification of geographic restrictions in location modeling using GIS. *Letters in Spatial and Resource Sciences* 1:61-71.

Murray, A. T., D. Tong, and K. Kim. 2010. Enhancing classic coverage location models. *International Regional Science Review* 33:115-133.

Nakanishi, M., and L. G. Cooper. 1974. Parameter Estimation for a Multiplicative Competitive Interaction Model-Least Squares Approach. *Journal of Marketing Research* 11:303-311.

NAS. 2004. *The hydrogen economy: opportunities, costs, barriers, and R&D needs*. Washington, D.C.: The National Academies Press.

Ni, J., N. Johnson, J. M. Ogden, C. Yang, and J. Johnson. 2005. Estimating Hydrogen Demand Distribution Using Geographic Information Systems (GIS). In *Presentation Series*. Davis, California: Institution of Transportation Studies.

Nicholas, M. A., S. L. Handy, and D. Sperling. 2004. Using Geographic Information Systems to Evaluate Siting and Networks of Hydrogen Stations. *Transportation Research Record: Journal of the Transportation Research Board* 1880:126-134.

Nyerges, T. L., R. Montejano, C. Oshiro, and M. Dadswell. 1997. Group-based geographic information systems for transportation improvement site selection. *Transportation Research C: Engineering Technologies* 5C:349-369.

O'Sullivan, D., and D. Unwin. 2003. *Geographic information analysis*. Hoboken, N.J.: J. Wiley.

Ogden, J. M. 1999a. Developing an infrastructure for hydrogen vehicles: a Southern California case study. *International Journal of Hydrogen Energy* 24 (8):709-730.

———. 1999b. Prospects for building a hydrogen energy infrastructure. *Annual Review of Energy and the Environment* 24 (1):227-279.

———. 2004. *Hydrogen Delivery Model for H2A Analysis: A Spreadsheet model for Hydrogen Delivery Scenarios*.

Openshaw, S. 1992. Some suggestions concerning the development of artificial intelligence tools for spatial modelling and analysis in GIS. *The Annals of Regional Science* 26 (1):35-51.

Openshaw, S., and P. J. Taylor. 1981. The modifiable areal unit problem. In *Quantitative geography: A british view*, eds. N. Wrigley and R. Bennett, 60-69. London: Routledge and Kegan Paul.

Owen, S. H., and M. S. Daskin. 1998. Strategic facility location: A review. *European Journal of Operational Research* 111 (3):423-447.

Ralston, B. A., G. Tharakan, and C. Liu. 1994. A spatial decision support system for transportation policy analysis in Bangladesh. *Journal of Transport Geography* 2 (2):101-110.

ReVelle, C. 1986. The Maximum Capture or 'Sphere of Influence' Location Problem: Hotelling Revisited on a Network. *Journal of Regional Science* 26 (2):343-358.

Revelle, C. 1987. Urban public facility location. In *Handbook of regional and urban economics, Vol II.* , ed. E. S. Mills, 1053-1096. Amsterdam: North-Holland.

ReVelle, C. S., and R. Swain. 1970. Central facilities location. *Geographical Analysis* 2:30-42.

Ribeiro, A., and A. P. Antunes. 2002. A GIS-based decision-support tool for public facility planning. *Environment and Planning B* 29:553-569.

Rinner, C. 2003. Web-based Spatial Decision Support: Status and Research Directions. *Journal of Geographic Information and Decision Analysis* 7 (1):14-31.

Shier, D. R. 1979. On algorithms for finding the k shortest paths in a network. *Networks* 9 (3):195-214.

Snediker, D. E., A. T. Murray, and T. C. Matisziw. 2008. Decision support for network disruption mitigation. *Decision Support Systems* 44:954-969.

Snyder, L. V. 2006. Facility location under uncertainty: a review. *IIE Transactions* 38 (7):547 - 564.

Spaulding, B., and R. Cromley. 2007. Integrating the maximum capture problem into a GIS framework. *Journal of Geographical Systems* 9 (3):267-288.

Sperling, D., and J. S. Cannon. 2004. *The hydrogen energy transition : moving toward the post petroleum age in transportation*. Amsterdam ; San Diego: Elsevier/Academic Press.

Steyaert, L. T., and M. F. Goodchild. 1994. Integrating geographic information systems and environmental simulation models: a status review. In *Environmental Information Management and Analysis: Ecosystem to Global Scales*, eds. W. K. Michener, J. W. Brunt and S. G. Stafford, 333-356. London: Taylor and Francis.

Suzuki, A., and A. Okabe. 1995. Using Voronoi diagrams. In *Facility location: A survey of applications and methods*, ed. Z. Drezner, 103-118. New York: Springer.

Teitz, M. B., and P. Bart. 1968. Heuristic Methods for Estimating the Generalized Vertex Median of a Weighted Graph. *Operations Research* 16 (5):955-961.

Tester, J. W. 2005. *Sustainable energy : choosing among options*. Cambridge, Mass.: MIT Press.

Tomlin, C. D. 1990. *Geographic information systems and cartographic modeling*. Englewood Cliffs, NJ: Prentice-Hall.

Tong, D., and A. T. Murray. 2008. Maximizing coverage of spatial demand for service. *Papers in Regional Science* 87:479-489.

Toregas, C., R. Swain, C. S. ReVelle, and L. Bergman. 1971. The Location of Emergency Service Facilities. *Operations Research* 19 (5):1363-1373.

Unwin, D. J. 1995. Geographical information systems and the problem of 'error and uncertainty'. *Progress in Human Geography* 19 (4):549-558.

Upchurch, C., M. Kuby, and S. Lim. 2009. A Model for Location of Capacitated Alternative-Fuel Stations. *Geographical Analysis* 41:85-106.

Wang, Y.-W., and C.-C. Lin. 2009. Locating road-vehicle refueling stations. *Transportation Research Part E: Logistics and Transportation Review* 45 (5):821-829.

Welch, C. 2006. Lessons Learned from Alternative Transportation Fuels: Modeling Transition Dynamics: National Renewable Energy Laboratory.

———. 2007a. *System Dynamics: HyDIVE(TM) (Hydrogen Dynamic Infrastructure and Vehicle Evolution) Model (Presentation)*.

Welch, C. J. 2007b. Quantifying Consumer Sensitivity to Hydrogen Refueling Station Coverage. In *2007 Annual Progress Report*: National Renewable Energy Laboratory, Department of Energy.

Williams, H. W., L. 1977. On the Formation of Travel Demand Models and Economic Evaluation Measures of User Benefit. *Environment and Planning A* 9:285-344.

Wu, T.-H., and J.-N. Lin. 2003. Solving the competitive discretionary service facility location problem. *European Journal of Operational Research* 144:366-378.

Xiao, N. C. 2008. A Unified Conceptual Framework for Geographical Optimization Using Evolutionary Algorithms. *Annals of the Association of American Geographers* 98 (4):795-817.

Yang, C., and J. Ogden. 2007. Determining the lowest-cost hydrogen delivery mode. *International Journal of Hydrogen Energy* 32 (2):268-286.

Yeh, A. G. O., and M. H. Chow. 1996. An integrated GIS and location-allocation approach to public facilities planning: An example of open space planning. *Computers, Environment and Urban Systems* 20:339-350.

Yen, J. Y. 1971. Finding the K Shortest Loopless Paths in a Network. *Management Science* 17 (11):712-716.

Zeng, W., I. Castillo, and M. Hodgson. 2010a. A Generalized Model for Locating Facilities on a Network with Flow-Based Demand. *Networks and Spatial Economics* 10 (4):579-611.

———. In Press. A Generalized Model for Locating Facilities on a Network with Flow-Based Demand. *Networks and Spatial Economics*.

Zeng, W., I. Castillo, and M. J. Hodgson. 2010b. Aggregating Data for the Flow-Intercepting Location Model: A Geographic Information System, Optimization, and Heuristic Framework. *Geographical Analysis* 42 (3):301-322.

Zeng, W., and R. L. Church. 2009. Finding shortest paths on real road networks: the case for A*. *International Journal of Geographical Information Science* 23 (4):531 - 543.

Zeng, W., M. J. Hodgson, and I. Castillo. 2009. The Pickup Problem: Consumers' Locational Preferences in Flow Interception. *Geographical Analysis* 41 (1):107-126.

Zhan, F. B. 1997. Three Fastest Shortest Path Algorithms on Real Road Networks: Data Structures and Procedures. *Journal of Geographic Information and Decision Analysis* 1 (1):69-82.

Zhan, F. B., and C. E. Noon. 1998. Shortest Path Algorithms: An Evaluation using Real Road Networks. *Transportation Science* 32 (1):65.